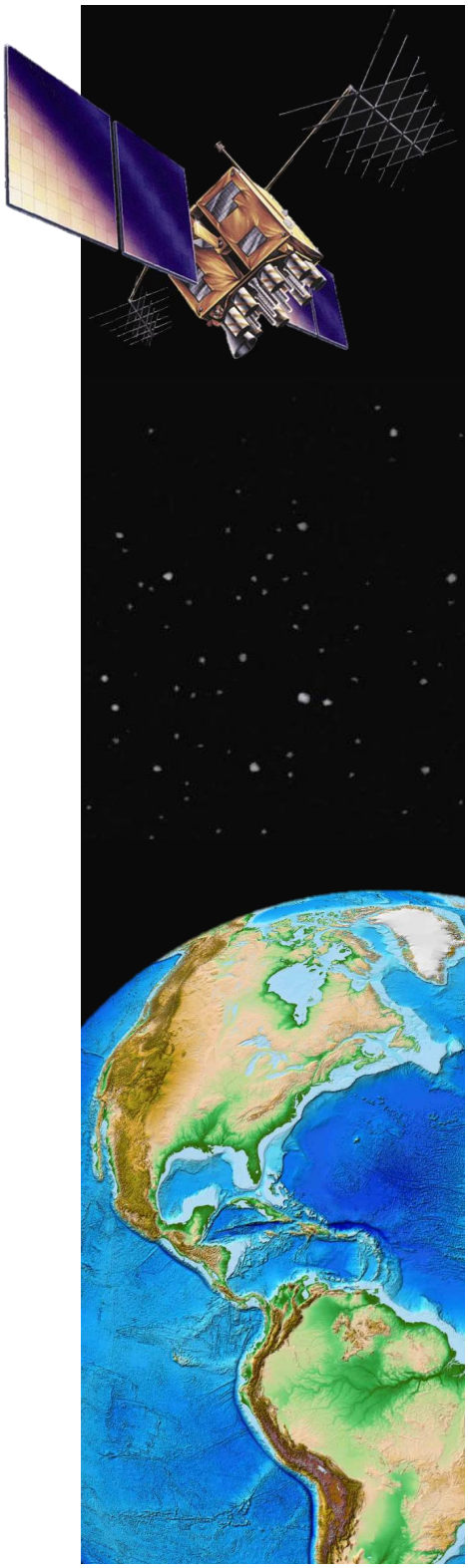

An Analysis of Global Positioning System (GPS) Standard Positioning Service (SPS) Performance for 2018

TR-SGL-19-02

March 13, 2019

Space and Geophysics Laboratory
Applied Research Laboratories
The University of Texas at Austin
P.O. Box 8029
Austin, TX 78713-8029

Brent A. Renfro,
Miquela Stein,
Nicholas Boeker,
Emery Reed,
Eduardo Villalba

Contract: NAVSEA Contract N00024-17-D-6421
Task Order: 5101192

This Page Added for Document Spacing

Executive Summary

Applied Research Laboratories, The University of Texas at Austin (ARL:UT) examined the performance of the Global Positioning System (GPS) throughout 2018 for the U.S. Air Force Space and Missile Systems Center Global Positioning Systems Directorate (SMC/GP). This report details the results of that performance analysis. This material is based upon work supported by SMC/GP through Naval Sea Systems Command Contract N00024-17-D-6421, task order 5101192, "GPS Data Collection and Performance Analysis."

Performance is defined by the 2008 Standard Positioning Service (SPS) Performance Standard (SPS PS) [1]. The performance standard provides the U.S. government's assertions regarding the expected performance of GPS. This report does not address all of the assertions in the performance standards. This report covers those assertions which can be verified by anyone with knowledge of standard GPS data analysis practices, familiarity with the relevant signal specification, and access to a Global Navigation Satellite System (GNSS) data archive.

The assertions evaluated include those of accuracy, integrity, continuity, and availability of the GPS signal-in-space (SIS) along with the assertions on accuracy of positioning and time transfer. Chapter 1 is an introduction to the report. Chapter 2 of the report includes a tabular summary of the assertions that were evaluated and a summary of the results. The remaining chapters present details on the analysis associated with each assertion.

All the SPS PS assertions examined in the report were met in 2018.

Contents

List of Figures

List of Tables

Chapter 1

Introduction

Applied Research Laboratories, The University of Texas at Austin (ARL:UT)[1] examined the performance of the Global Positioning System (GPS) throughout 2018 for the U.S. Air Force Space and Missile Systems Center Global Positioning Systems Directorate (SMC/GP). This report details the results of that analysis. This material is based upon work supported by SMC/GP through Naval Sea Systems Command Contract N00024-17-D-6421, task order 5101192, "GPS Data Collection and Performance Analysis."

Performance is assessed relative to selected assertions in the 2008 Standard Positioning Service (SPS) Performance Standard (SPS PS) [1]. (Hereafter the term SPS PS, or SPSPS08, is used when referring to the 2008 SPS PS.) Chapter 2 contains a tabular summary of performance stated in terms of the metrics provided in the performance standard. Chapter 3 presents a more detailed explanation of the analysis conducted in evaluating each assertion. The assertions are presented in the order of appearance in the performance standards. Chapter 4 details additional findings of the performance analysis.

The performance standards define the services delivered through the L1 C/A code signal. The metrics are limited to the signal-in-space (SIS) and do not address atmospheric errors, receiver errors, or errors due to the user environment (e.g. multipath errors, terrain masking, and foliage). This report addresses assertions in the SPS PS that can be verified by anyone with knowledge of standard GPS data analysis practices, familiarity with the relevant signal specification [2], and access to a data archive (such as that available via the International Global Navigation Satellite System (GNSS) Service (IGS)) [3]. The assertions examined include those related to user range error (URE), availability of service, and position domain standards.

[1] *A complete list of abbreviations found in this document is provided in Appendix G.*

The majority of the assertions related to URE values are evaluated by comparison of the space vehicle (SV) clock and position representations as computed from the broadcast Legacy Navigation (LNAV) message data against the SV truth clock and position data as provided by a precise orbit calculated after the time of interest. The broadcast clock and position data is denoted in this report by BCP and the truth clock and position data by TCP. The process by which the URE values are calculated is described in Appendix B of this report.

Observation data from tracking stations are used to cross-check the URE values and to evaluate non-URE assertions. Examples of the latter application include the areas of Continuity (3.4), Availability (3.5), and Position/Time Availability (3.6). In these cases, data from two networks are used. The two networks considered are the National Geospatial-Intelligence Agency (NGA) Monitor Station Network (MSN) [4] and a subset of the tracking stations that contribute to the IGS. The geographic distribution of these stations is shown in Figure 1.1. The selection of these sets of stations ensure continuous simultaneous observation of all space vehicles by multiple stations.

Navigation message data used in this report were collected from the NGA MSN. The collection and selection of navigation message data are described in general terms in Appendix B.2.

Several metrics in the performance standards are stated in terms of either the Base 24 constellation, which consists of six orbital planes and four slots per plane, or the Expandable 24 constellation, in which three of the 24 slots may be occupied by two SVs. Currently, there are more than 32 GPS SVs on-orbit. Of these, at most 31 SVs may be operationally broadcasting at any time. Of the SVs on-orbit, 27 are located in the Expandable 24 constellation. The SVs in excess of those located in defined slots are assigned to locations in various planes in accordance with operational considerations.

The majority of the metrics in this report are evaluated on either a per-SV basis or for the full constellation. The metrics associated with continuity and availability are defined with respect to the slot definitions.

Each of the GPS SVs are identified by pseudo-random noise ID (PRN) and by space vehicle number (SVN). PRN IDs are assigned to SVs for periods of time. A given SV may be assigned different PRNs at different times during its operational life. The SVN represents the permanent unique identifier for the vehicle under discussion. As the number of active SVs has increased to nearly the total available, PRNs are now being used by multiple SVs within a given year (but by no more than one SV at a time). In general, we list the SVN first and the PRN second because the SVN is the unique identifier of the two. The SVN-to-PRN relationships were provided by the GPS Master Control Station (MCS), however other useful summaries of this information may be found on the U.S. Coast Guard Navigation Center website [5] and the U.S. Naval Observatory (USNO) website [6].

The authors acknowledge and appreciate the effort of several ARL:UT staff members who reviewed these results. For 2018 this included Molly Lee, Jon Little, Scott Sellers, and Johnathan York.

Karl Kovach of The Aerospace Corporation provided valuable assistance in interpreting the SPSPS08 assertions. John Lavrakas of Advanced Research Corporation and P.J. Mendicki of The Aerospace Corporation have long been interested in GPS performance metrics and have provided valuable comments on the final draft. However, the results presented in this report are derived by ARL:UT, and any errors in this report are the responsibility of ARL:UT.

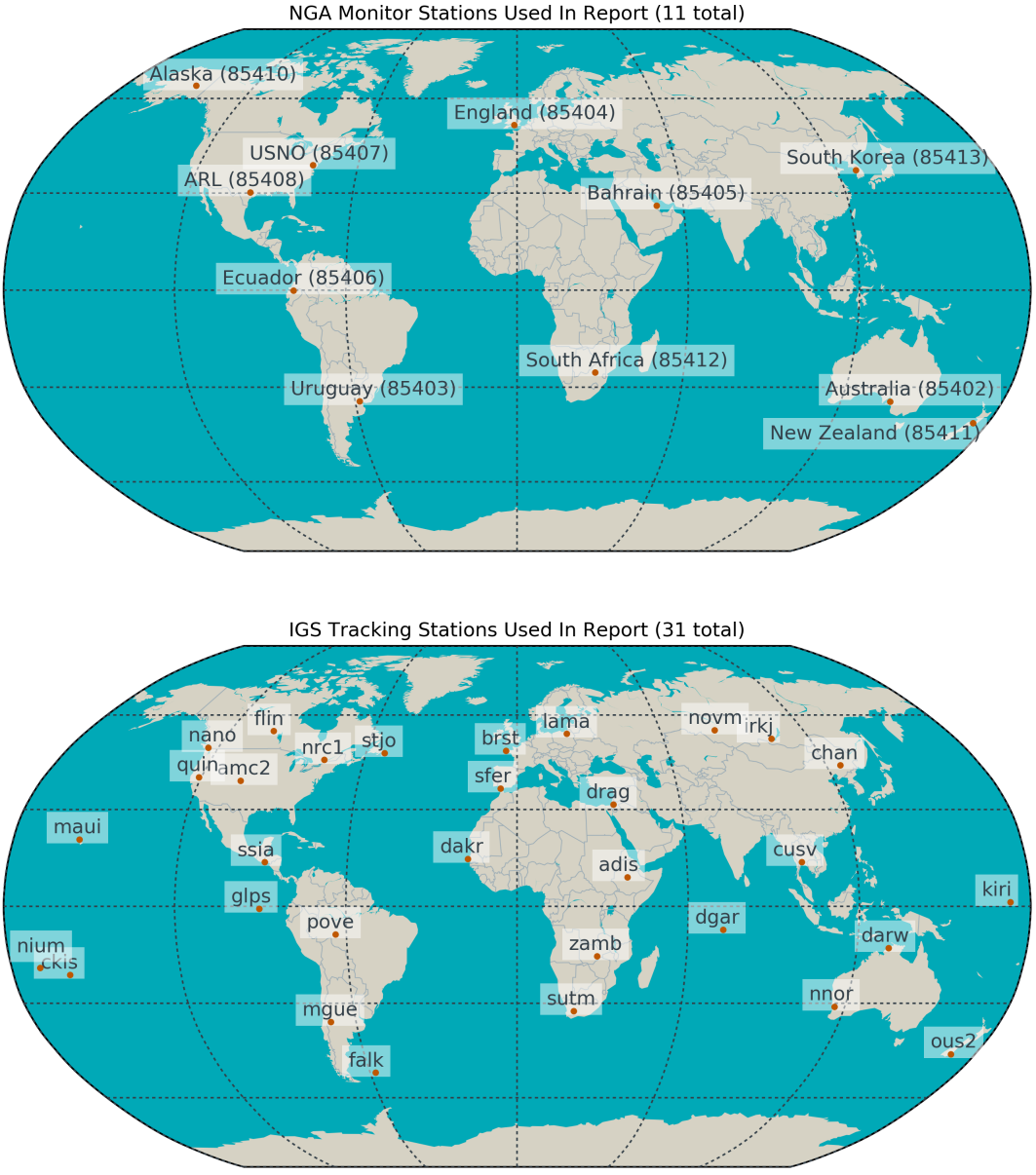

Figure 1.1: Maps of the Network of Stations Used in this Report

Chapter 2

Summary of Results

Table 2.1 provides a summary of the assertions defined in the performance standards. The table is annotated to show which assertions are evaluated in this report and the status of each assertion.

Of the assertions evaluated, all were met in 2018.

Details regarding each result may be found in Chapter 3. All abbreviations used in Table 2.1 may be found in Appendix G.

Table 2.1: Summary of SPS PS Metrics Examined for 2018

SPSPS08 Section	SPS PS Assertion	2018 Status	Report Section
3.3.1 SIS Per-Satellite Coverage	100% Coverage of Terrestrial Service Volume	not eval.	3.1.1
3.3.2 SIS Constellation Coverage	100% Coverage of Terrestrial Service Volume	✔	3.1.2
3.4.1 SIS URE Accuracy	$\leq$ 7.8 m 95% Global average URE during normal operations over all AODs	✔	3.2.1
	$\leq$ 12.8 m 95% Global average URE during normal operations at any AOD	✔	3.2.2
	$\leq$ 6.0 m 95% Global average URE during normal operations at zero AOD	✔	3.2.3
	$\leq$ 30 m 99.94% Global average URE during normal operations	✔	3.2.4
	$\leq$ 30 m 99.79% Worst case single point average URE during normal operations	✔	
	$\leq$ 388 m 95% Global average URE after 14 days without upload	N/A	–
3.4.2 SIS URRE Accuracy	$\leq$ 0.006 m/s 95% Global average at any AOD	✔	3.2.5
3.4.3 SIS URAE Accuracy	$\leq$ 0.002 m/s^2 95% Global average at any AOD	✔	3.2.6
3.4.4 SIS UTCOE Accuracy	$\leq$ 40 nsec 95% Global average at any AOD	✔	3.2.7
3.5.1 SIS Instantaneous URE Integrity	$\leq 1X10^{-5}$ Probability over any hour of exceeding the NTE tolerance without a timely alert	✔	3.3.1
3.5.4 SIS Instantaneous UTCOE Integrity	$\leq 1X10^{-5}$ Probability over any hour of exceeding the NTE tolerance without a timely alert	✔	3.3.2
3.6.1 SIS Continuity - Unscheduled Failure Interruptions	$\geq$ 0.9998 Probability over any hour of not losing the SPS SIS availability from the slot due to unscheduled interruption	✔	3.4.1
3.6.3 Status and Problem Reporting	Appropriate NANU issue at least 48 hours prior to a scheduled event	✔	3.4.2.1
3.7.1 SIS Per-Slot Availability	$\geq$ 0.957 Probability that (a.) a slot in the baseline 24-slot will be occupied by a satellite broadcasting a healthy SPS SIS, or (b.) a slot in the expanded configuration will be occupied by a pair of satellites each broadcasting a healthy SIS	✔	3.5.1
3.7.2 SIS Constellation Availability	$\geq$ 0.98 Probability that at least 21 slots out of the 24 slots will be occupied by a satellite (or pair of satellites for expanded slots) broadcasting a healthy SIS	✔	3.5.2
	$\geq$ 0.99999 Probability that at least 20 slots out of the 24 slots will be occupied by a satellite (or pair of satellites for expanded slots) broadcasting a healthy SIS	✔	
3.7.3 Operational Satellite Counts	$\geq$ 0.95 Probability that the constellation will have at least 24 operational satellites regardless of whether those operational satellites are located in slots or not	✔	3.5.3
3.8.1 PDOP Availability	$\geq$ 98% Global PDOP of 6 or less	✔	3.6.1
	$\geq$ 88% Worst site PDOP of 6 or less	✔	
3.8.2 Position Service Availability	$\geq$ 99% Horizontal, average location	✔	3.6.3
	$\geq$ 99% Vertical, average location	✔	
	$\geq$ 90% Horizontal, worst-case location	✔	
	$\geq$ 90% Vertical, worst-case location	✔	
3.8.3 Position Accuracy	$\leq$ 9 m 95% Horizontal, global average	✔	3.6.4
	$\leq$ 15 m 95% Vertical, global average	✔	
	$\leq$ 17 m 95% Horizontal, worst site	✔	
	$\leq$ 37 m 95% Vertical, worst site	✔	
	$\leq$ 40 nsec time transfer error 95% of the time	✔	3.6.5

✔ - Met
N/A - No SVs were in this mode in 2018
not eval. - see report text for more information

Chapter 3

Discussion of Performance Standard Metrics and Results

While Chapter 2 summarizes the status of the SPSPS08 metrics for 2018, the statistics and trends reported in this chapter provide both additional information and support for these conclusions.

3.1 SIS Coverage

3.1.1 Per-Satellite Coverage

SIS per-satellite coverage is asserted in Section 3.3.1 of the SPSPS08. The following standard is provided (from Table 3.3-1).

- *"100% Coverage of Terrestrial Service Volume"*

This is interpreted to mean that the direction of the Earth coverage beam of each GPS SV will be managed such that the beam will cover the Terrestrial Service volume visible to that SV providing at least the minimum required received power. This assertion is not evaluated at this time. Within the control segment, the operators have various tools to enable them to monitor and control SV pointing. Monitoring this assertion external to the control segment will require both SV-specific antenna gain pattern information and calibrated power observations. The potential for cost-effective evaluation will be examined again as future reports are prepared.

3.1.2 Constellation Coverage

SIS constellation coverage is asserted in Section 3.3.2 of the SPSPS08. The following standard is provided (from Table 3.3-2).

- *"100% Coverage of Terrestrial Service Volume"*

This assertion is interpreted to mean that a user will have at least four SVs transmitting a healthy or marginal signal visible at any moment. This is evaluated as part of the examination of DOP (see Section 3.6 of this report). The condition was true throughout 2018. As a result, the assertion is considered verified for 2018.

3.2 SIS Accuracy

SIS URE accuracy is asserted in Section 3.4 of the SPSPS08. The following standards (from Tables 3.4-1 through 3.4-4 in the SPS PS) are considered in this report:

- *"≤ 7.8 m 95% Global Average URE during Normal Operations over all AODs"*
- *"≤ 12.8 m 95% Global Average URE during Normal Operations at any AOD"*
- *"≤ 6.0 m 95% Global Average URE during Normal Operations at Zero AOD"*
- *"≤ 30 m 99.94% Global Average URE during Normal Operations"*
- *"≤ 30 m 99.79% Worst Case Single Point Average URE during Normal Operations"*
- *"≤ 0.006 m/s 95% Global Average URRE over any 3-second interval during Normal Operations at Any AOD"*
- *"≤ 0.002 m/s^2 95% Global Average URAE over any 3-second interval during Normal Operations at Any AOD"*
- *"≤ 40 nsec 95% Global Average UTCOE during Normal Operations at Any AOD"*

The remaining standard associated with operations after extended periods without an upload is not applicable in 2018 as periods of extended operations were very limited.

The URE statistics presented in this report are based on a comparison of the BCP against the TCP. (Refer to Appendix B for further details on the process by which the URE are computed.) This is a useful approach, but one that has specific limitations, the most significant being that the TCP may not capture the effect of individual discontinuities or large effects over short time scales (e.g. a frequency step or clock run-off). Nonetheless, this approach is appropriate given the 30 day period of averaging implemented in determining URE compared to brief (less than an hour) periods of the rare discontinuities. Briefly, this approach allows the computation of URE without direct reference to observations from any particular ground sites, though the TCP carries an implicit network dependency based on the set of ground stations used to derive the precise orbits from which the TCP is derived.

In the case of this report, the BCP and TCP are both referenced to the ionosphere-free linear combination of the L1/L2 P(Y)-code signal. As a result, the resulting URE values are best characterized as Precise Positioning Service (PPS) dual-frequency URE values. The SPS results are derived from the PPS dual-frequency results by a process described in Appendix F.

Throughout this section and the next, there are references to several distinct SIS URE expressions. Each of these SIS URE expressions means something slightly different. It is important to pay careful attention to the particular SIS URE expression being used in each case to avoid misinterpreting the associated URE numbers.

Appendix C of the SPSPS08 provides definitions for the two ways SIS URE are computed, *Instantaneous SIS URE*, which expresses URE on an instantaneous basis and *root mean square (RMS) SIS URE*, which expresses URE on a statistical basis. When the BCP and TCP are used to estimate the range residual along a specific satellite-to-receiver line-of-sight vector at a given instant in time, then that is an "Instantaneous SIS URE." Some of the primary differences between instantaneous basis SIS UREs and statistical basis SIS UREs are given below.

Table 3.1: Characteristics of SIS URE Methods

Instantaneous Basis SIS URE	**Statistical Basis SIS URE**
Always algebraically signed (±) number	Never algebraically signed
Never a statistical qualifier	Always a statistical qualifier (RMS, 95%, etc.)
Specific to a particular time and place	Statistic over span of times, or places, or both
Next section of this report (Section 3.3)	This section of this report (Section 3.2)

Throughout this section, there are references to the "Instantaneous RMS SIS URE." This is a statistical basis SIS URE (note the "RMS" statistical qualifier), where the measurement quantity is the Instantaneous SIS URE, and the span of the statistic covers that one particular point ("instant") in time across a large range of spatial points. This is effectively the evaluation of the Instantaneous SIS URE across every spatial point in the area of the service volume visible to the SV at that particular instant in time. Put another way; consider the signal from a given SV at a given point in time. That signal intersects the surface of the Earth over an area, and at each point in that area there is a unique Instantaneous SIS URE value based on geometric relationship between the SV and the point of interest. In the name "Instantaneous RMS SIS URE," the "Instantaneous" means that no time averaging occurs. The "RMS" refers to taking the RMS of all the individual Instantaneous SIS URE values across the area visible to the SV for a single time. This concept is explained in SPSPS08 Section A.4.11, and the relevant equation is presented in Appendix B.1.2 of this report.

3.2.1 URE Over All AOD

The performance standard URE metric that is most closely related to a user's observations is the calculation of the 95^{th} percentile Global Average URE over all ages of data (AODs). This is associated with the SPSPS08 Section 3.4 metrics:

- *"$\leq$ 7.8 m 95% Global Average URE during Normal Operations over all AODs"*

These metrics can be decomposed into several pieces to better understand the process. For example, the first metric may be decomposed as follows:

- *7.8 m* - This is the limit against which to test. The value is unique to the signal under evaluation.
- *95%* - This is the statistical measure applied to the data. In this case, there are a sufficiently large number of samples to allow direct sorting of the results across time and selection of the 95^{th} percentile.
- *Global Average URE* - This is another term for the Instantaneous RMS SIS URE, a statistical quantity representing the average URE across the area of the service volume visible to the SV at a given point in time. The expression used to compute this quantity is provided in Appendix B.1.2.
- *Normal Operations* - This is a constraint related to normal vs. extended mode operations. See IS-GPS-200 20.3.4.4 [2].
- *over all AODs* - This constraint means that the Global Average URE is considered at each evaluation time regardless of the AOD at the evaluation time. A more detailed explanation of the AOD and how this quantity is computed can be found in Section 4.2.

In addition, there are three general statements in Section 3.4 of SPSPS08 that have a bearing on this calculation:

- These statistics include data only from periods when each SV was healthy. Throughout this report, an SV is considered healthy based on the definition in SPS PS Section 2.3.2.
- These statistics are "per SV" - that is, they apply to the signal from each satellite, not for averages across the constellation.
- *"The ergodic period contains the minimum number of samples such that the sample statistic is representative of the population statistic. Under a one-upload-per-day scenario, for example, the traditional approximation of the URE ergodic period is 30 days."* (SPSPS08 Section 3.4, Note 2)

The statistics are computed over monthly periods and not daily. Monthly periods approximate the suggested 30 day period while conforming to a familiar time scale and avoiding the complication that a year is not evenly divisible by 30. We have computed the monthly statistic regardless of the number of days of availability in each month but have identified SV-months with less than 25 days of availability to note any SV-month with significantly less data than expected.

Table 3.2 contains the monthly 95^{th} percentile values of the RMS SIS URE based on the assumptions and constraints described above. For each SV, the worst value across the year is marked in red. In all cases, no values exceed 7.8 m, and so this requirement is met for 2018.

Figure 3.1 provides a summary of these results for the entire constellation. For each SV, shown along the horizontal axis, the median value of the monthly 95^{th} percentile SIS URE is displayed as a point. The full range of the monthly 95^{th} percentile SIS URE is shown by the vertical bars. Color distinguishes between the Block IIA, Block IIR, Block IIR-M, and Block IIF SVs. The red horizontal line at 7.8 m is the performance threshold asserted by the SPSPS08 Section 3.4 performance metric.

A number of points are evident from Table 3.2 and Figure 3.1:

1. All SVs meet the performance assertion of the SPSPS08, even when only the worst performing month is considered. Even the worst value for each SV (indicated by the upper extent of the range bars) is more than factor of 2 smaller than the threshold.
2. For most of the SVs, the value of the 95^{th} percentile SIS URE metric is relatively stable over the course of the year, as indicated by relatively small range bars.
3. The "best" SVs are those which cluster at the 1.0 m level and whose range variation is small.
4. The values for SVN 65/PRN 24 and SVN 72/PRN 8 are noticeably different than the other Block IIF SVs. These are the only Block IIF SVs operating on a Cesium frequency standard.

Table 3.2: Monthly 95^{th} Percentile Values of SIS RMS URE for All SVs in Meters

SVN	PRN	Block	Jan	Feb	Mar	Apr	May	Jun	Jul	Aug	Sep	Oct	Nov	Dec	2018
34	18	IIA	–	–	2.42	1.55	1.65	1.71	1.60	1.82	1.92	2.08	1.57	1.49	1.73
41	14	IIR	0.95	1.02	0.96	1.06	1.10	1.09	0.99	1.10	0.99	1.12	1.11	0.99	1.04
43	13	IIR	1.18	1.06	1.07	1.30	1.14	1.19	1.01	0.99	1.39	1.18	1.27	1.22	1.17
44	28	IIR	2.31	2.13	2.18	2.47	2.50	2.36	2.20	2.04	2.35	2.32	2.49	2.05	2.30
45	21	IIR	1.00	1.01	1.20	0.99	1.04	1.09	1.03	1.00	1.00	1.00	1.01	1.02	1.03
46	11	IIR	1.33	1.28	1.45	1.33	1.19	1.32	1.20	1.09	1.18	1.22	0.98	1.04	1.21
47	22	IIR	0.92	0.97	0.99	0.88	0.91	0.91	0.99	1.02	0.96	0.98	0.90	0.97	0.96
48	7	IIR-M	1.12	1.12	1.25	1.30	1.24	1.24	1.23	1.17	1.12	1.23	1.17	1.14	1.19
50	5	IIR-M	0.93	0.95	0.96	0.97	0.95	0.92	0.95	0.98	0.97	0.97	0.99	0.96	0.96
51	20	IIR	0.96	0.97	0.94	0.95	0.96	0.94	0.95	1.00	1.02	0.95	0.96	0.93	0.96
52	31	IIR-M	1.28	1.18	1.40	1.28	1.15	1.30	1.11	1.19	1.23	1.30	1.24	1.17	1.24
53	17	IIR-M	1.96	1.75	1.65	1.45	1.72	1.72	1.72	1.84	1.71	1.43	1.77	1.19	1.67
54	18	IIR	0.94	–	–	–	–	–	–	–	–	–	–	–	0.94
55	15	IIR-M	0.92	0.92	0.90	0.90	0.96	0.95	0.92	0.95	0.99	0.93	0.94	0.89	0.93
56	16	IIR	0.96	0.95	1.02	0.96	0.91	0.93	0.93	0.94	0.90	0.91	0.90	0.91	0.94
57	29	IIR-M	1.22	1.20	1.21	1.32	1.49	1.42	1.65	1.42	1.47	1.34	1.61	1.50	1.41
58	12	IIR-M	1.04	0.97	0.93	0.95	0.93	0.92	0.94	0.98	0.92	0.96	0.95	0.96	0.96
59	19	IIR	1.03	1.03	1.02	0.95	0.97	0.96	0.95	0.94	0.93	0.96	0.96	0.98	0.97
60	23	IIR	0.92	1.01	1.04	0.98	0.92	0.92	0.95	1.02	0.93	0.97	0.96	0.91	0.96
61	2	IIR	0.96	0.94	0.92	1.01	1.01	1.04	1.12	0.93	0.93	0.96	0.99	1.02	0.98
62	25	IIF	0.93	1.06	1.03	1.01	1.03	1.10	1.20	1.04	1.06	0.96	1.00	0.97	1.05
63	1	IIF	1.18	1.29	1.29	1.21	1.38	1.56	1.40	1.27	1.18	1.17	1.02	1.16	1.29
64	30	IIF	1.00	0.94	0.93	1.03	1.05	1.06	1.00	0.94	0.90	0.91	1.00	1.21	1.02
65	24	IIF	2.60	2.55	2.57	2.61	2.71	2.81	2.78	2.71	2.72	2.58	2.57	2.54	2.65
66	27	IIF	0.94	0.94	1.01	0.97	0.99	0.95	0.95	1.02	0.98	1.08	0.94	0.98	0.98
67	6	IIF	1.00	1.00	1.03	0.97	0.96	1.02	1.10	1.12	1.11	1.13	1.05	1.04	1.06
68	9	IIF	0.90	0.99	1.06	1.16	1.12	0.98	0.97	1.42	0.98	1.09	0.93	1.04	1.05
69	3	IIF	1.39	1.21	1.16	1.11	1.03	1.07	1.16	1.25	1.23	1.10	0.98	0.97	1.14
70	32	IIF	0.93	0.98	0.98	0.96	0.90	1.00	1.25	0.93	0.96	1.01	0.94	0.92	0.96
71	26	IIF	1.06	1.14	0.99	1.06	1.10	1.15	1.13	1.09	1.00	1.01	1.01	1.09	1.08
72	8	IIF	2.31	2.14	2.26	2.23	2.42	2.26	2.36	2.29	2.11	2.27	2.27	2.26	2.28
73	10	IIF	0.95	1.02	0.98	0.97	0.95	0.98	0.97	1.02	0.99	0.97	0.89	0.92	0.97
Block IIA			–	–	2.42	1.55	1.65	1.71	1.60	1.82	1.92	2.08	1.57	1.49	1.73
Block IIR			1.16	1.12	1.19	1.19	1.20	1.17	1.14	1.15	1.19	1.15	1.19	1.08	1.16
Block IIF			1.53	1.41	1.42	1.44	1.49	1.55	1.64	1.58	1.44	1.40	1.54	1.44	1.49
All SVs			1.28	1.22	1.29	1.30	1.34	1.34	1.35	1.33	1.32	1.27	1.31	1.22	1.30

Notes: Values not present indicate that the satellite was unavailable during this period. Months during which an SV was available for less than 25 days are shown shaded. Months with the highest SIS RMS URE for a given SV are colored red. The column labeled "2018" is the 95^{th} percentile over all the days in the year. The four rows at the bottom are the monthly 95^{th} percentile values over various sets of SVs.

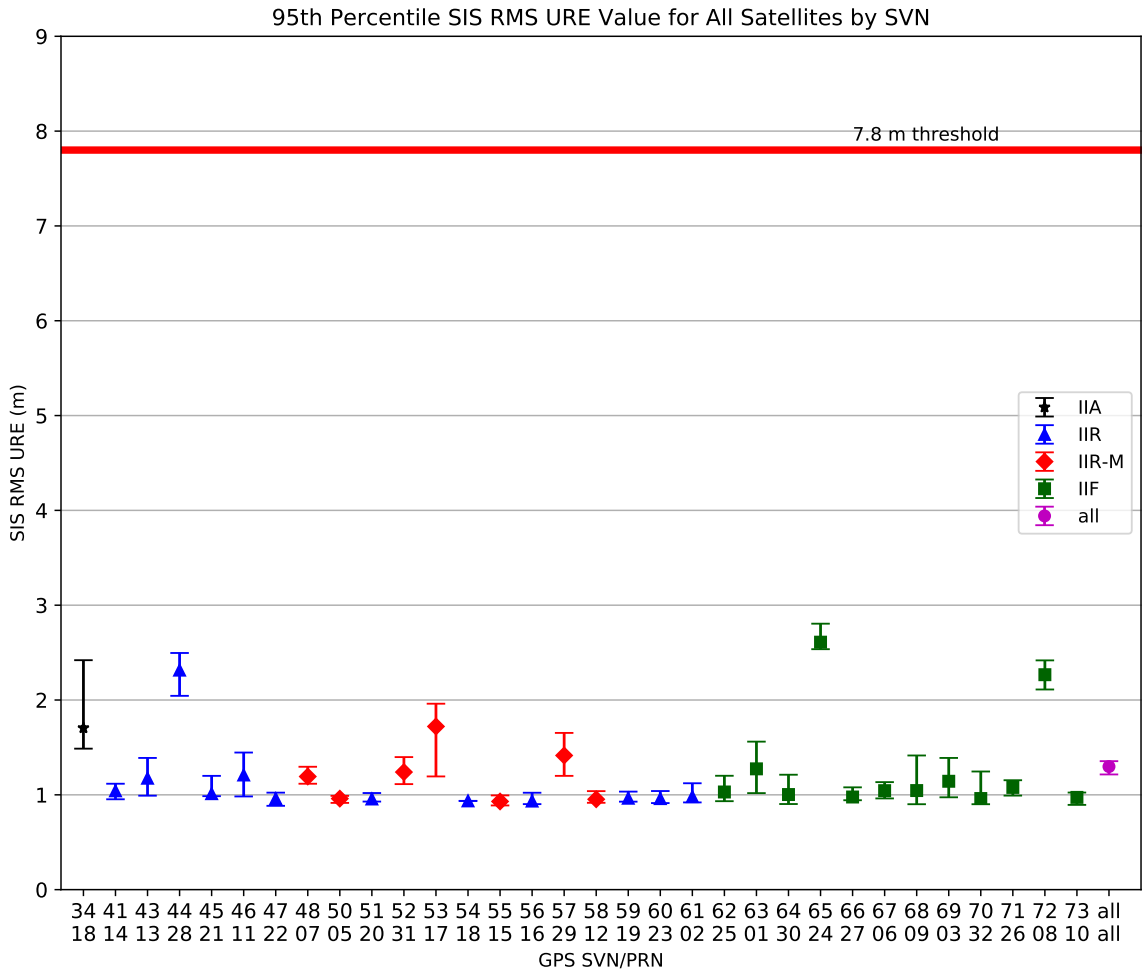

Figure 3.1: Range of the Monthly 95^{th} Percentile Values for All SVs

Notes: Each SVN with valid data is shown sequentially along the horizontal axis. The median value of the monthly 95^{th} percentile SIS URE is displayed as a point along the vertical axis. The minimum and maximum of the monthly 95^{th} percentile SIS URE for 2018 are shown by whiskers on the vertical bars. Color distinguishes between the Block IIA, Block IIR, Block IIR-M, and Block IIF SVs. The red horizontal line at 7.8 m indicates the upper bound given by the SPSPS08 Section 3.4 performance metric. The marker for "all" represents the monthly 95^{th} percentile values across all satellites.

3.2.1.1 An Alternate Method

As described toward the end of Section 3.2, the 95^{th} percentile Global Average URE values are formed by first deriving the Instantaneous RMS SIS URE at a succession of time points, then picking the 95^{th} percentile value over that set of results. This has the computational advantage that the Instantaneous RMS SIS URE is derived from a single equation errors in radial, along-track, cross-track, and time components at a given instant in time (as explained in Appendix B.1.2). However, it leads to a two-step implementation under which we first compute an RMS over a spatial area at a series of time points, then compute a 95^{th} percentile statistic over time.

Given current computation and storage capability, it is practical to compute a set of 95^{th} percentile URE values in which the Instantaneous SIS URE values are computed over a sufficiently dense grid and at fixed time intervals separated by uniform time steps throughout the period of interest. The 95^{th} percentile value is then selected from the entire set of Instantaneous SIS URE values. This was done in parallel to the process that produced the results shown in Section 3.2.1. The evaluation was performed at a 5 minute cadence. For each SV at each evaluation time, the point on the Earth immediately below the SV (nadir direction) was used as the center of the uniformly spaced 577 point grid that extends over the area visible to the satellite above the 5° minimum elevation angle. Further details on the implementation are provided in Appendix B.1.3.

Table 3.3 presents a summary of the results obtained by this alternate method. This table is in the same format as Table 3.2. Figure 3.2 (which is in the same format as Figure 3.1) presents the values in Table 3.3 in a graphical manner. The values in Table 3.3 are larger than the values in Table 3.2 by an average of 0.024 m. The maximum difference [alternate - original] for a given SV-month is +0.109 m; the minimum difference is -0.103 m.

Figure 3.3 is an illustration of the differences between the monthly 95^{th} percentile SIS URE values calculated by the two different methods. Each pair of monthly values for a given SV found in Table 3.2 and Table 3.3 were taken and the difference computed as the quantity [alternate - original]. The median, maximum, and minimum differences were then selected from each set and plotted in Figure 3.3. Figure 3.3 illustrates that the two methods agree to within 20 cm and generally a good deal less with the alternate method typically being a few cm larger.

None of the values in Table 3.3 exceed the threshold of 7.8 m. Therefore, the threshold is met for 2018 even under this alternate interpretation of the metric.

Table 3.3: Monthly 95^{th} Percentile Values of SIS Instantaneous URE for All SVs in Meters (via Alternate Method)

SVN	PRN	Block	Jan	Feb	Mar	Apr	May	Jun	Jul	Aug	Sep	Oct	Nov	Dec	2018
34	18	IIA	–	–	2.32	1.57	1.65	1.71	1.63	1.83	1.90	2.08	1.51	1.54	1.74
41	14	IIR	0.99	1.04	0.98	1.11	1.15	1.12	1.00	1.13	1.04	1.12	1.15	1.01	1.07
43	13	IIR	1.20	1.07	1.09	1.32	1.18	1.20	1.02	1.02	1.42	1.20	1.29	1.25	1.19
44	28	IIR	2.33	2.12	2.18	2.46	2.47	2.38	2.21	2.06	2.35	2.31	2.52	2.07	2.30
45	21	IIR	1.05	1.04	1.24	1.00	1.08	1.15	1.09	1.06	1.03	1.03	1.05	1.06	1.07
46	11	IIR	1.36	1.34	1.45	1.32	1.21	1.34	1.26	1.14	1.25	1.25	1.02	1.06	1.25
47	22	IIR	0.95	1.00	1.00	0.90	0.93	0.93	1.03	1.09	0.98	1.00	0.92	0.99	0.98
48	7	IIR-M	1.13	1.14	1.27	1.30	1.24	1.29	1.26	1.18	1.15	1.24	1.19	1.16	1.21
50	5	IIR-M	0.95	0.98	1.00	1.00	0.97	0.93	0.97	1.00	1.01	0.99	1.01	0.99	0.99
51	20	IIR	0.99	1.00	0.96	0.97	0.98	0.97	0.97	1.01	1.03	0.99	0.97	0.97	0.99
52	31	IIR-M	1.33	1.20	1.44	1.30	1.15	1.34	1.14	1.22	1.23	1.31	1.29	1.17	1.26
53	17	IIR-M	1.93	1.75	1.69	1.50	1.74	1.72	1.74	1.81	1.73	1.46	1.80	1.22	1.68
54	18	IIR	0.95	–	–	–	–	–	–	–	–	–	–	–	0.95
55	15	IIR-M	0.94	0.94	0.92	0.92	0.96	0.98	0.95	1.01	1.09	0.97	0.96	0.91	0.96
56	16	IIR	0.97	0.98	1.06	0.99	0.92	0.97	0.96	0.95	0.92	0.93	0.92	0.92	0.96
57	29	IIR-M	1.25	1.30	1.25	1.33	1.53	1.41	1.59	1.50	1.54	1.35	1.61	1.53	1.44
58	12	IIR-M	1.05	0.99	0.95	0.97	0.96	0.96	0.96	1.01	0.94	0.99	1.00	0.98	0.98
59	19	IIR	1.05	1.05	1.03	0.98	1.00	0.99	0.98	0.95	0.94	0.98	0.98	0.98	0.99
60	23	IIR	0.94	1.02	1.06	1.00	0.94	0.95	0.97	1.03	0.94	1.01	0.99	0.95	0.98
61	2	IIR	0.98	0.96	0.95	1.04	1.03	1.05	1.17	0.95	0.93	0.97	1.03	1.04	1.00
62	25	IIF	0.96	1.09	1.06	1.03	1.06	1.15	1.30	1.07	1.09	0.99	1.03	1.00	1.08
63	1	IIF	1.23	1.33	1.33	1.23	1.40	1.60	1.44	1.34	1.25	1.19	1.07	1.19	1.32
64	30	IIF	1.02	0.96	0.97	1.05	1.08	1.08	1.02	0.97	0.92	0.92	1.02	1.26	1.03
65	24	IIF	2.63	2.57	2.59	2.63	2.73	2.81	2.81	2.72	2.72	2.59	2.61	2.54	2.67
66	27	IIF	0.96	0.96	1.03	0.99	1.00	0.97	0.97	1.04	1.00	1.10	0.97	1.01	1.00
67	6	IIF	1.03	1.02	1.05	0.99	0.97	1.05	1.17	1.22	1.22	1.21	1.07	1.07	1.10
68	9	IIF	0.91	1.01	1.07	1.20	1.13	1.00	0.98	1.39	0.98	1.12	0.95	1.06	1.06
69	3	IIF	1.39	1.25	1.19	1.13	1.04	1.09	1.19	1.26	1.25	1.13	1.00	1.00	1.17
70	32	IIF	0.95	0.98	1.01	0.98	0.91	1.04	1.21	0.96	0.98	1.03	0.96	0.96	0.98
71	26	IIF	1.08	1.18	1.03	1.09	1.13	1.19	1.19	1.14	1.09	1.11	1.07	1.09	1.12
72	8	IIF	2.38	2.16	2.29	2.25	2.43	2.27	2.38	2.32	2.14	2.30	2.31	2.26	2.30
73	10	IIF	0.98	1.04	1.02	0.99	0.97	1.01	1.01	1.05	1.06	1.03	0.92	0.94	1.00
Block IIA			–	–	2.32	1.57	1.65	1.71	1.63	1.83	1.90	2.08	1.51	1.54	1.74
Block IIR			1.19	1.14	1.22	1.21	1.23	1.20	1.18	1.18	1.22	1.18	1.21	1.11	1.19
Block IIF			1.53	1.42	1.45	1.45	1.49	1.56	1.66	1.59	1.46	1.43	1.54	1.45	1.50
All SVs			1.30	1.25	1.31	1.31	1.35	1.36	1.38	1.36	1.35	1.30	1.32	1.24	1.32

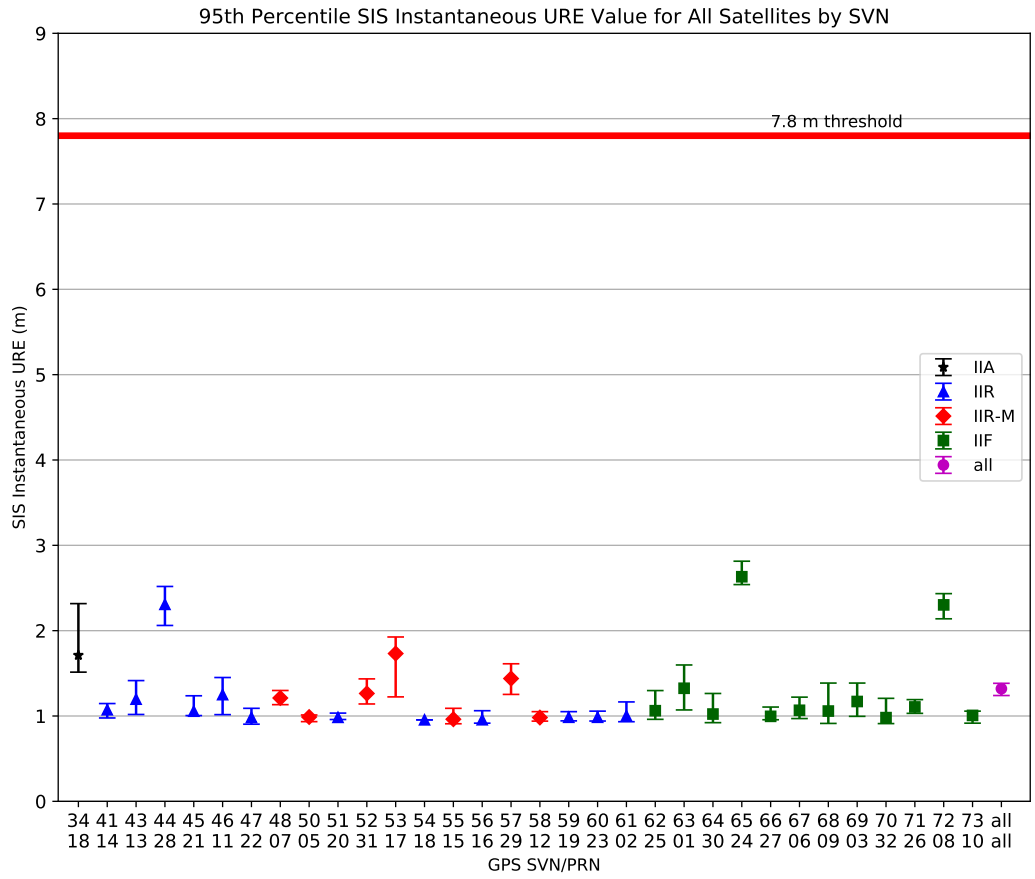

Figure 3.2: Range of the Monthly 95^{th} Percentile Values for All SVs (via Alternate Method)

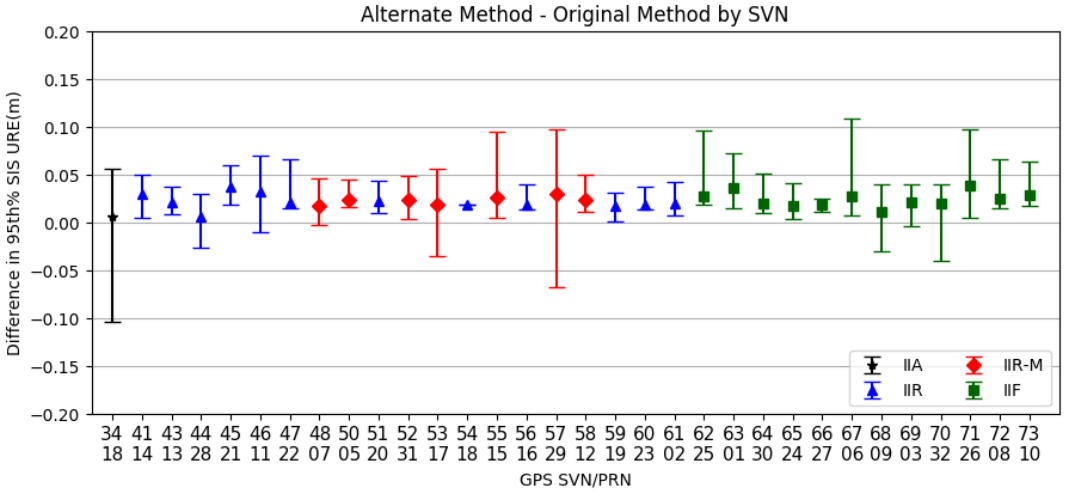

Figure 3.3: Range of Differences in Monthly Values for All SVs

3.2.2 URE at Any AOD

The next URE metric considered is the calculation of URE at any AOD. This is associated with the following SPSPS08 Section 3.4 metric:

- *"≤ 12.8 m 95% Global Average URE during Normal Operations at Any AOD"*

This metric may be decomposed in a manner similar to the previous metrics. The key differences are the term "at any AOD" and the change in the threshold values. The phrase "at any AOD" is interpreted to mean that at any AOD where sufficient data can be collected to constitute a reasonable statistical set the value of the required statistic should be ≤ 12.8 m. See Section 4.2 for a discussion of how the AOD is computed.

To examine this requirement, the set of 30 s Instantaneous RMS SIS URE values used in Section 3.2.1 was analyzed as described in Appendix A. In summary, the RMS SIS URE values for each satellite for the entire year were divided into bins based on 15 minute intervals of AOD. The 95^{th} percentile values for each bin were selected and the results were plotted as a function of the AOD.

Figures 3.4 through 3.7 show two curves: shown in blue is the 95^{th} percentile URE vs. AOD (in hours), and shown in green is the count of points in each bin as a function of AOD. For satellites that are operating on the normal pattern (roughly one upload per day), the count of points in each bin is roughly equal from the time the upload becomes available until about 24 hours AOD. In fact, the nominal number of points can be calculated by multiplying the number of expected 30 s estimates in a 15 minute bin (30 estimates per bin) by the number of days in the year. There are just under 11,000 points in each bin. This corresponds well to the plateau area of the green curve for the well-performing satellites (e.g. Figures 3.4 and 3.5). For satellites that are uploaded more frequently, the green curve will show a left-hand peak higher than the nominal count decreasing to the right. This is a result of the fact that there will be fewer points at higher AOD due to the more frequent uploads. The vertical scales on Figures 3.4 through 3.7 and the figures in Appendix A have been constrained to a constant value to aid in comparisons between the charts. In 2018, SVs with lower than nominal counts were SVN 54/PRN 18 (decommissioned in early March) and SVN 34/PRN 18 (brought back into the constellation in late March).

The representative best performers for Block IIR/IIR-M and Block IIF are shown in Figures 3.4 and 3.5. These are SVN 55/PRN 15 and SVN 62/PRN 25, respectively. For both blocks, several SVs have similar good results. Best performers exhibit a low and very flat distribution of AODs, and the UREs appear to degrade roughly linearly with time, at least to the point that the distribution (represented by the green curve) shows a marked reduction in the number of points.

Figures 3.6 and 3.7 show the worst performing (i.e. highest URE values) Block IIR/IIR-M and Block IIF SVs. These are SVN 44/PRN 28 and SVN 65/PRN 24, respectively. Note that the distribution of AOD samples for SVN 65/PRN 24 is biased toward shorter values of AOD, which indicates that uploads are occurring more frequently than once-per-day on occasion.

The plots for all satellites are contained in Appendix A. A review of the full set of plots leads to the conclusion that the rate of URE growth for the two Block IIF SVs using Cesium frequency standards is noticeably higher. While there are differences between individual satellites, all the results are well within the assertion for this metric.

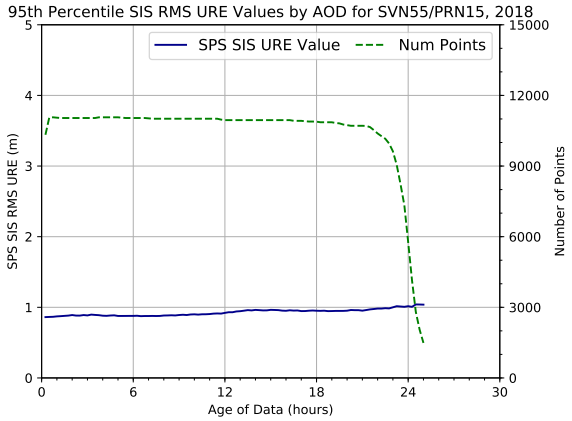

Figure 3.4: Best Performing Block IIR/IIR-M SV in Terms of URE over Any AOD

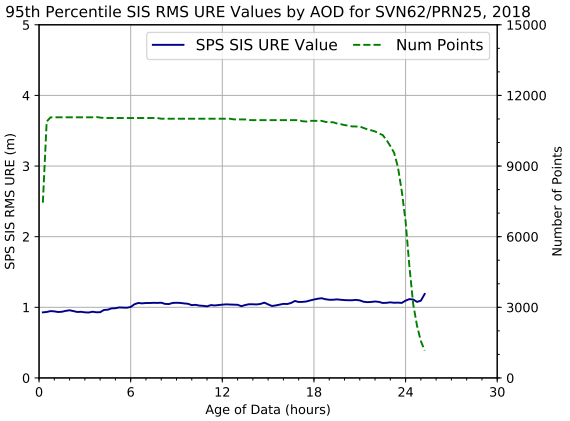

Figure 3.5: Best Performing Block IIF SV in Terms of URE over Any AOD

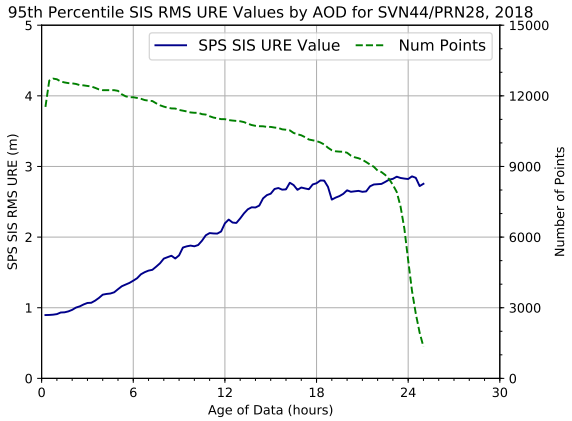

Figure 3.6: Worst Performing Block IIR/IIR-M SV in Terms of URE over Any AOD

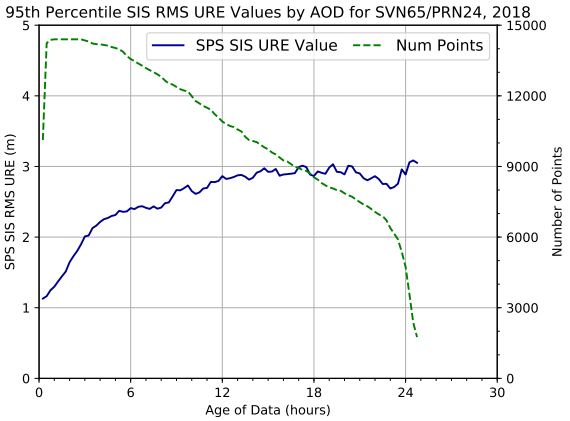

Figure 3.7: Worst Performing Block IIF SV in Terms of URE over Any AOD

3.2.3 URE at Zero AOD

Another URE metric considered is the calculation of URE at Zero Age of Data (ZAOD). This is associated with the SPSPS08 Section 3.4 metric:

- *"≤ 6.0 m 95% Global Average URE during Normal Operations at Zero AOD"*

This metric may be decomposed in a manner similar to the previous two metrics. The key differences are the term "at Zero AOD" and the change in the threshold values.

The broadcast ephemeris is never available to user equipment at ZAOD due to the delays inherent in preparing the broadcast ephemeris and uploading it to the SV. However, we can still make a case that this assertion is met by examining the 95^{th} percentile SIS RMS URE value at 15 minutes AOD. These values are represented by the left-most data point on the red lines shown in Figure 3.4 through Figure 3.7. The ZAOD values should be slightly better than the 15 minute AOD values, or at worst roughly comparable. Inspection of the 15 minute AOD values shows that the values for all SVs are well within the 6.0 m value associated with the assertion. Therefore the assertion is considered fulfilled.

3.2.4 URE Bounding

The SPSPS08 asserts the following requirements for single-frequency C/A code:

- *"≤ 30 m 99.94% Global Average URE during Normal Operations"*
- *"≤ 30 m 99.79% Worst Case Single Point Average URE during Normal Operations"*

Note that the first assertion states "Global Average URE", which is interpreted to mean the Instantaneous SIS RMS URE values, while the second assertion states "Worst Case Single Point Average URE", which is interpreted to mean the Instantaneous SIS URE. Therefore, to evaluate the first assertion, the 30 s Instantaneous SIS RMS URE values computed as part of the evaluation described in Section 3.2.1 were checked to determine whether any exceeded the 30 m threshold.

To evaluate the second assertion, the Instantaneous SIS URE values computed as part of the evaluation described in Section 3.2.1.1 were checked to determine whether any exceeded the 30 m threshold. This provides a set of 577 Instantaneous SIS URE values distributed across the area visible to a given SV at each 30 s epoch.(The 577 point grid and the distribution of the points is described in Appendix B.1.3.) This yields a set of over 60 million Instantaneous SIS URE values per SV per year. (577 values/300 s epoch * 288 30 s epochs/day * 365 days/year.)

However, there are limitations to our technique of estimating UREs that are worth noting such as fits across orbit/clock discontinuities, thrust events, and clock run-offs. These are discussed in Appendix B.1.4. As a result of these limitations, a set of observed range deviations (ORDs) was also examined as a cross-check.

The ORDs were formed using the NGA observation data collected to support the position accuracy analysis described in Section 3.6.4. In the case of ORDs, the observed range is differenced from the range predicted by the geometric distance from the known station position to the SV location derived from the broadcast ephemeris. The ORDs are similar to the Instantaneous SIS URE in that both represent the error along a specific line-of-sight. However, the ORDs are not true SIS measurements due to the presence of residual atmospheric effects and receiver noise. The selected stations are geographically distributed such that at least two sets of observations are available for each SV at all times. As a result, any actual SV problems that would lead to a violation of this assertion will produce large ORDs from multiple stations.

None of these three checks found any values that exceeded the 30m threshold. Based on these results, these assertions are considered satisfied.

3.2.5 URRE Over All AOD

The performance standard provides the following assertion for the user range rate error (URRE).

- *"≤0.006 m/sec 95% Global Average URRE over any 3-second interval during Normal Operations at Any AOD"*

This is subject to the same general constraints from SPSPS08 Section 3.4 as the URE assertions.

The URRE cannot be evaluated by comparison of the BCP to the TCP. This is due to two factors:

1. as described in Note 1 to SPS PS Table 3.4-2, the primary contributing factor to the URRE is the noise from the SV frequency standards (clocks), and
2. the assertion states "over any 3-second interval".

In the precise orbits used for the TCP, the noise due to the SV clocks is smoothed over long periods. As a result, the comparison of BCP and TCP derivatives will not reveal short term (i.e. 3 s) changes in SV clock behavior.

To address this, a different evaluation process is used. This process uses the TCP along with the measured carrier phase observations and the known station positions to form the URRE values by differencing the range errors. The carrier phase observations have much lower noise than the pseudorange values, and since both phase and range are based on the same SV clock and the same receiver clock, the result will be a more precise measurement of the range rate error.

The observation data from the NGA MSN is collected at a 1.5 s rate. This rate allows examination of the URRE at the desired cadence. Dual-frequency observations are used in order to reduce ionospheric errors and come as close as practical to the constraint that the results are to be based on SIS. In a similar manner, tropospheric models based on weather observed at the stations is used to reduce tropospheric errors.

These steps are all helpful, but the individual observations retain enough noise to be unable to verify the assertion based on data from single receivers. However, there are additional conditions that provide a way to further reduce the effects of the noise in the data.

- Note 2 to SPS PS Table 3.4-2 states that all correlated errors should be ignored. Therefore any constant biases in the URRE values for a given SV-receiver pass may be removed.
- The assertion states that the URRE is to be considered as a global average. SV clock errors will have constant effect across the area that can view the SV. Therefore, URRE errors for a specific SV-epoch will be constant across the field of view. This is not true for orbit errors where the effect on URE will vary from station-to-station due to geometry. However, the URRE effect on orbit errors over a 3 s interval will be negligible (assuming no thrust events). This allows us to average all the URRE values for a given SV-epoch in order to reduce the noise in the URRE samples.

Table 3.4 contains the monthly 95^{th} percentile values of the URRE based on the assumptions and constraints described above. For each SV, the worst value across the year is marked in red. Figure 3.8 provides a summary of these results for the entire constellation. For each SV, shown along the horizontal axis, the monthly values from Table 3.4 are plotted. These results are conservative in the sense that there has been no attempt to account for receiver noise in the observation data.

No values in Table 3.4 exceed 0.006 m/sec and so this requirement is considered met for 2018.

3.2.6 URAE Over All AOD

The performance standard provides the following assertion for the user range acceleration error (URAE).

- *"$\leq$0.002 m/sec/sec 95% Global Average URAE over any 3-second interval during Normal Operations at Any AOD"*

This is subject to the same general constraints from and SPSPS08 Section 3.4 as the URE assertions.

The URAE values were obtained by differencing the URRE values derived in support of the previous section. Table 3.5 contains the monthly 95^{th} percentile values of the URRE based on the assumptions and constraints described above. For each SV, the worst value across the year is marked in red. Figure 3.9 provides a summary of these results for the entire constellation. No values exceed 0.002 m/sec/sec and so this requirement is considered met for 2018.

Table 3.4: Monthly 95^{th} Percentile Values of URRE for All SVs in mm/s

SVN	PRN	Block	Jan	Feb	Mar	Apr	May	Jun	Jul	Aug	Sep	Oct	Nov	Dec
34	18	IIA	–	–	3.35	3.30	3.28	3.29	3.33	3.30	3.48	3.46	3.47	3.50
41	14	IIR	2.58	2.59	2.57	2.47	2.40	2.41	2.41	2.42	2.60	2.61	2.55	2.78
43	13	IIR	2.57	2.63	2.69	2.68	2.67	2.61	2.47	2.52	2.76	2.85	2.78	2.62
44	28	IIR	2.62	2.60	2.54	2.46	2.47	2.49	2.50	2.51	2.67	2.67	2.65	2.97
45	21	IIR	3.08	2.90	2.72	2.75	2.88	2.98	2.86	2.74	2.73	2.72	2.79	3.34
46	11	IIR	3.06	3.02	2.85	2.88	2.90	2.88	2.91	2.87	2.99	2.93	2.93	2.92
47	22	IIR	2.50	2.57	2.40	2.40	2.31	2.33	2.39	2.44	2.49	2.44	2.34	2.50
48	7	IIR-M	2.56	2.55	2.52	2.57	2.67	2.71	2.65	2.58	2.66	2.63	2.69	2.83
50	5	IIR-M	3.02	3.25	3.08	2.89	2.75	2.74	2.94	3.14	3.08	3.00	2.77	3.01
51	20	IIR	2.74	2.73	2.66	2.65	2.54	2.54	2.57	2.58	2.60	2.56	2.54	2.66
52	31	IIR-M	2.52	2.48	2.36	2.38	2.38	2.39	2.34	2.31	2.38	2.51	2.50	2.66
53	17	IIR-M	2.91	2.91	2.90	2.86	2.77	2.69	2.64	2.63	2.95	3.11	3.03	3.26
54	18	IIR	2.76	–	–	–	–	–	–	–	–	–	–	–
55	15	IIR-M	2.64	2.66	2.61	2.64	2.58	2.56	2.50	2.53	2.68	2.72	2.66	2.72
56	16	IIR	3.03	3.04	2.86	2.76	2.67	2.64	2.73	2.82	2.80	2.78	2.84	3.03
57	29	IIR-M	2.51	2.51	2.49	2.58	2.55	2.50	2.45	2.48	2.66	2.64	2.57	2.56
58	12	IIR-M	3.07	3.10	2.93	2.88	2.85	2.88	2.95	3.01	2.96	2.92	2.88	2.93
59	19	IIR	2.72	2.72	2.60	2.75	2.71	2.70	2.73	2.74	2.73	2.76	2.73	2.76
60	23	IIR	2.47	2.46	2.44	2.50	2.49	2.49	2.47	2.49	2.56	2.56	2.51	2.57
61	2	IIR	2.61	2.61	2.62	2.46	2.38	2.40	2.41	2.39	2.72	2.76	2.71	3.05
62	25	IIF	2.31	2.28	2.24	2.24	2.17	2.18	2.18	2.14	2.39	2.35	2.32	2.35
63	1	IIF	2.27	2.27	2.25	2.25	2.23	2.23	2.25	2.24	2.36	2.36	2.39	2.43
64	30	IIF	1.87	1.88	1.87	1.93	1.90	1.90	1.88	1.87	2.09	2.10	1.94	2.00
65	24	IIF	4.78	4.81	4.78	4.82	4.83	4.88	4.87	4.89	4.97	5.00	5.00	4.98
66	27	IIF	2.18	2.18	2.09	2.10	2.05	2.07	2.07	2.07	2.17	2.13	2.13	2.21
67	6	IIF	1.98	1.98	1.79	1.81	1.77	1.78	1.75	1.75	1.89	1.89	1.86	2.08
68	9	IIF	1.98	1.99	1.88	1.89	1.87	1.88	1.84	1.85	1.96	1.97	1.96	1.93
69	3	IIF	2.06	2.04	1.93	1.96	1.92	1.92	1.92	1.93	2.04	1.99	2.00	2.05
70	32	IIF	2.05	2.07	2.03	2.03	1.94	1.95	1.98	1.98	2.08	2.09	2.04	2.23
71	26	IIF	1.93	1.92	1.81	1.88	1.86	1.88	1.86	1.83	1.89	1.90	1.86	2.11
72	8	IIF	3.34	3.32	3.29	3.35	3.36	3.39	3.38	3.40	3.47	3.47	3.46	3.63
73	10	IIF	1.86	1.86	1.78	1.81	1.82	1.85	1.88	1.84	2.11	2.07	1.95	2.03
All SVs			2.62	2.63	2.57	2.58	2.55	2.56	2.56	2.56	2.68	2.68	2.63	2.76

Notes: Values not present indicate that the satellite was unavailable during this period. Months during which an SV was available for less than 25 days are shown shaded. Months with the highest value for a given SV are colored red.

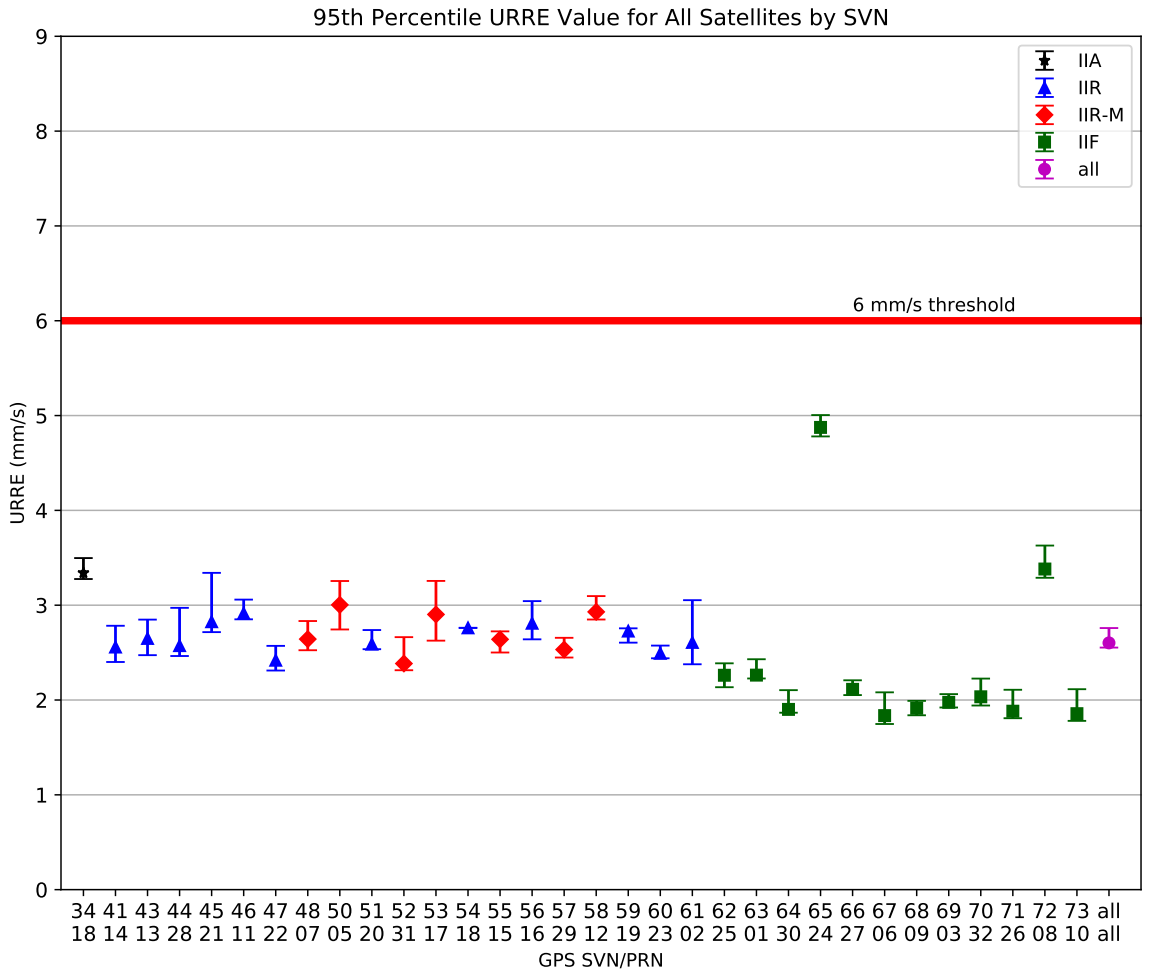

Figure 3.8: Range of the Monthly URRE 95^{th} Percentile Values for All SVs

Notes: Each SVN with valid data is shown sequentially along the horizontal axis. The median value of the monthly 95^{th} percentile URRE is displayed as a point along the vertical axis. The minimum and maximum of the monthly 95^{th} percentile URRE for 2018 are shown by whiskers on the vertical bars. Color distinguishes between the Block IIA, Block IIR, Block IIR-M, and Block IIF SVs. The red horizontal line at 6.0 mm/s indicates the upper bound given by the SPSPS08 Section 3.4 performance metric. The marker for "all" represents the monthly 95^{th} percentile values across all satellites.

Table 3.5: Monthly 95^{th} Percentile Values of URAE for All SVs in mm/s^2

SVN	PRN	Block	Jan	Feb	Mar	Apr	May	Jun	Jul	Aug	Sep	Oct	Nov	Dec
34	18	IIA	–	–	1.26	1.30	1.29	1.29	1.28	1.28	1.28	1.28	1.28	1.28
41	14	IIR	0.78	0.78	0.75	0.78	0.76	0.76	0.77	0.77	0.76	0.76	0.76	0.76
43	13	IIR	0.80	0.80	0.79	0.81	0.80	0.81	0.80	0.80	0.81	0.82	0.81	0.79
44	28	IIR	0.80	0.80	0.77	0.80	0.79	0.79	0.80	0.80	0.79	0.78	0.78	0.78
45	21	IIR	0.81	0.79	0.74	0.77	0.78	0.79	0.78	0.76	0.75	0.74	0.75	0.78
46	11	IIR	0.82	0.81	0.78	0.81	0.80	0.81	0.81	0.81	0.82	0.82	0.81	0.82
47	22	IIR	0.73	0.74	0.70	0.74	0.72	0.72	0.73	0.74	0.72	0.72	0.70	0.72
48	7	IIR-M	0.79	0.78	0.73	0.77	0.76	0.77	0.76	0.76	0.76	0.75	0.78	0.77
50	5	IIR-M	0.84	0.87	0.83	0.82	0.80	0.80	0.82	0.85	0.83	0.83	0.80	0.83
51	20	IIR	0.76	0.76	0.73	0.76	0.74	0.74	0.74	0.75	0.75	0.74	0.73	0.74
52	31	IIR-M	0.74	0.74	0.71	0.74	0.72	0.73	0.73	0.72	0.72	0.76	0.74	0.73
53	17	IIR-M	0.78	0.77	0.74	0.79	0.77	0.76	0.76	0.76	0.75	0.77	0.77	0.76
54	18	IIR	0.82	–	–	–	–	–	–	–	–	–	–	–
55	15	IIR-M	0.76	0.77	0.74	0.77	0.76	0.75	0.74	0.75	0.75	0.76	0.76	0.76
56	16	IIR	0.79	0.80	0.75	0.77	0.75	0.76	0.78	0.78	0.76	0.76	0.76	0.77
57	29	IIR-M	0.74	0.73	0.71	0.76	0.74	0.73	0.73	0.73	0.73	0.73	0.72	0.73
58	12	IIR-M	0.77	0.78	0.73	0.78	0.76	0.77	0.78	0.78	0.75	0.75	0.75	0.75
59	19	IIR	0.78	0.78	0.75	0.79	0.77	0.78	0.78	0.77	0.77	0.77	0.76	0.78
60	23	IIR	0.76	0.76	0.72	0.78	0.76	0.76	0.76	0.76	0.76	0.75	0.75	0.74
61	2	IIR	0.72	0.72	0.69	0.73	0.72	0.72	0.72	0.72	0.74	0.73	0.73	0.72
62	25	IIF	0.70	0.70	0.67	0.72	0.71	0.72	0.72	0.71	0.72	0.71	0.69	0.70
63	1	IIF	0.75	0.75	0.71	0.75	0.74	0.75	0.74	0.74	0.74	0.75	0.75	0.75
64	30	IIF	0.69	0.69	0.66	0.70	0.68	0.69	0.68	0.69	0.72	0.72	0.68	0.68
65	24	IIF	1.63	1.64	1.62	1.64	1.65	1.66	1.66	1.67	1.69	1.69	1.69	1.69
66	27	IIF	0.72	0.72	0.69	0.72	0.72	0.72	0.72	0.72	0.72	0.72	0.70	0.72
67	6	IIF	0.70	0.70	0.65	0.69	0.68	0.68	0.68	0.68	0.68	0.68	0.68	0.68
68	9	IIF	0.70	0.71	0.67	0.72	0.70	0.71	0.71	0.71	0.70	0.71	0.70	0.69
69	3	IIF	0.68	0.68	0.65	0.70	0.68	0.68	0.68	0.69	0.68	0.68	0.68	0.67
70	32	IIF	0.69	0.69	0.65	0.70	0.68	0.69	0.69	0.69	0.68	0.68	0.67	0.68
71	26	IIF	0.71	0.71	0.67	0.70	0.69	0.70	0.69	0.69	0.70	0.70	0.69	0.71
72	8	IIF	1.17	1.17	1.15	1.17	1.18	1.19	1.19	1.20	1.20	1.21	1.21	1.22
73	10	IIF	0.70	0.70	0.66	0.69	0.68	0.68	0.68	0.68	0.73	0.73	0.69	0.67
All SVs			0.80	0.80	0.78	0.82	0.81	0.81	0.81	0.81	0.81	0.81	0.80	0.81

Notes: Values not present indicate that the satellite was unavailable during this period. Months during which an SV was available for less than 25 days are shown shaded. Months with the highest value for a given SV are colored red.

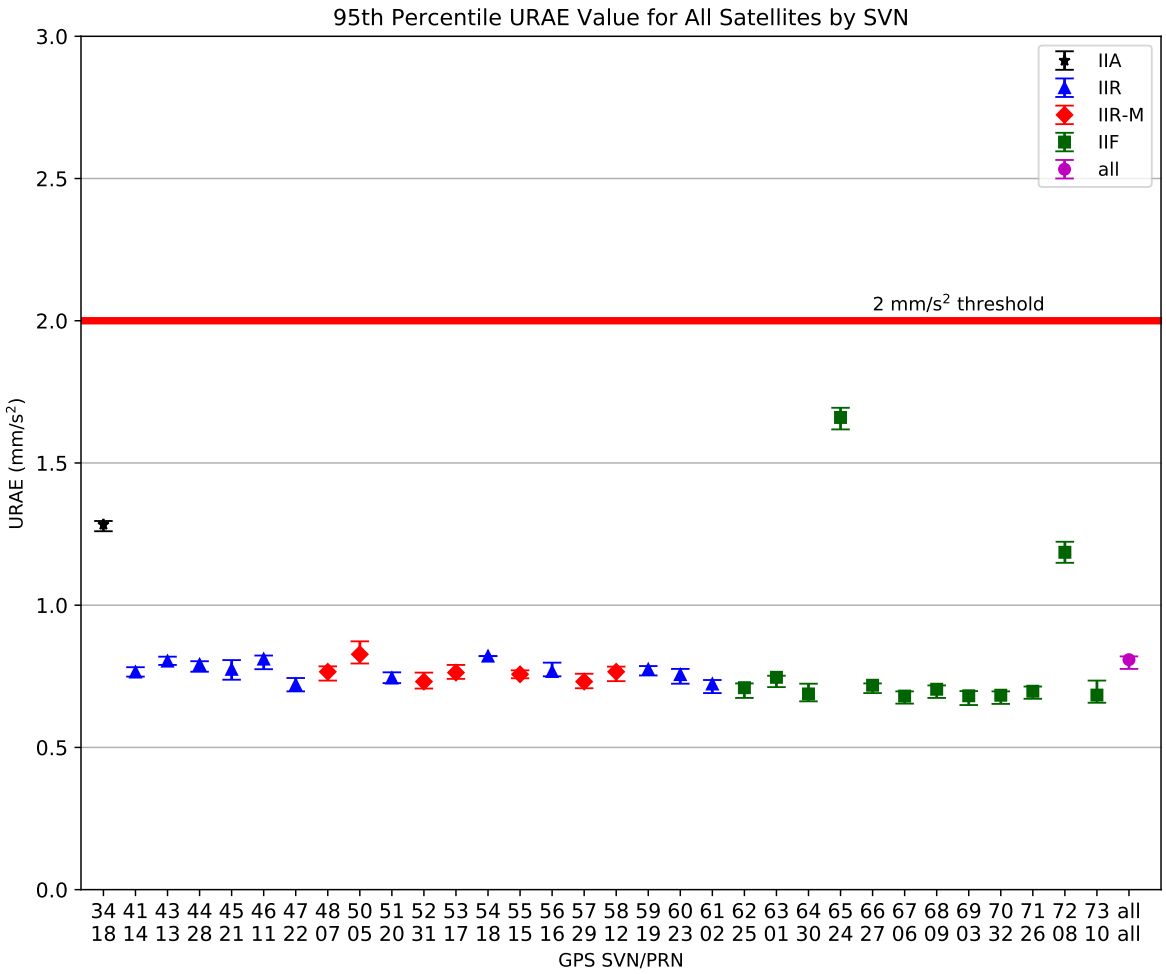

Figure 3.9: Range of the Monthly URAE 95^{th} Percentile Values for All SVs

Notes: Each SVN with valid data is shown sequentially along the horizontal axis. The median value of the monthly 95^{th} percentile URAE is displayed as a point along the vertical axis. The minimum and maximum of the monthly 95^{th} percentile URAE for 2018 are shown by whiskers on the vertical bars. Color distinguishes between the Block IIA, Block IIR, Block IIR-M, and Block IIF SVs. The red horizontal line at 2.0 mm/s^2 indicates the upper bound given by the SPSPS08 Section 3.4 performance metric. The marker for "all" represents the monthly 95^{th} percentile values across all satellites.

3.2.7 UTC Offset Error Accuracy

The SPS PS provides the following assertion regarding the UTC offset error (UTCOE) Accuracy:

- *"≤ 40 nsec 95% Global Average UTCOE during Normal Operations at Any AOD"*

The conditions and constraints state that this assertion should be true for any healthy SPS SIS.

This assertion was evaluated by calculating the global average UTCOE at each 15 minute interval in the year. The GPS-UTC offset available to the user was calculated based on the GPS broadcast navigation message data available from the SV at that time. The GPS-UTC offset truth information was provided by the USNO daily GPS-UTC offset values. The USNO value for GPS-UTC at each evaluation epoch was derived from a multi-day spline fit to the daily truth values.

The selection and averaging algorithms are a key part of this process. The global average at each 15 minute epoch is determined by evaluating the UTCOE across the surface of the earth at each point on a 111 km × 111 km grid. (This grid spacing corresponds to roughly 1° at the Equator.) At each grid point, the algorithm determines the set of SVs visible at or above the 5° minimum elevation angle that are broadcasting a healthy indication in the navigation message. For each of these SVs, the UTC offset information in subframe 4 page 18 of the navigation message is compared to determine the data set that has an epoch time (t_{ot}) that is the latest of those that fall in the range *current time* $\leq t_{ot} \leq$ *current time + 72 hours*. These data are used to form the UTC offset and UTCOE for that time-grid point. (The 72 hour value is derived from the 144 hour fit interval shown in IS-GPS-200 Table 20-XIII [2].)

The global averages at each evaluation epoch are assembled into monthly data sets. The 95^{th} percentile values are then selected from these sets.

Table 3.6 provides the results for each month of 2018. None of these values exceed the assertion of 40 nsec. Therefore the assertion is verified for 2018. Figure 3.10 provides additional supporting information in the form of a time-history of global average UTCOE values at each 15 minute epoch for the year.

Table 3.6 contains a noticeably larger value for July than any other month. There is also an excursion in the daily values in Figure 3.10. A review of the USNO daily GPS-UTC offset values shows that the value for 16 July 2018 was based on roughly half the usual number of data points. This led to daily values for the offset and slope that are clearly different than the surrounding days. Given that the result is still an order of magnitude better than the assertion, this was not examined further.

Table 3.6: 95^{th} Percentile Global Average UTCOE for 2018

Month	**95$^{\text{th}}$ Percentile Global Avg. UTCOE (nsec)**
Jan.	1.240
Feb.	1.717
Mar.	1.375
Apr.	1.616
May	1.122
Jun.	1.998
Jul.	3.370
Aug.	1.449
Sep.	1.413
Oct.	1.486
Nov.	1.575
Dec.	1.550

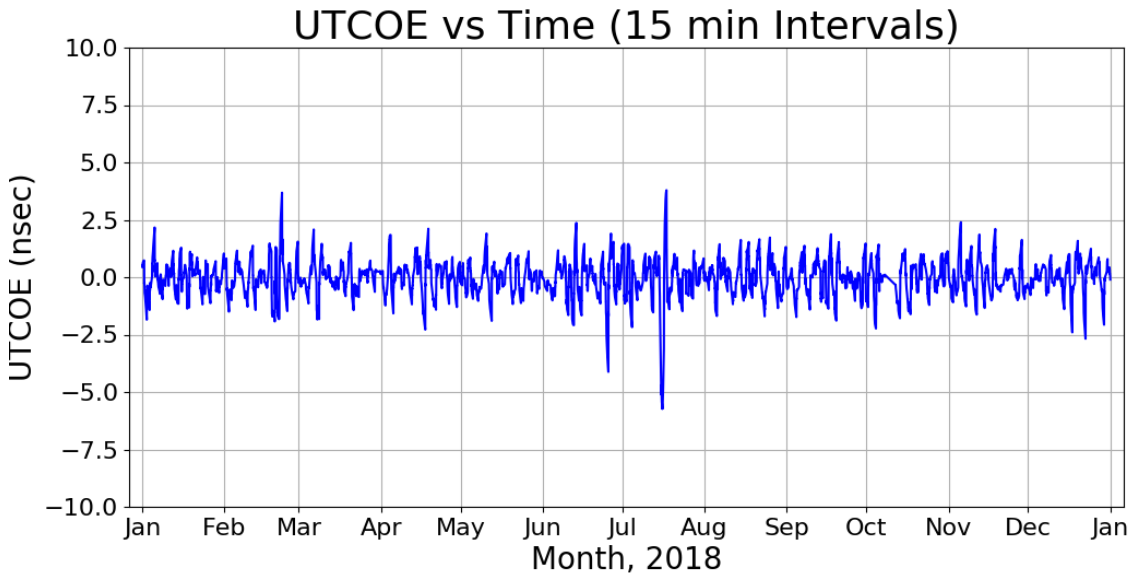

Figure 3.10: UTCOE Time Series for 2018

3.3 SIS Integrity

3.3.1 URE Integrity

Under the heading of SIS Integrity, the SPSPS08 makes the following assertion in Section 3.5.1, Table 3.5-1:

- *"$\leq 1 \times 10^{-5}$ Probability Over Any Hour of the SPS SIS Instantaneous URE Exceeding the NTE Tolerance Without a Timely Alert During Normal Operations"*

The associated conditions and constraints include a limitation to healthy SIS, a Not to Exceed (NTE) tolerance ±4.42 times the upper bound on the user range accuracy (URA) currently broadcast, and a worst case for a delayed alert of 6 hours.

The reference to "a Timely Alert" in the assertion refers to any of a number of ways to issue an alert to the user through the GPS signal or navigation message. See SPSPS08 Section A.5.5 for a complete description.

To estimate the worst-case probability of users experiencing misleading signal information (MSI), note that immediately below SPSPS08 Table 3.5-1 is an explanation that for a 32 SV constellation (full broadcast almanac) the corresponding average annual number of SPS SIS Instantaneous URE integrity losses is 3. Assuming each of the 3 losses lasts no more than 6 hours over one year, the fraction of time in which MSI will occur is 0.002.

This assertion was verified using two methods:

- The Instantaneous SIS URE values at the worst case location in view of each SV at each 30 s interval were examined to determine the number of values that exceed ±4.42 times the URA. (The worst location was selected from the set of Instantaneous SIS URE values computed for each SV as described in Section 3.2.1.1.)
- ORDs from a network of tracking stations were examined to determine the number of values that exceed ±4.42 times the URA.

Two methods were used due to the fact that each method may result in false positives in rare cases. For example, the URE values may be incorrect near discontinuities in the URE (as described in Appendix B). Similarly, the ORD values may be incorrect due to receiver or reception issues. Therefore, all reported violations are examined manually to determine whether a violation actually occurred, and if so, the extent of the violation.

Screening the 30 s Instantaneous SIS URE values and the ORD data did not reveal any events for which this threshold was exceeded. Therefore the assertion is verified for 2018.

3.3.2 UTCOE Integrity

The SPS PS provides the following assertion regarding UTCOE Integrity in Section 3.5.4:

- *"$\leq$ 1 $\times$ 10^{-5} Probability Over Any Hour of the SPS SIS Instantaneous UTCOE Exceeding the NTE Tolerance Without A Timely Alert during Normal Operations"*

The associated conditions and constraints include a limitation to healthy SIS, a NTE tolerance of ±120 nsec, and the note that this holds true for any healthy SPS SIS. The reference to "a Timely Alert" in the assertion refers to any of a number of ways to issue an alert. See SPSPS08 Section A.5.5 for a complete description.

This assertion was evaluated by calculating the UTC offset for the navigation message subframe 4 page 18 data broadcast by each SV transmitting a healthy indication in the navigation message at each 15 minute interval. As in Section 3.2.7, only UTC offset information with an epoch time (t_{ot}) that is in the range *current time* $\leq t_{ot} \leq$ *current time + 72 hours* were considered valid. That offset was used to compute the corresponding UTCOE from truth data obtained from USNO [7]. Any UTCOE values that exceed the NTE threshold of ±120 nsec were investigated to determine if they represented actual violations of the NTE threshold or were artifacts of data processing.

No values exceeding the NTE threshold were found in 2018. The value farthest from zero for the year was -5.729 nsec (during July). Therefore the assertion is verified for 2018.

3.4 SIS Continuity

3.4.1 Unscheduled Failure Interruptions

The SIS Continuity metric is stated in SPSPS08 Table 3.6-1 as follows:

- *"≥ 0.9998 Probability Over Any Hour of Not Losing the SPS SIS Availability from a Slot Due to Unscheduled Interruption"*

The conditions and constraints note the following:

- The empirical estimate of the probability is calculated as an average over all slots in the 24-slot constellation, normalized annually.
- The SPS SIS is available from the slot at the start of the hour.

The notion of SIS continuity is slightly more complex for an expandable slot, because multiple SVs are involved. Following SPSPS08 Section A.6.5, a loss of continuity is considered to occur when,

> *"The expandable slot is in the expanded configuration, and either one of the pair of satellites occupying the orbital locations defined in Table 3.2-2 for the slot loses continuity."*

Hence, the continuity of signal of the expanded slot will be determined by whether either SV loses continuity.

Another point is that there is some ambiguity in this metric, which is stated in terms of "a slot" while the associated conditions and constraints note that this is an average over all slots. Therefore both the per-slot and 24-slot constellation averages have been computed. As discussed below, while the per-slot values are interesting, the constellation average is the correct value to compare to the performance standard metric.

Three factors must be considered in looking at this metric:

1. We must establish which SVs were assigned to which slots during the period of the evaluation.
2. We must determine when SVs were not transmitting (or not transmitting a PRN available to users).
3. We must determine which interruptions were scheduled vs. unscheduled.

The derivation of the SV/slot assignments is described in Appendix E.

For purposes of this report, interruptions were considered to have occurred if one or more of the SVs assigned to the given slot are unhealthy in the sense of SPSPS08 Section 2.3.2.

The following specific indications were considered:

- If the health bits in navigation message subframe 1 are set to anything other than all zeros.
- If an appropriately distributed worldwide network of stations failed to collect any pseudorange data sets for a given measurement interval.

The latter case (failure to collect any data) indicates that the satellite signal was removed from service (e.g. non-standard code or some other means). The NGA MSN provides at least two-station visibility (and at least 90% three-station visibility) with redundant receivers at each station, both continuously monitoring up to 12 SVs in view. Therefore, if no data for a satellite are received for a specific time, it is highly likely that the satellite was not transmitting on the assigned PRN at that time. The 30 s Receiver Independent Exchange format (RINEX) [8] observation files from this network were examined for each measurement interval (i.e. every 30 s) for each SV. If at least one receiver collected a pseudorange data set on L1 C/A, L1 P(Y), and L2 P(Y) with a signal-to-noise level of at least 25 dB-Hz on all frequencies and no loss-of-lock flags, the SV is considered trackable at that moment. In addition, the 30 s IGS data collected to support the position accuracy estimates (Section 3.6.4) were examined in a similar fashion to guard against any MSN control center outages that could have led to missing data across multiple stations simultaneously. This allows us to define an epoch-by-epoch availability for each satellite. Then, for each slot, each hour in the year was examined, and if an SV occupying the slot was not available at the start of the hour, the hour was not considered as part of the evaluation of the metric. If the slot was determined to be available, then the remaining data was examined to determine if an outage occurred during the hour.

The preceding criteria were applied to determine times and durations of interruptions. After this, the Notice Advisories to Navstar Users (NANUs) effective in 2018 were reviewed to determine which of these interruptions could be considered scheduled interruptions as defined in SPSPS08 Section 3.6. The scheduled interruptions were removed from consideration for purposes of assessing continuity of service. When a slot was available at the start of an hour but a scheduled interruption occurred during the hour, the hour was assessed based on whether data were available prior to the scheduled outage.

Scheduled interruptions as defined in the ICD-GPS-240 [9] have a nominal notification time of 96 hours prior to the outage. Following the SPSPS08 Section 2.3.5, scheduled interruptions announced 48 hours in advance are not to be considered as contributing to the loss of continuity. So to contribute to a loss of continuity, the notification time for a scheduled interruption must occur less than 48 hours in advance of the interruption. In the case of an interruption not announced in a timely manner, the time from the start of the interruption to the moment 48 hours after notification time can be considered as a potential unscheduled interruption (for continuity purposes).

The following NANU types are considered to represent (or modify) scheduled interruptions (assuming the 48-hour advance notice is met):

- FCSTDV - Forecast Delta-V
- FCSTMX - Forecast Maintenance
- FCSTEXTD - Forecast Extension
- FCSTRESCD - Forecast Rescheduled
- FCSTUUFN - Forecast Unusable Until Further Notice

The FCSTSUMM (Forecast Summary) NANU that occurs after the outage is referenced to confirm the actual beginning and ending time of the outage.

For scheduled interruptions that extend beyond the period covered by a FCSTDV or FCSTMX NANU, the uncovered portion will be considered an unscheduled interruption. However, if a FCSTEXTD NANU extending the length of a scheduled interruption is published 48 hours in advance of the effective time of extension, the interruption will remain categorized as scheduled. It is worth reiterating that, for the computation of the metric, only those hours for which a valid SIS is available from the slot at the start of the hour are actually considered in the computation of the values.

The results of the assessment of SIS continuity are summarized in Table 3.7. The metric is averaged over the constellation, therefore the value in the bottom row (labeled "All Slots") must be greater than 0.9998 in order to meet the assertion.

To put this in perspective, there are 8760 hours in a year (8784 for a leap year). The required probability of not losing SPS SIS availability is calculated as an average over all slots in the 24-slot constellation, which implies that the maximum number of unscheduled interruptions over the year is given by $8760 \times (1 - 0.9998) \times 24 = 42$ unscheduled hours that experience interruptions. This is less than two unscheduled interruptions per SV per year but allows for the possibility that some SVs may have no unscheduled interruptions while others may have more than one.

Returning to Table 3.7, across the slots in the Expanded 24 constellation the total number of hours lost was 4. This is smaller than the maximum number of hours of unscheduled interruptions (42) available to meet the metric and leads to empirical value for the fraction of hours in which SPS SIS continuity was maintained of 0.999981. Therefore, this assertion is considered fulfilled in 2018.

Table 3.7: Probability Over Any Hour of Not Losing Availability Due to Unscheduled Interruption for 2018

Plane-Slot	# of Hours with the SPS SIS available at the start of the hour[b]	# of Hours with Unscheduled Interruption[c]	Fraction of Hours in Which Availability was Not Lost
A1	8760	0	1.000000
A2	8760	0	1.000000
A3	8760	1	0.999886
A4	8760	0	1.000000
B1[a]	8756	1	0.999886
B2	8760	0	1.000000
B3	8760	0	1.000000
B4	8760	0	1.000000
C1	8760	0	1.000000
C2	8750	1	0.999886
C3	8760	0	1.000000
C4	8760	0	1.000000
D1	8760	0	1.000000
D2[a]	8760	0	1.000000
D3	8760	0	1.000000
D4	8760	0	1.000000
E1	8760	0	1.000000
E2	8760	0	1.000000
E3	8760	0	1.000000
E4	5513[d]	1	0.999819
F1	8760	0	1.000000
F2[a]	8760	0	1.000000
F3	8760	0	1.000000
F4	8760	0	1.000000
All Slots	206979	4	0.999981

[a] *When B1, D2, and F2 are configured as expandable slots, both slot locations must be occupied by an available satellite for the slot to be counted as available.*

[b] *There were 8760 hours in 2018.*

[c] *Number of hours in which SPS SIS was available at the start of the hour and during the hour either (1.) an SV transmitted navigation message with subframe 1 health bits set to other than all zeroes without a scheduled outage, (2.) signal lost without a scheduled outage, or (3.) the URE NTE tolerance was violated.*

[d] *This value is lower due to the period starting after SVN 54/PRN 18 became unusable (NANU 2018001) until SVN 51/PRN 20 completed the transition to E4.*

3.4.2 Status and Problem Reporting Standards

3.4.2.1 Scheduled Events

The SPSPS08 makes the following assertion in Section 3.6.3 regarding notification of scheduled events affecting service:

- *"Appropriate NANU issued to the Coast Guard and the FAA at least 48 hours prior to the event"*

While beyond the assertion in the performance standards, ICD-GPS-240 [9] states a nominal notification time of 96 hours prior to outage start and an objective of 7 days (168 hours) prior to outage start.

This metric was evaluated by comparing the NANU periods to outages observed in the data. In general, scheduled events are described in a pair of NANUs. The first NANU is a forecast of when the outage will occur. The second NANU is provided after the outage and summarizes the actual start and end times of the outage. (This is described in ICD-GPS-240 Section 10.1.1.)

Table 3.8 summarizes the pairs found for 2018. The two leftmost columns provide the SVN/PRN of the subject SV. The next three columns specify the NANU #, type, and date/time of the NANU for the forecast NANU. These are followed by three columns that specify the NANU #, the date/time of the NANU for the FCSTSUMM NANU provided after the outage, and the date/time of the beginning of the outage. The final column is the time difference between the time the forecast NANU was released and the beginning of the actual outage (in hours). This represents the length of time between the release of the forecast and the actual start of the outage.

Table 3.8: Scheduled Events Covered in NANUs for 2018

SVN	PRN	Prediction NANU			Summary NANU (FCSTSUMM)			Notice (hrs)
		NANU #	TYPE	Release Time	NANU #	Release Time	Start Of Outage	
64	30	2018004	FCSTDV	08 Feb 1704Z	2018005	14 Feb 0153Z	13 Feb 1933Z	122.48
46	11	2018006	FCSTDV	22 Feb 2217Z	2018007	01 Mar 2048Z	01 Mar 1431Z	160.23
51	20	2018008	FCSTDV	02 Mar 2140Z	2018012	09 Mar 0624Z	08 Mar 2321Z	145.68
69	03	2018011	FCSTDV	08 Mar 1936Z	2018013	15 Mar 1956Z	15 Mar 1355Z	162.32
72	08	2018016	FCSTDV	28 Mar 1948Z	2018018	06 Apr 0033Z	05 Apr 1927Z	191.65
53	17	2018020	FCSTDV	13 Apr 1953Z	2018022	18 Apr 0357Z	17 Apr 2229Z	98.60
47	22	2018021	FCSTDV	16 Apr 2028Z	2018024	27 Apr 1345Z	27 Apr 0827Z	251.98
60	23	2018023	FCSTDV	25 Apr 2131Z	2018025	03 May 2037Z	03 May 1423Z	184.87
41	14	2018026	FCSTDV	08 May 1829Z	2018027	18 May 1324Z	18 May 0817Z	229.80
51	20	2018029	FCSTDV	15 Jun 1526Z	2018030	22 Jun 0824Z	22 Jun 0202Z	154.60
58	12	2018031	FCSTDV	10 Aug 2011Z	2018032	16 Aug 2251Z	16 Aug 1721Z	141.17
61	02	2018035	FCSTDV	30 Aug 1718Z	2018037	06 Sep 2128Z	06 Sep 1521Z	166.05
55	15	2018036	FCSTDV	04 Sep 2325Z	2018039	11 Sep 1846Z	11 Sep 1145Z	156.33
59	19	2018038	FCSTDV	07 Sep 1702Z	2018040	14 Sep 1410Z	14 Sep 0839Z	159.62
68	09	2018041	FCSTDV	26 Sep 1741Z	2018043	04 Oct 0749Z	04 Oct 0204Z	176.38
50	05	2018046	FCSTDV	10 Oct 1502Z	2018047	16 Oct 1938Z	16 Oct 1400Z	142.97
65	24	2018054	FCSTDV	30 Nov 1503Z	2018058	07 Dec 1114Z	07 Dec 0450Z	157.78
62	25	2018062	FCSTDV	11 Dec 1534Z	2018064	14 Dec 1145Z	14 Dec 0534Z	62.00
Average Notice Period								159.14

To meet the assertion in the performance standard, the number of hours in the rightmost column of Table 3.8 should always be greater than 48.0. There were no cases in which the forecast was less than the 48 hour assertion. In previous years, such events were shown in red in Table 3.8. The average notice was over 159 hours. Therefore, the assertion has been met.

One satellite was decommissioned in 2018. Table 3.9 provides the details on how this was represented in the NANUs.

Table 3.9: Decommissioning Events Covered in NANUs for 2018

SVN	PRN	UNUSUFN NANU		DECOM NANU		
		NANU #	Release Time	NANU #	Release Time	End of Unusable Period
54	18	2018001	23 Jan 1656Z	2018009	05 Mar 2211Z	23 Jan 1650Z

3.4.2.2 Unscheduled Outages

The SPS PS provides the following assertion in Section 3.6.3 regarding notification of unscheduled outages or problems affecting service:

- *"Appropriate NANU issued to the Coast Guard and the FAA as soon as possible after the event"*

The ICD-GPS-240 states that the nominal notification time is less than 1 hour after the start of the outage with an objective of 15 minutes.

This metric was evaluated by examining the NANUs provided throughout the year and comparing the NANU periods to outages observed in the data. Unscheduled events may be covered by either a single NANU or a pair of NANUs. In the case of a brief outage, a NANU with type UNUNOREF (unusable with no reference) is provided to detail the period of the outage. In the case of longer outages, a UNUSUFN (unusable until further notice) is provided to inform users of an ongoing outage or problem. This is followed by a NANU with type UNUSABLE after the outage is resolved. (This is described in detail in ICD-GPS-240 Section 10.1.2.)

Table 3.10 provides a list of the unscheduled outages found in the NANU information for 2018. The two leftmost columns provide the SVN/PRN of the subject SV. The third column provides the plane-slot of the SV to assist in relating these events to the information in Table 3.7. The next two columns provide the NANU # and date/time of the UNUSUFN NANU. These are followed by three columns that specify the NANU #, the date/time of the NANU for the UNUSABLE NANU provided after the outage, and the date/time of the beginning of the outage. The final column is the time difference between the outage start time and the UNUSUFN NANU release time (in minutes). Values shown in red in the final column have a lag time of greater than 60 minutes.

Table 3.10 contains 21 entries, 15 of which are related to NANUs of type UNUNOREF. This is a far greater number of UNUNOREF NANUs than either 2016 or 2017, each of which had none. The majority of these (14 of 15) were related to SVN 34/PRN 18. Aside from the NANUs for SVN 34/PRN 18, the rate of unscheduled events was comparable to the previous two years.

Table 3.10: Unscheduled Events Covered in NANUs for 2018

SVN	PRN	Plane-Slot[a]	UNUSUFN NANU		UNUSABLE/UNUNOREF NANU			Lag Time (minutes)
			NANU #	Release Time	NANU #	Release Time	Start Of Event	
54	18	E4	2018001	23 Jan 1656Z	2018009[b]	05 Mar 2211Z	23 Jan 1650Z	6.00
64	30	A3	–	–	2018014	20 Mar 1211Z	20 Mar 1050Z	81.00
34	18	D	–	–	2018028	26 May 1004Z	26 May 0948Z	16.00
66	27	C2	2018044	07 Oct 0834Z	2018045	07 Oct 1818Z	07 Oct 0807Z	27.00
34	18	D	–	–	2018048	08 Nov 1634Z	08 Nov 1625Z	9.00
34	18	D	2018048	08 Nov 1634Z	2018049	12 Nov 1605Z	08 Nov 1625Z	9.00
34	18	D	–	–	2018050	12 Nov 1622Z	12 Nov 1528Z	54.00
34	18	D	–	–	2018052	14 Nov 1525Z	14 Nov 1515Z	10.00
34	18	D	2018053	17 Nov 1722Z	2018055	03 Dec 2010Z	17 Nov 1701Z	21.00
34	18	D	2018056	03 Dec 2317Z	2018059	10 Dec 2045Z	03 Dec 2309Z	8.00
34	18	D	–	–	2018061	11 Dec 0311Z	11 Dec 0302Z	9.00
34	18	D	–	–	2018063	12 Dec 0402Z	12 Dec 0352Z	10.00
34	18	D	–	–	2018065	16 Dec 0200Z	16 Dec 0153Z	7.00
34	18	D	–	–	2018066	17 Dec 0231Z	17 Dec 0225Z	6.00
34	18	D	–	–	2018067	18 Dec 0108Z	18 Dec 0123Z	-15.00[c]
34	18	D	–	–	2018068	19 Dec 0224Z	19 Dec 0222Z	2.00
34	18	D	–	–	2018069	20 Dec 0058Z	20 Dec 0055Z	3.00
34	18	D	–	–	2018070	21 Dec 0207Z	21 Dec 0205Z	2.00
56	16	B1A	2018071	21 Dec 1313Z	2018072	21 Dec 1734Z	21 Dec 1304Z	9.00
34	18	D	–	–	2018073	27 Dec 0208Z	27 Dec 0157Z	11.00
34	18	D	–	–	2018075	29 Dec 0109Z	29 Dec 0102Z	7.00
Average Lag Time								15.35

[a] *Only plane is specified for SVs that are not in a defined slot.*
[b] *UNUSUFN NANU was closed with a DECOM NANU*
[c] *NANU release time is prior to event start time. Event not included in average lag time.*

Because the performance standard states only "as soon as possible after the event," there is no evaluation to be performed. However, the data are provided for information. With respect to the nominal notification times provided in ICD-GPS-240, the nominal times are met in 2018 except for NANU 2018014.

3.5 SIS Availability

3.5.1 Per-Slot Availability

The SPS PS makes the following assertions in Section 3.7.1:

- *"≥ 0.957 Probability that a Slot in the Baseline 24-Slot Configuration will be Occupied by a Satellite Broadcasting a Healthy SPS SIS"*
- *"≥ 0.957 Probability that a Slot in the Expanded Configuration will be Occupied by a Pair of Satellites Each Broadcasting a Healthy SPS SIS"*

The constraints include the note that this is to be calculated as an average over all slots in the 24-slot constellation, normalized annually.

The derivation of the SV/slot assignments is described in Appendix E.

This metric was verified by examining the status of each SV in the Baseline 24-Slot configuration (or pair of SVs in an expandable slot) at every 30 s interval throughout the year. The health status was determined from the subframe 1 health bits of the ephemeris being broadcast at the time of interest. In addition, data from both the MSN and the IGS networks were examined to verify that the SV was broadcasting a trackable signal at the time. The results are summarized in Table 3.11. The metric is averaged over the constellation, therefore the value in the bottom row (labeled "All Slots") must be greater than 0.957 in order for the assertion to be met.

Slot E4 has a lower availability than other slots in 2018 due to the decommissioning of SVN 54/PRN 18 on January 23 (NANU 2018001). This left a gap in the defined constellation until the move of SVN 51/PRN 20 was completed in early June.

We should note that even though E4 had poor occupancy numbers, dilution of precision metrics do not reflect this. This is a result of the fact that for positioning and navigation, overall satellite geometry is more important than slot occupancy, and the close adjacency of the SVs in a slot does not substantially improve the geometry.

Regardless of the individual slot availabilities, the average availability for the constellation was 0.984, which is above the threshold of 0.957. Therefore the assertion being evaluated in this section was met.

Table 3.11: Per-Slot Availability for 2018

Plane-Slot	# Missing Epochs	Available
A1	764	0.999273
A2	0	1.000000
A3	755	0.999282
A4	0	1.000000
B1[a]	536	0.999490
B2	736	0.999300
B3	0	1.000000
B4	687	0.999346
C1	0	1.000000
C2	1213	0.998846
C3	639	0.999392
C4	655	0.999377
D1	725	0.999310
D2[a]	775	0.999263
D3	0	1.000000
D4	0	1.000000
E1	673	0.999360
E2	0	1.000000
E3	655	0.999377
E4	390406	0.628609
F1	0	1.000000
F2[a]	820	0.999220
F3	681	0.999352
F4	770	0.999268
All Slots	401490	0.984086

Note: For each slot there were 1051200 total 30 s epochs in 2018.

[a] *When B1, D2, and F2 are configured as expandable slots, both slot locations must be occupied by an available satellite for the slot to be counted as available.*

3.5.2 Constellation Availability

The SPSPS08 makes the following assertions in Section 3.7.2:

- *"≥ 0.98 Probability that at least 21 Slots out of the 24 Slots will be Occupied Either by a Satellite Broadcasting a Healthy SPS SIS in the Baseline 24-Slot Configuration or by a Pair of Satellites Each Broadcasting a Healthy SPS SIS in the Expanded Slot Configuration"*
- *"≥ 0.99999 Probability that at least 20 Slots out of the 24 Slots will be Occupied Either by a Satellite Broadcasting a Healthy SPS SIS in the Baseline 24-Slot Configuration or by a Pair of Satellites Each Broadcasting a Healthy SPS SIS in the Expanded Slot Configuration"*

To evaluate this metric the subframe 1 health condition and the availability of signal were evaluated for each SV every 30 s for all of 2018. Following a literal reading of the requirement, the number of SVs broadcasting a healthy SIS was examined for each measurement interval and assigned to the correct slot. For non-expanded baseline slots, if an SV qualified as being in the slot and was transmitting a healthy signal, the slot was counted as occupied. For expanded slots, the slot was counted as occupied if two healthy SVs were found: one in each of the two portions of the expanded slot. If the count of occupied slots was greater than 20, the measurement interval was counted as a 1; otherwise the measurement interval was assigned a zero. The sum of the 1 values was then divided by the total number of measurement intervals. The value for 2018 is 1.00. Thus, both requirements are satisfied.

While this satisfies the metric, it does not provide much information on exactly how many SVs are typically healthy. To address this, at each 30 s interval the number of SVs broadcasting a healthy SIS was counted. This was done for both the count of occupied slots and for the number of SVs. The daily averages as a function of time are shown in Figure 3.11. As is clear, the number of occupied slots always exceeded 21.

3.5.3 Operational Satellite Counts

Table 3.7-3 of the SPSPS08 states:

- *"$\geq$ 0.95 Probability that the Constellation will Have at least 24 Operational Satellites Regardless of Whether Those Operational Satellites are Located in Slots or Not"*

Under "Conditions and Constraints" the term Operational is defined as

> *"any satellite which appears in the transmitted navigation message almanac... regardless of whether that satellite is currently broadcasting a healthy SPS SIS or not or whether the broadcast SPS SIS also satisfies the other performance standards in this SPS PS or not."*

Given the information presented in Sections 3.5.1 and 3.5.2, we conclude that at least 24 SVs were operational 100% of the time for 2018. However, to evaluate this more explicity, the almanac status was examined directly. The process consisted of selecting an almanac for each day in 2018. IS-GPS-200 Section 20.3.3.5.1.3 [2] assigns a special meaning to the SV health bits in the almanac's subframe 4 page 25 and subframe 5 page 25 (Data ID 51 and 63). When these bits are set to all ones it indicates "the SV which has that ID is not available, and there might be no data regarding that SV in that page of subframes 4 and 5..." Given this definition, the process examines the subframe 4 and 5 health bits for the individual SVs and counts the number of SVs for which the health bits are other than all ones. The results are shown in Figure 3.12. This plot is very similar to the full constellation healthy satellite count shown in Figure 3.11. The almanac health data are not updated as frequently as those in subframe 1. As a result, the plot in Figure 3.12 contains only integer values. Therefore, on days when it appears the operational SV count is lower than the number of healthy SVs in the constellation, these reflect cases where an SV was set unhealthy for a small portion of the day. In Figure 3.11, such effects are averaged over the day, yielding a higher availability.

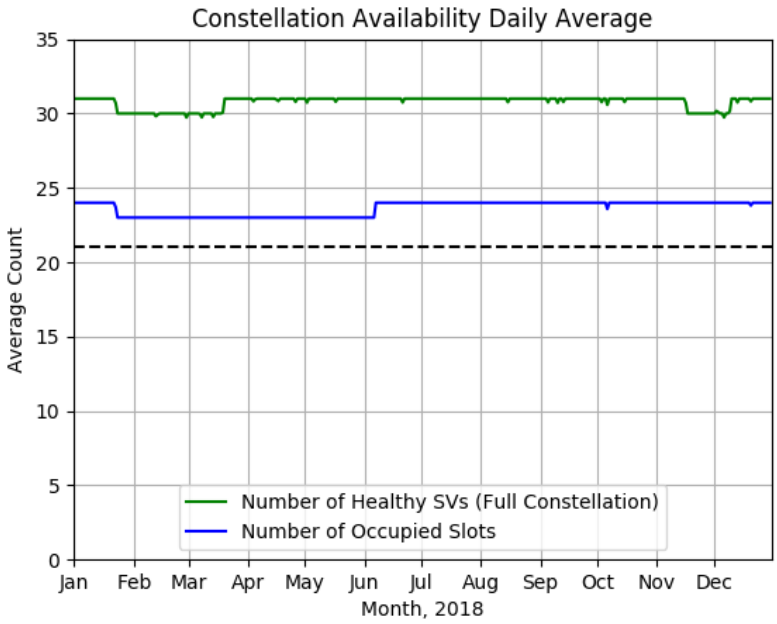

Figure 3.11: Daily Average Number of Occupied Slots

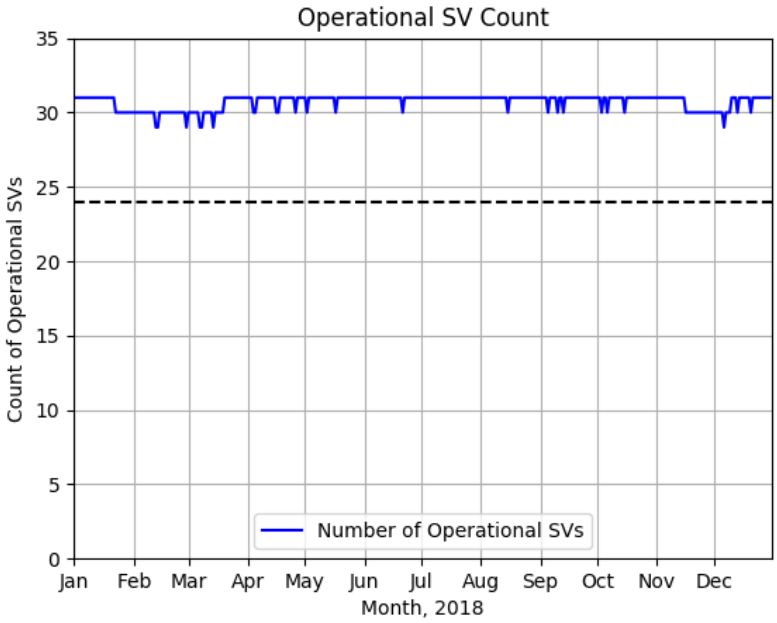

Figure 3.12: Count of Operational SVs by Day for 2018

3.6 Position/Time Domain Standards

3.6.1 PDOP Availability

Given representative user conditions and considering any 24 hour interval the SPSPS08 calls for:

- *"≥ 98% global PDOP of 6 or less"*
- *"≥ 88% worst site PDOP of 6 or less"*

Based on the definition of a representative receiver contained in SPS PS Section 3.8, a 5° minimum elevation angle is used for this evaluation.

These assertions were verified empirically throughout 2018 using a uniformly-spaced grid, containing N_{grid} points, to represent the terrestrial service volume at zero altitude, and an archive of the broadcast ephemerides transmitted by the SVs throughout the year. All healthy, transmitting SVs were considered. The grid was 111 km × 111 km (roughly 1° × 1° at the Equator). The time started at 0000Z each day and stepped through the entire day at one minute intervals (1440 points/day, defined as $1 \leq N_t \leq 1440$). The overall process followed is similar to that defined in Section 5.4.6 of the GPS Civil Monitoring Performance Specification (CMPS) [10].

The Position Dilution of Precision (PDOP) values were formed using the traditional PDOP algorithm [11], without regard for the impact of terrain. The coordinates of the grid locations provided the ground positions at which the PDOP was computed. The position of each SV was computed from the broadcast ephemeris available to a receiver at the time of interest. The only filtering performed was the exclusion of any unhealthy SVs (those with subframe 1 health bits set to other than all zeroes). The results of each calculation were tested with respect to the threshold of PDOP ≤ 6. If the condition was violated, a bad PDOP counter associated with the particular grid point, b_i for $1 \leq i \leq N_{grid}$, was incremented.

At least four SVs must be available to a receiver for a valid PDOP computation. This condition was fulfilled for all grid points at all times in 2018.

Once the PDOPs had been computed across all grid points, for each of the 1440 time increments during the day, the percentage of time the PDOP was less than or equal to 6 for the day was computed using the formula:

$$(\%PDOP \leq 6) = 100 \left(1 - \frac{\sum_{i=1}^{N_{grid}} b_i}{N_{grid} N_t} \right)$$

The worst site for a given day was identified from the same set of counters by finding the site with the maximum bad count: $b_{max} = \max_i(b_i)$. The ratio of b_{max} to N_t is an estimate of the fraction of time the worst site PDOP exceeds the threshold. This value was averaged over the year, and the percentage of time the PDOP is less than or equal to 6 was computed.

Table 3.12 summarizes the results of this analysis for the configurations of all SVs available. The second column ("Average daily % over 2018") provides the values for the assertions. The additional column is provided to verify that no single-day value actually dropped below the goal. From this table we conclude that the PDOP availability metrics are met for 2018.

Table 3.12: Summary of PDOP Availability

Metric	Average daily % over 2018	Minimum daily % over 2018
$\geq 98\%$ Global Average PDOP ≤ 6	99.999	99.387
$\geq 88\%$ Worst site PDOP ≤ 6	99.994	98.264

In addition to verifying the assertion, several additional analyses go beyond the direct question and speak to the matter of how well the system is performing on a more granular basis. The remainder of this chapter describes those analyses and results.

3.6.2 Additional DOP Analysis

There are several ways to look at Dilution of Precision (DOP) values when various averaging techniques are taken into account. Assuming a set of DOP values, each identified by latitude (λ), longitude (θ), and time (t), then each individual value is represented by $DOP_{\lambda,\theta,t}$.

The global average DOP for a day, $\langle DOP \rangle(day)$, is defined to be

$$\langle DOP \rangle(day) = \frac{\sum_t \sum_\theta \sum_\lambda DOP_{\lambda,\theta,t}}{N_{grid} \times N_t}$$

Another measure of performance is the average DOP over the day at the worst site,$\langle DOP \rangle_{worst\,site}$. In this case the average over a day is computed for each unique latitude/longitude combination and the worst average of the day is taken as the result.

$$\langle DOP \rangle_{worst\,site}(day) = \max_{\lambda,\theta} \left(\frac{\sum_t DOP_{\lambda,\theta,t}}{N_t} \right)$$

This statistic is the most closely related to the description of worst site used in Section 3.6.1.

The average of worst site DOP, $\langle DOP_{worst\,site} \rangle$, is calculated by obtaining the worst DOP in the latitude/longitude grid at each time, then averaging these values over the day.

$$\langle DOP_{worst\,site} \rangle(day) = \frac{\sum_t \max_{\lambda,\theta} (DOP_{\lambda,\theta,t})}{N_t}$$

This represents a measure of the worst DOP performance. It is not particularly useful from the user's point of view because the location of the worst site varies throughout the day.

Finally, the absolute worst time-point in a day is given by taking the maximum of the individual DOP values for all locations and all times.

$$DOP_{abs.\,worst}(day) = \max_{\lambda,\theta,t} (DOP_{\lambda,\theta,t})$$

Given that the $\langle DOP \rangle_{worst\,site}(day)$ is most closely related to the worse site definition used in Section 3.6.1, this is the statistic that will be used for "worst site" in the remainder of this section. For 2018, both $\langle DOP \rangle_{worst\,site}(day)$ and $\langle DOP_{worst\,site} \rangle(day)$ satisfy the SPS PS assertions.

It is worth noting the following mathematical relationship between these quantities:

$$\langle DOP \rangle \leq \langle DOP \rangle_{worst\,site} \leq \langle DOP_{worst\,site} \rangle \leq DOP_{abs.\,worst}$$

This serves as a sanity check on the DOP results in general and establishes that these metrics are increasingly sensitive to outliers in $DOP_{\lambda,\theta,t}$.

In calculating the percentage of the time that the $\langle DOP \rangle$ and $\langle DOP \rangle_{worst\,site}$ are within bounds, several other statistics were calculated which provide insight into the availability of the GPS constellation throughout the world. Included in these statistics are the annual means of the daily global average DOP and the $\langle DOP \rangle_{worst\,site}$ values. These values are presented in Table 3.13, with values for 2015 through 2017 provided for comparison. The average number of satellites and the fewest satellites visible across the grid are calculated as part of the DOP calculations. Also shown in Table 3.13 are the annual means of the global average number of satellites visible to grid cells on a 111 km $\times$ 111 km (latitude by longitude) global grid and the annual means of the number of satellites in the worst-site grid cell (defined as seeing the fewest number of satellites). It should be noted that the worst site for each of these values was not only determined independently from day-to-day, it was also determined independently for each metric. That is to say, it is not guaranteed that the worst site with respect to Horizontal DOP (HDOP) is the same as the worst site with respect to PDOP. For all quantities shown in Table 3.13 the values are very similar across all four years.

There are a few other statistics that can add insight regarding the GPS system availability. The primary availability metric requires that the globally averaged PDOP be in-bounds at least 98% of the time. There are two related values: the number of days for which the PDOP is in bounds and the 98^{th} percentile of the daily globally averaged PDOP values. Similarly, calculations can be done for $\langle DOP \rangle_{worst\,site}$ criteria of having the PDOP ≤ 6 greater than 88% of the time. Table 3.14 presents these values.

Table 3.13: Additional DOP Annually-Averaged Visibility Statistics for 2015 through 2018

	$\langle$**DOP**$\rangle$				$\langle$**DOP**$\rangle_{\textbf{worst site}}$			
	2015	**2016**	**2017**	**2018**	**2015**	**2016**	**2017**	**2018**
Horizontal DOP	0.85	0.83	0.83	0.84	0.97	0.94	0.94	0.95
Vertical DOP	1.37	1.34	1.35	1.36	1.72	1.68	1.68	1.70
Time DOP	0.80	0.78	0.78	0.79	0.92	0.89	0.89	0.91
Position DOP	1.62	1.58	1.59	1.60	1.89	1.84	1.83	1.86
Geometry DOP	1.81	1.77	1.77	1.79	2.10	2.04	2.04	2.07
Number of visible SVs	10.33	10.39	10.49	10.42	5.28	5.93	5.95	5.32

Table 3.14: Additional PDOP Statistics

	2015	**2016**	**2017**	**2018**
% of Days with the $\langle PDOP \rangle \leq 6$	100.00	100.00	100.00	100.00
% of Days with the $\langle PDOP \rangle$ at Worst Site ≤ 6	100.00	100.00	100.00	100.00
98^{th} Percentile of $\langle PDOP \rangle$	1.65	1.63	1.60	1.64
88^{th} Percentile of $\langle PDOP \rangle_{worst\,site}$	1.92	1.89	1.84	1.87

Table 3.14 shows that the average DOP values for 2018 are nearly identical to previous years.

Behind the statistics are the day-to-day variations. Figure 3.13 provides a time history of the four PDOP metrics considering all satellites for 2018. Four metrics are plotted:

- Daily Global Average PDOP: $\langle PDOP \rangle$
- Average Worst Site PDOP: $\langle PDOP \rangle_{worst\,site}$
- Average PDOP at Worst Site: $\langle PDOP_{worst\,site} \rangle$
- Absolute Worst PDOP: $PDOP_{abs.\,worst}$

$PDOP_{abs.\,worst}$ is the only quantity that does not include averaging. As such, $PDOP_{abs.\,worst}$ is the quantity most sensitive to events such as SV outages and to short-duration periods of higher PDOP as SVs drift within the constellation. In addition, the fact that the PDOP evaluation is conducted on a five minute cadence coupled with the fact that the SV ground tracks advance four minutes per day means a period of higher PDOP that lasts less than five minutes can be alternately observed/not-observed on successive days as the two cadences interact. An example of this is seen in early January where the $PDOP_{abs.\,worst}$ exhibits daily oscillations. During this time, a very short-duration period of localized somewhat higher PDOP is coming in-and-out of view as it overlaps (or does not overlap) with the five minute evaluation cadence.

There are two periods in which the $PDOP_{abs.\,worst}$ is noticeably high for several weeks. The first period is a sudden rise in late January which slowly decreases until early June. The onset of this period coincides with the unusable period (and decommisioning) of SVN 54/PRN 18. The replacement SV for that slot was SVN 51/PRN 20, which was not close at the time SVN 54/PRN 18 became unusable. The PDOP improves as SVN 51/PRN 20 drifts into position. The second period is from mid-June to the end of the year. An examination of daily maps of the worst PDOP shows a very small (few degree) high-latitude hole opens up for about 15 minutes per day in mid-June and recurs daily throughout the remainder of the year.

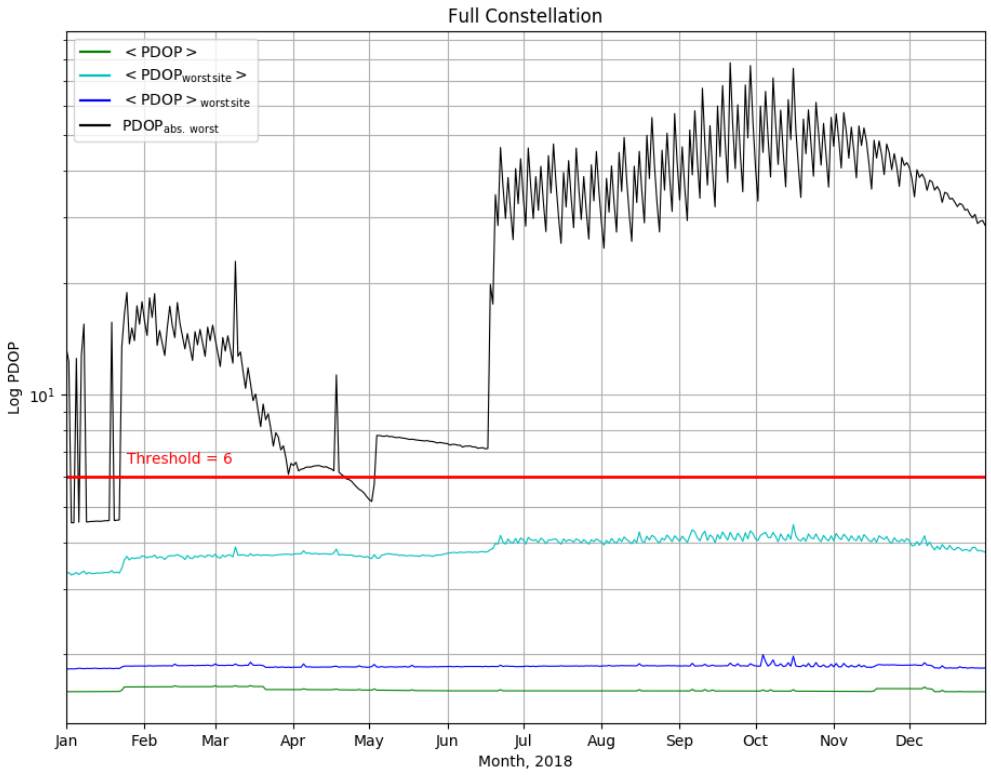

Figure 3.13: Daily PDOP Metrics Using All SVs for 2018

3.6.3 Position Service Availability

The positioning and timing availability standards are stated in Table 3.8-2 of SPSPS08 as follows:

- *"≥ 99% Horizontal Service Availability, average location"*
- *"≥ 99% Vertical Service Availability, average location"*
- *"≥ 90% Horizontal Service Availability, worst-case location"*
- *"≥ 90% Vertical Service Availability, worst-case location"*

The conditions and constraints associated with the standards include the specification of a 17 m horizontal 95^{th} percentile threshold and a 37 m vertical 95^{th} percentile threshold.

These are derived values as described in the sentence preceding SPSPS08 Table 3.8-2:

> *"The commitments for maintaining PDOP (Table 3.8-1) and SPS SIS URE accuracy (Table 3.4-1) result in support for position service availability standards as presented in Table 3.8-2."*

Because the commitments for PDOP and constellation SPS SIS URE have been met, this assertion in the SPSPS08 implies that the position and timing availability standards have also been fulfilled. A direct assessment of these metrics was not undertaken.

3.6.4 Position Accuracy

The positioning accuracy standards are stated in Table 3.8-3 of SPSPS08 as follows:

- *"≤ 9 m 95% Horizontal Error Global Average Position Domain Accuracy"*
- *"≤ 15 m 95% Vertical Error Global Average Position Domain Accuracy"*
- *"≤ 17 m 95% Horizontal Error Worst Site Position Domain Accuracy"*
- *"≤ 37 m 95% Vertical Error Worst Site Position Domain Accuracy"*

These are derived values as described in the sentence preceding SPSPS08 Table 3.8-3:

> *"The commitments for maintaining PDOP (Table 3.8-1) and SPS SIS URE accuracy (Table 3.4-1) result in support for position service availability standards as presented in Table 3.8-3."*

Since the commitments for PDOP and constellation SPS SIS URE have been met, the position and timing accuracy standards have also been fulfilled.

While this answer is technically correct, it is not very helpful. Position and time determination are the primary reasons that GPS exists. At the same time, position accuracy is a particularly difficult metric to evaluate due to the fact that GPS provides the SIS, but the user is responsible for appropriately processing the SIS to determine a position. The position processing used by ARL:UT is described in Appendix B.4.

The process generates position solutions using both NGA and IGS observation data (see Figure 1.1) and using both a simplistic approach with no data editing and a receiver autonomous integrity monitoring (RAIM) approach.

We conducted the elevation angle processing with a 5° minimum elevation angle in agreement with the standard.

This process yields four sets of results organized as detailed in Table 3.15.

Table 3.15: Organization of Positioning Results

	Data Editing	**Data Source**	
		IGS	**NGA**
Cases	RAIM	1	2
	None	3	4

Once the solutions are computed, two sets of statistics were developed. The first set is a set of daily average values across all stations. In the second set, the worst site is determined on a day-to-day basis and the worst site 95^{th} percentile values are computed.

These are empirical results and should not be construed to represent proof that the metrics presented in the standard have been met. Instead, they are presented as a means of corroboration that the standards have been met through the fulfillment of the more basic commitments of PDOP and SPS SIS URE.

3.6.4.1 Results for Daily Average

Using the approach outlined above, position solutions were computed at each 30 s interval for data from both the NGA and IGS stations. In the nominal case in which all stations are operating for a complete day, this yields 2880 solutions per station per day. Truth positions for the IGS stations were taken from the weekly Station Independent Exchange format (SINEX) files. Truth locations for the NGA stations were taken from station locations defined as part of the latest WGS 84 reference frame [12] with corrections for station velocities applied.

Residuals between estimated locations and the truth locations were computed in the form of North, East and Up components in meters. The horizontal residual was computed from the root sum square (RSS) of the North and East components, and the vertical residual was computed from the absolute value of the Up component. As a result, the residuals will have non-zero mean values. The statistics on the residuals were compiled across all stations in a set for a given day. Figures 3.14-3.17 show the daily average for the horizontal and vertical residuals corresponding to the options shown in Table 3.15.

The statistics associated with the processing are provided in Table 3.16. The table contains the mean, median, maximum, and standard deviation of the daily values across 2018. The results are organized in this fashion to facilitate comparison of the same quantity across the various processing options. The results are expressed to the centimeter level of precision. This choice of precision is based on the fact that the truth station positions are known only at the few-centimeter level.

The following general observations may be drawn from the charts and the supporting statistics in Table 3.16:

- Outliers - Figure 3.15 shows a number of large outliers for the IGS averages computed with a simple pseudorange solution and no data editing. The outliers are distributed among several stations. These outliers are largely missing from Figure 3.14. This indicates the importance of conducting at least some level of data editing in the positioning process.

- Mean & Median values - The means and medians of the position residuals given in Table 3.16 are nearly identical for the NGA data sets, suggesting that if there are any 30 s position residual outliers, they are few in number and not too large. The means for the RAIM solutions from IGS are less than 5% higher than the medians. The means and medians for the IGS data set solutions with no data editing are significantly different. This is consistent with the outliers observed in Figure 3.14 and Figure 3.15 and with the maximum and standard deviation values for the IGS data set solutions with no editing. This suggests that there are some large 30 s position residuals in the epoch-by-epoch results for these data sets.

- Maximum values and Standard Deviation - The values shown in Table 3.16 for the IGS data sets are quite a bit larger than the corresponding values for the NGA data sets. Once again, this suggests that there are some large 30 s position residuals in the epoch-by-epoch results for these data sets.

- Differences between NGA and IGS results - The mean magnitude of the position residual as reported in Table 3.16 is slightly smaller for the NGA stations than for the IGS stations. There are a number of differences between the two station sets. The NGA station set is more homogeneous in that the same receiver model is used throughout the data processed for this analysis, the data are derived from full-code tracking, and a single organization prepared all the data sets using a single set of algorithms. By contrast, the IGS data sets come from a variety of receivers and were prepared and submitted by a variety of organizations. These differences likely account for the greater variability in the results derived from the IGS data sets.

Table 3.16: Daily Average Position Errors for 2018

Statistic	**Data Editing**	**Horizontal**		**Vertical**	
		IGS	**NGA**	**IGS**	**NGA**
Mean (m)	RAIM	1.35	1.09	2.24	1.46
	None	3.40	1.10	5.60	1.46
Median (m)	RAIM	1.30	1.09	2.14	1.46
	None	1.35	1.10	2.20	1.46
Maximum (m)	RAIM	8.67	1.27	29.73	1.67
	None	52.18	1.28	83.90	1.68
Std. Dev. (m)	RAIM	0.43	0.03	1.45	0.04
	None	6.09	0.03	9.94	0.04

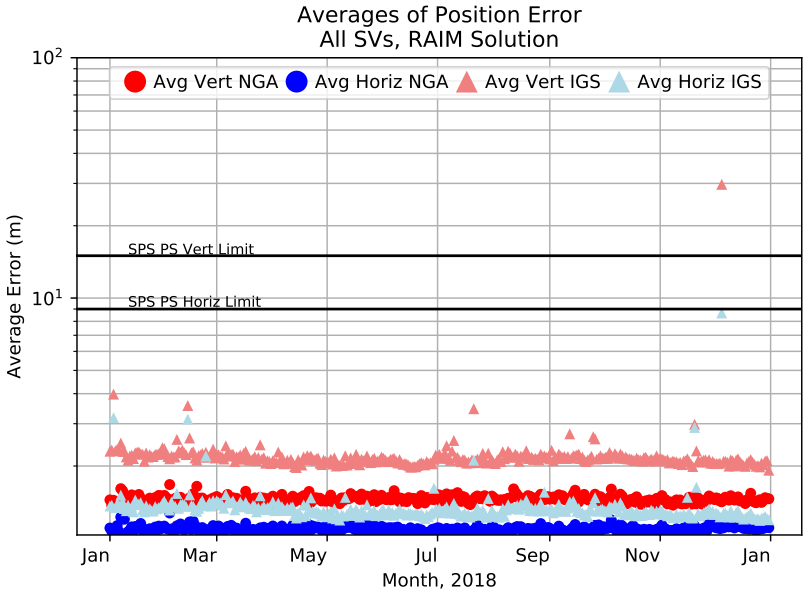

Figure 3.14: Daily Averaged Position Residuals Computed Using a RAIM Solution

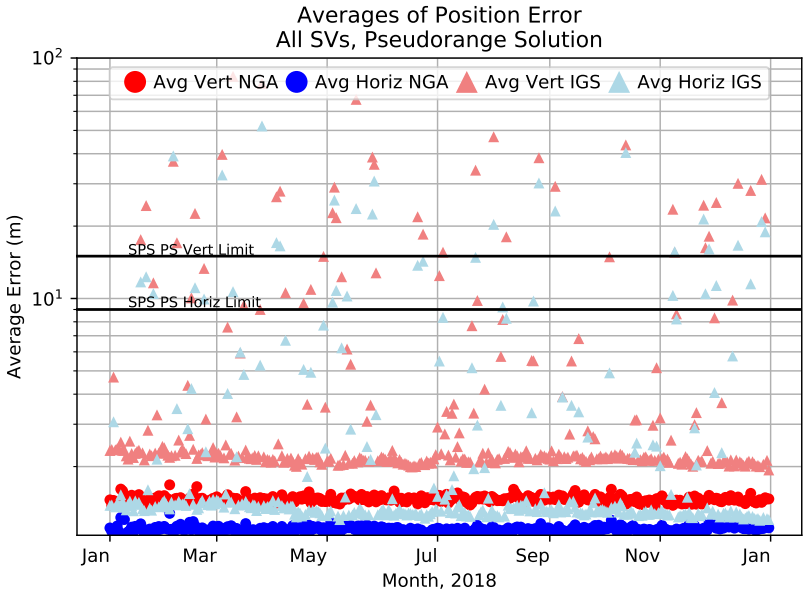

Figure 3.15: Daily Averaged Position Residuals Computed Using No Data Editing

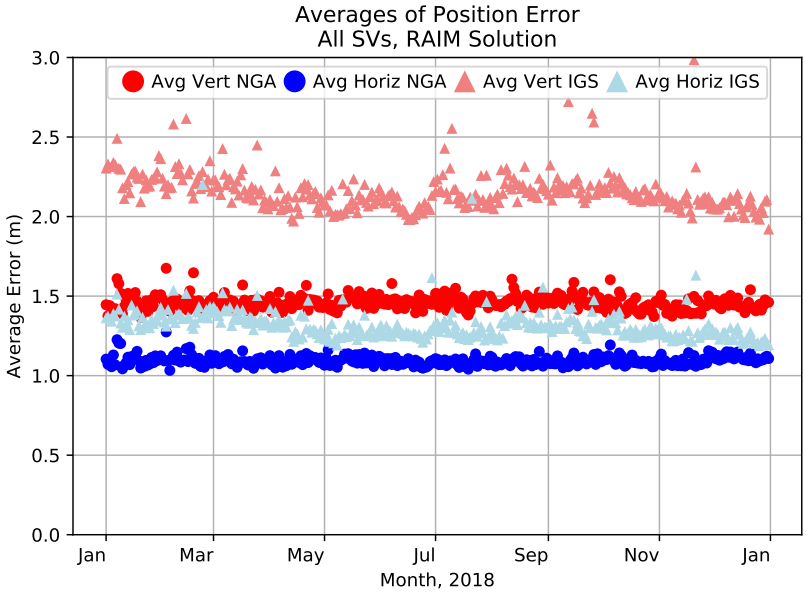

Figure 3.16: Daily Averaged Position Residuals Computed Using a RAIM Solution (enlarged)

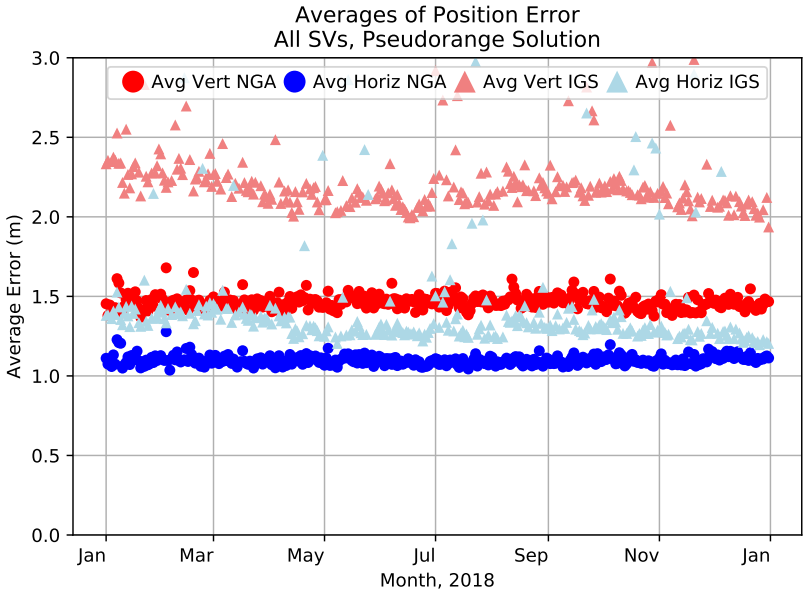

Figure 3.17: Daily Averaged Position Residuals Computed Using No Data Editing (enlarged)

3.6.4.2 Results for Worst Site 95th Percentile

The edited and non-edited 30 s position residuals were then independently processed to determine the worst site 95^{th} percentile values. In this case, the 95^{th} percentile was determined for each station in a given set, and the worst of these was used as the final 95^{th} percentile value for that day. Figures 3.18-3.21 show these values for the various processing options described in the previous section. The plots are followed a table of the statistics for the mean, median, maximum, and standard deviation of the daily worst site 95^{th} percentile values. Some general observations on the results are included following the tables.

The statistics associated with the worst site 95^{th} percentile values are provided in Table 3.17. As before, the results are organized in this fashion to facilitate comparison of the same quantity across the various processing options. Values are reported with a precision of one centimeter due to (a.) the magnitude of the standard deviation and (b.) the fact that the station positions are known only at the few-centimeter level.

Most of the observations from the daily averaged position residuals hold true in the case of the results for the worst site 95^{th} percentile case. However, there are a few additional observations to be drawn from Figures 3.18-3.21 and Table 3.17:

- Comparison to threshold - The values for both mean and median of the worst 95^{th} percentile for both horizontal and vertical errors are well within the standard for both solutions. Compared to the thresholds of 17 m 95^{th} percentile horizontal and 37 m 95^{th} percentile vertical these results are outstanding.
- Comparison between processing options - The statistics for the RAIM solutions are slightly better than the statistics for the pseudorange solutions with respect to mean and median. However, the maximum values for the IGS data with no editing are larger than the IGS RAIM maximum values by an order of magnitude. This illustrates the importance of some form of data editing.

Table 3.17: Daily Worst Site 95^{th} Percentile Position Errors for 2018

Statistic	Data Editing	Horizontal		Vertical	
		IGS	NGA	IGS	NGA
Mean (m)	RAIM	5.00	2.87	7.29	4.16
	None	8.29	2.88	11.62	4.18
Median (m)	RAIM	4.37	2.84	6.88	4.08
	None	4.67	2.85	6.94	4.11
Maximum (m)	RAIM	54.91	7.15	53.85	11.73
	None	759.13	7.15	343.82	11.73
Std. Dev. (m)	RAIM	4.38	0.25	2.86	0.59
	None	40.43	0.25	31.26	0.58

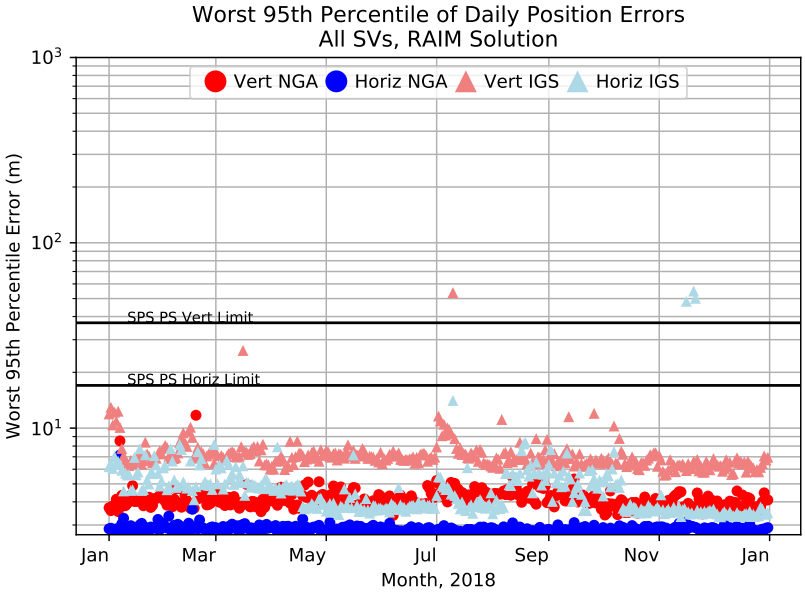

Figure 3.18: Worst Site 95^{th} Daily Averaged Position Residuals Computed Using a RAIM Solution

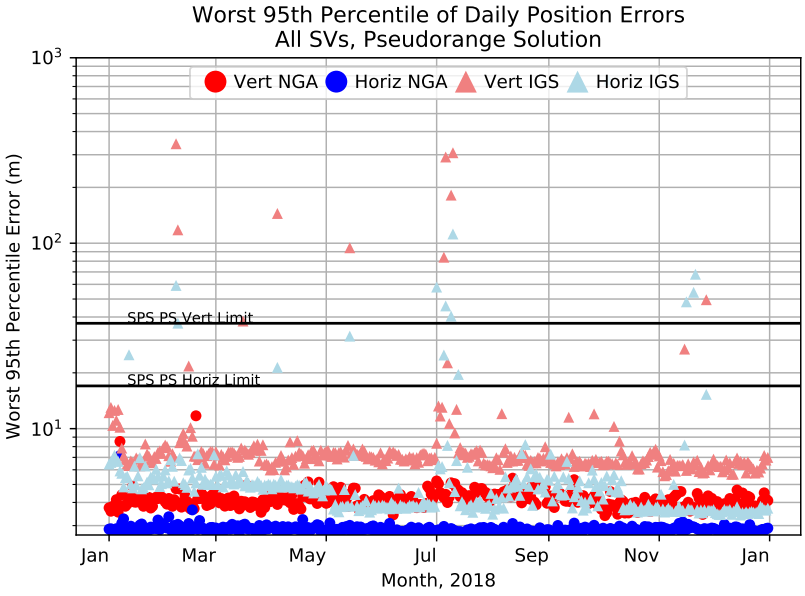

Figure 3.19: Worst Site 95^{th} Daily Averaged Position Residuals Computed Using No Data Editing

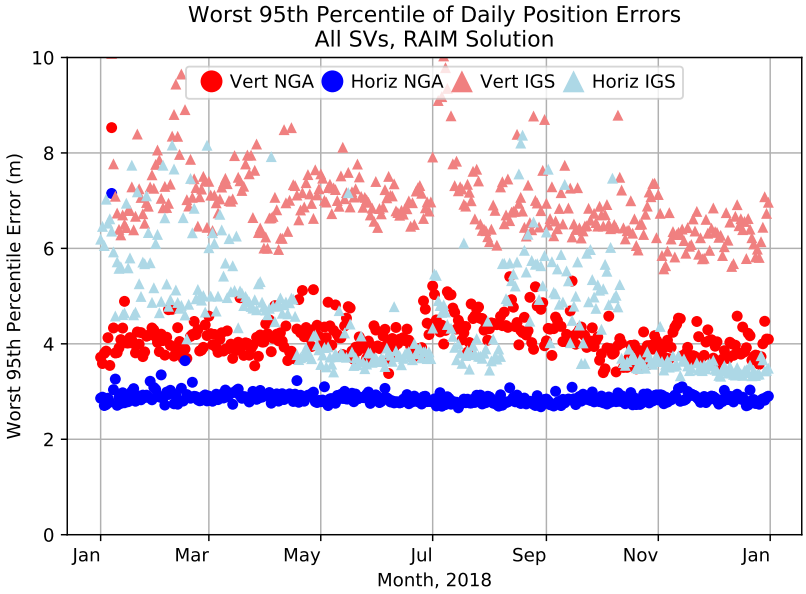

Figure 3.20: Worst Site 95^{th} Daily Averaged Position Residuals Computed Using a RAIM Solution (enlarged)

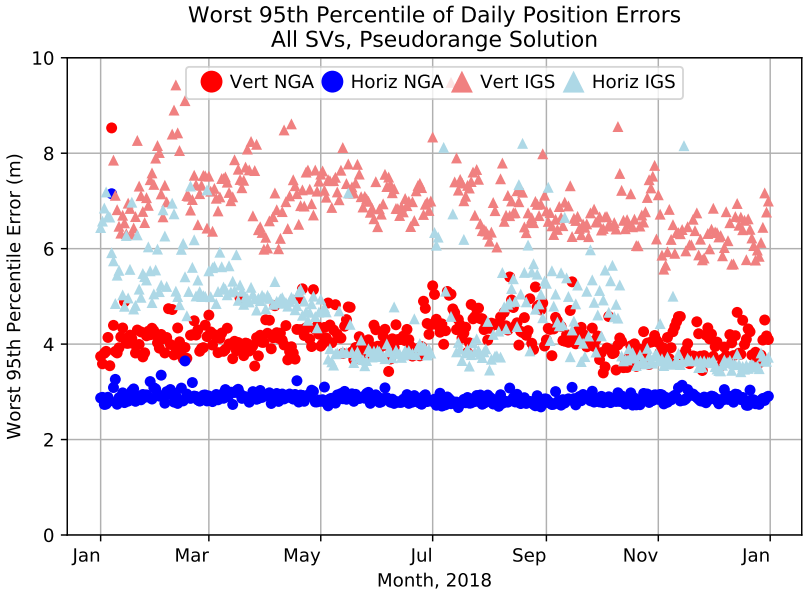

Figure 3.21: Worst Site 95^{th} Daily Averaged Position Residuals Computed Using No Data Editing (enlarged)

3.6.5 Time Accuracy

The timing accuracy standard is stated in Table 3.8-3 of SPSPS08 as follows:

- *"≤ 40 nsec 95% Error Time Transfer Domain Accuracy"* (SIS only)

Conditions and Constraints:

- *Defined for a time transfer solution meeting the representative user conditions*
- *Standard based on a measurement interval of 24 hours averaged over all points in the service volume.*

The equation for time transfer accuracy relative to UTC(USNO) in GPS is found in the SPSPS08, Appendix B.2.2.

$$\text{UUTCE} = \sqrt{(\text{UERE} * \text{TTDOP}/c)^2 + (\text{UTCOE})^2)} \tag{3.6.1}$$

Time transfer dilution of precision (TTDOP) is $1/\sqrt{\text{N}}$, where N is the number is satellites visible to the user[1]. The User UTC(USNO) Error (UUTCE) calculation was performed for each day of the year.

This computation was done only for satellites that meet the criteria of: healthy, trackable, operational, and have no NANU at each given time. To meet the requirement of an average over all points in the service volume a worldwide grid with 425 points was created (see Figure 3.22). Since time transfer accuracy can be dependent on which SVs are in view of a given location, the grid was selected to provide a representative sampling of possible user locations around the world with a variety of possible SV combinations. The grid has 10° separation in latitude, and 10° separation in longitude at the equator. The longitude spacing for latitudes away from the equator was selected to be as close as possible to the distance between longitude points along the equator while maintaining an even number of intervals. This yields a spacing of roughly 1100 km.

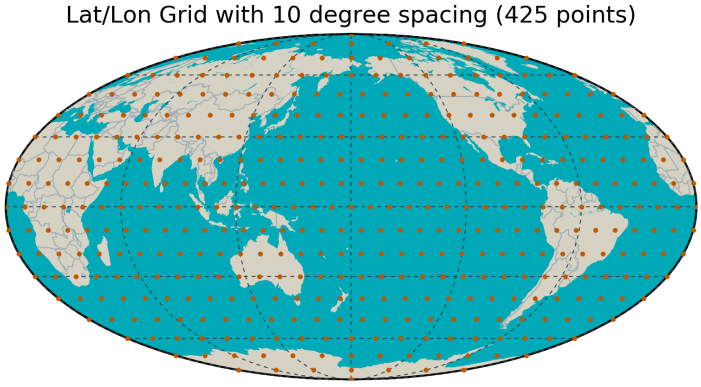

Figure 3.22: 10° Grid for UUTCE Calculation

[1] *as per conversation with Mr. Karl Kovach, author of the SPS PS, 31 August 2017*

Statistics were performed for each day over the grid of 425 points and time step of 15 minutes (96 time points), resulting in 40800 points to determine the 95^{th} percentile UUTCE value.

The computation steps are:

1. Compute satellite positions for each time point in day using the broadcast ephemeris,
2. For each time and grid point,
   (a) find visible satellites (above 5° elevation) that meet the above criteria,
   (b) determine the appropriate UTCO data set ($UTCO_i$). The appropriate data set is the valid data set that has the latest reference time (t_{ot}) of all valid data sets received at that location at that time. Calculate $UTCOE_i$ = $UTCO_i$ - USNO, where USNO is the daily truth value,
   (c) get the Instantaneous SIS URE for each visible satellite, then take the mean of all values ($UERE_i$) and assign as the value for that time and grid point,
3. Calculate all 40800 UUTCE values for the day, find 95% containment of all values.

The daily UUTCE results over all grid points and times per day are shown in Figure 3.23. In Figure 3.23 there is a noticeable spike in the values in mid-July. This aligns with the data anomaly described near the end of Section 3.2.7. All of these results are well below 40 nsec. Therefore this assertion is met.

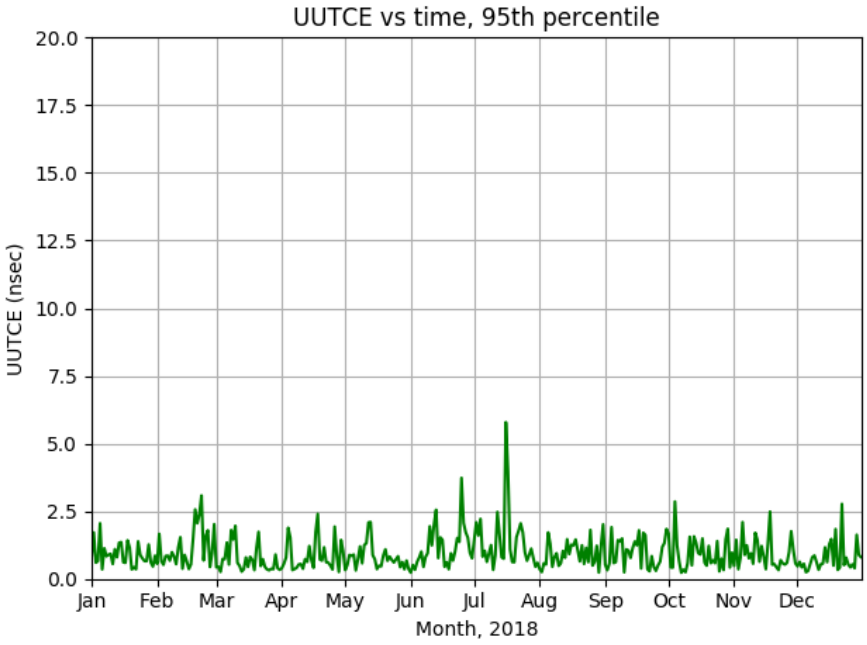

Figure 3.23: UUTCE 95^{th} Percentile Values

Chapter 4

Additional Results of Interest

4.1 Frequency of Different SV Health States

Several of the assertions require examination of the health information transmitted by each SV. We have found it useful to examine the rate of occurrence for all possible combinations of the six health bits transmitted in subframe 1.

Table 4.1 presents a summary of health bit usage in the ephemerides broadcast during 2018. Each row in the table presents a summary for a specific SV. The summary across all SVs is shown at the bottom. The table contains the count of the number of times each unique health code was seen, the raw count of unique sets of subframes 1, 2, and 3 collected during the year, and the percentage of sets of subframe 1, 2, and 3 data that contained specific health codes. Only two unique health settings were observed throughout 2018: binary 000000_2 (0x00) and binary 111111_2 (0x3F).

4.2 Age of Data

The Age of Data (AOD) represents the elapsed time between the observations that were used to create the broadcast navigation message and the time when the contents of subframes 1, 2, and 3 became available to the user to estimate the position of a SV. The accuracy of GPS (at least for users that depend on the broadcast ephemeris) is indirectly tied to the AOD because the prediction accuracy degrades over time (see Section 3.2.2). This is especially true for the clock prediction. It has been recognized that reducing the AOD improves position, velocity, or time (PVT) solutions for autonomous users; however, there is an impact in terms of increased operations tempo at 2^{nd} Space Operations Squadron (2SOPS).

Note that there is no need for a GPS receiver to refer to AOD in any PVT computation other than the optional application of the navigation message correction table (NMCT). (See IS-GPS-200 Section 20.3.3.5.1.9 for a description of the NMCT.) The AOD is computed here to validate that the operators at 2SOPS are not modifying the operational tempo to maintain the URE accuracy described in Section 3.2.

Table 4.1: Frequency of Health Codes

SVN	PRN	Count by Health Code		Total # SF 1, 2, 3 Collected	% of Time by Health Code		Operational Days for 2018	Avg # SF 1, 2, 3 per Operational Day
		0x3F	0x00		0x3F	0x00		
34	18	122	3432	3554	3.4	96.6	277	12.8
41	14	3	4747	4750	0.1	99.9	365	13.0
43	13	0	4742	4742	0.0	100.0	365	13.0
44	28	0	4801	4801	0.0	100.0	365	13.2
45	21	0	4747	4747	0.0	100.0	365	13.0
46	11	4	4742	4746	0.1	99.9	365	13.0
47	22	3	4744	4747	0.1	99.9	365	13.0
48	07	0	4746	4746	0.0	100.0	365	13.0
50	05	3	4741	4744	0.1	99.9	365	13.0
51	20	9	4740	4749	0.2	99.8	365	13.0
52	31	0	4753	4753	0.0	100.0	365	13.0
53	17	3	4742	4745	0.1	99.9	365	13.0
54	18	223	296	519	43.0	57.0	40	13.0
55	15	5	4741	4746	0.1	99.9	365	13.0
56	16	1	4750	4751	0.0	100.0	365	13.0
57	29	0	4757	4757	0.0	100.0	365	13.0
58	12	4	4746	4750	0.1	99.9	365	13.0
59	19	4	4743	4747	0.1	99.9	365	13.0
60	23	4	4743	4747	0.1	99.9	365	13.0
61	02	4	4743	4747	0.1	99.9	365	13.0
62	25	4	4746	4750	0.1	99.9	365	13.0
63	01	0	4751	4751	0.0	100.0	365	13.0
64	30	4	4745	4749	0.1	99.9	365	13.0
65	24	4	4855	4859	0.1	99.9	365	13.3
66	27	3	4746	4749	0.1	99.9	365	13.0
67	06	0	4753	4753	0.0	100.0	365	13.0
68	09	3	4747	4750	0.1	99.9	365	13.0
69	03	4	4751	4755	0.1	99.9	365	13.0
70	32	0	4753	4753	0.0	100.0	365	13.0
71	26	0	4749	4749	0.0	100.0	365	13.0
72	08	4	4769	4773	0.1	99.9	365	13.1
73	10	0	4750	4750	0.0	100.0	365	13.0
All SVs		418	146311	146729	0.3	99.7	365	402.0

The daily average AOD throughout 2018 is shown in Table 4.2, along with values for the previous three years. Details on how AOD was computed are provided in Appendix B.3. The daily average AOD for the constellation, Block IIR/IIR-M, and Block IIF is illustrated in Figure 4.1. The single Block IIA SV, SVN 34/PRN 18, is not shown in Figure 4.1 as there were no other Block IIA SVs with which to conduct an average. In addition, this SV was subject of several NANUs starting in mid-November (see Figure D.1), which resulted in erratic average AOD values. Except for SVN 34/PRN 18, the average AOD is generally constant throughout 2018, which indicates that any variations in the URE results discussed earlier are not due to changes in operations tempo at 2SOPS.

Table 4.2: Age of Data of the Navigation Message by SV Type

	Average Age of Data (hrs)			
	2015	**2016**	**2017**	**2018**
Full Constellation	11.6	11.9	12.1	12.1
Block II/IIA	11.6	11.7	–	11.9
Block IIR/IIR-M	11.7	11.9	12.1	12.1
Block IIF	11.4	11.8	12.1	12.1

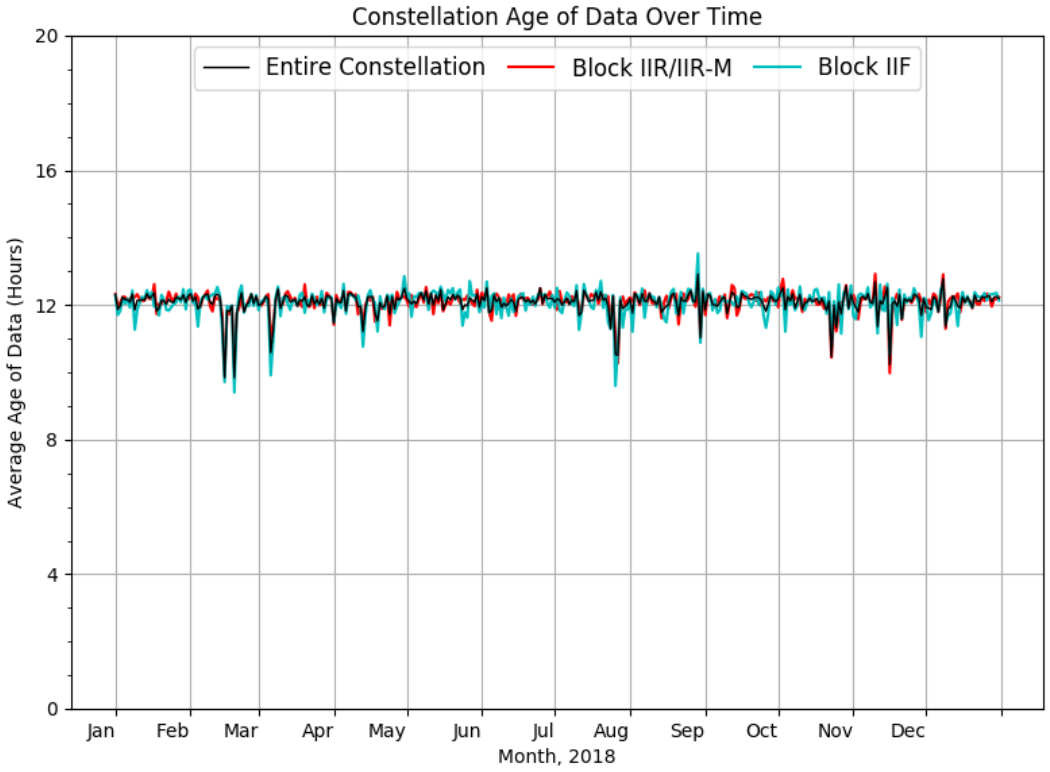

Figure 4.1: Constellation Age of Data for 2018

4.3 User Range Accuracy Index Trends

Tables 4.3 and 4.4 present a summary of the analysis of the URA index values throughout 2018. The total number of navigation messages examined differs from the health summary in Section 4.1 as only URA index values corresponding to health settings of 0x00 are included in this analysis. Both the absolute count and the count as a percentage of the total are shown.

The vast majority of the values are 0, 1, or 2 (over 99.9%). Index values between 3 and 4 were very rare. No values over 4 were observed.

4.4 Extended Mode Operations

IS-GPS-200 defines Normal Operations as the period of time when subframe 1, 2, and 3 data sets are transmitted by the SV for periods of two hours with a curve fit interval of four hours (IS-GPS-200 Section 20.3.4.4). This definition is taken to be the same as the definition of Normal Operations in SPSPS08 for the URE metrics. To determine if any SV operated in other than Normal Operations at any time in 2018, the broadcast ephemerides were examined to determine if any contained fit interval flags were set to 1. (See IS-GPS-200 20.3.3.4.3.1 for definition of the fit interval flag.)

The analysis found a total of 46 examples of extended operations for satellites set healthy. The examples were distributed across 29 days. The average time of an occurrence was 55 minutes. The minimum duration was 90 seconds and the maximum duration was 4 hours 48 minutes. These results are summarized in Table 4.5.

Given the relative rarity of occurrence, the URE values for the periods summarized in Table 4.5 are included in the statistics presented in Section 3.2.1, even though a strict interpretation of the SPSPS08 would suggest that they be removed. However, the SVs involved were still set healthy and (presumably) being used by user equipment, it is appropriate to include these results to reflect performance seen by the users.

Examination of the ephemerides from past years reveals that 2018 is not an anomaly. Such periods have been found in all years checked (back to 2005).

Past discussions with the operators have revealed several reasons for these occurrences. Some are associated with Alternate MCS (AMCS) testing. When operations are transitioned from the MCS to the AMCS (and reverse) it is possible that SVs nearing the end of their daily cycle may experience a longer-than-normal upload cycle. Other occurrences may be caused by delays due to ground antenna maintenance or due to operator concentration on higher-priority issues with the constellation at the time.

Table 4.3: Distribution of URA Index Values

SVN	PRN	URA Index						Total # SF 1, 2, 3 examined[a]	Avg # SF 1, 2, 3 per Oper. Day[a]	Oper. Days for 2018
		5	4	3	2	1	0			
34	18					307	3125	3432	12.9	266
41	14			2	5	184	4556	4747	13.0	365
43	13					258	4484	4742	13.0	365
44	28			1	857	1164	2779	4801	13.2	365
45	21					178	4569	4747	13.0	365
46	11				2	448	4292	4742	13.0	365
47	22		2	5	1	77	4659	4744	13.0	365
48	07				1	500	4245	4746	13.0	365
50	05				1	95	4645	4741	13.0	365
51	20				9	69	4662	4740	13.0	365
52	31				1	478	4274	4753	13.0	365
53	17				2	742	3998	4742	13.0	365
54	18					5	291	296	12.3	24
55	15				3	248	4490	4741	13.0	365
56	16					318	4432	4750	13.0	365
57	29				2	712	4043	4757	13.0	365
58	12			2	1	277	4466	4746	13.0	365
59	19				2	323	4418	4743	13.0	365
60	23			1	4	245	4493	4743	13.0	365
61	02			2	4	267	4470	4743	13.0	365
62	25				3	357	4386	4746	13.0	365
63	01				82	1136	3533	4751	13.0	365
64	30				1	366	4378	4745	13.0	365
65	24				44	1242	3569	4855	13.3	365
66	27				1	323	4422	4746	13.0	365
67	06					156	4597	4753	13.0	365
68	09				1	279	4467	4747	13.0	365
69	03				2	151	4598	4751	13.0	365
70	32				1	214	4538	4753	13.0	365
71	26					344	4405	4749	13.0	365
72	08				2	530	4237	4769	13.1	365
73	10					76	4674	4750	13.0	365
All SVs		0	2	13	1032	12069	133195	146311	400.9	365

[a] *Only sets of SF 1,2,3 that include a healthy indication are included.*

Table 4.4: Distribution of URA Index Values As a Percentage of All Values Collected

SVN	PRN	URA Index					
		5	**4**	**3**	**2**	**1**	**0**
34	18					8.9	91.1
41	14				0.1	3.9	96.0
43	13					5.4	94.6
44	28				17.9	24.2	57.9
45	21					3.7	96.3
46	11					9.4	90.5
47	22			0.1		1.6	98.2
48	07					10.5	89.4
50	05					2.0	98.0
51	20				0.2	1.5	98.4
52	31					10.1	89.9
53	17					15.6	84.3
54	18					1.7	98.3
55	15				0.1	5.2	94.7
56	16					6.7	93.3
57	29					15.0	85.0
58	12					5.8	94.1
59	19					6.8	93.1
60	23				0.1	5.2	94.7
61	02				0.1	5.6	94.2
62	25				0.1	7.5	92.4
63	01				1.7	23.9	74.4
64	30					7.7	92.3
65	24				0.9	25.6	73.5
66	27					6.8	93.2
67	06					3.3	96.7
68	09					5.9	94.1
69	03					3.2	96.8
70	32					4.5	95.5
71	26					7.2	92.8
72	08					11.1	88.8
73	10					1.6	98.4
Constellation Average		0.0	0.0	0.0	0.7	8.2	91.0

Notes: Values smaller than 0.1 are not shown. Constellation averages are weighted by the number of observations.

Table 4.5: Summary of Occurrences of Extended Mode Operations

SVN	PRN	# of Occurrences		Duration (minutes)	
		Healthy	Unhealthy	Healthy	Unhealthy
34	18	2	0	153	0
41	14	1	0	75	0
44	28	1	0	2	0
45	21	1	0	75	0
47	22	3	0	306	0
48	07	1	0	53	0
50	05	3	0	47	0
51	20	1	0	32	0
52	31	2	0	46	0
53	17	3	0	66	0
55	15	1	0	97	0
56	16	3	0	104	0
57	29	3	0	278	0
60	23	2	0	23	0
62	25	1	0	24	0
63	01	3	0	243	0
64	30	2	0	4	0
66	27	3	0	101	0
67	06	2	0	256	0
68	09	3	0	366	0
70	32	1	0	10	0
71	26	1	0	12	0
72	08	2	0	120	0
73	10	1	0	51	0
Totals		46	0	2544	0

Appendix A

URE as a Function of AOD

This appendix contains supporting information for the results presented in Section 3.2.2. Charts of SIS RMS URE vs. AOD similar to Figures 3.4-3.7 are presented for each GPS SV. The charts are organized by SV block and by ascending SVN within each block.

These charts are based on the same set of 30 s Instantaneous RMS SIS URE values used in Section 3.2.1. For each SV, a period of 48 hours of AOD was divided into a set of 192 bins, each 15 minutes of AOD in duration. An additional bin was added for any AOD that appeared beyond 48 hours. All of the 30 s URE values for the year for a given SV were grouped according to AOD bin. The values in each bin were sorted and the 95^{th} percentile and the maximum were determined. Once the analysis was complete, it was clear that most bins beyond the 26 hour mark contained too few points to be considered statistically relevant. Therefore, when the number of points in a bin falls below 10% of the number of points in most populated bin, the bin is not used for plotting purposes. The problem with bins with low counts is that, in our experience, the results tend to dominated by one or two very good or very bad observations and this can lead to erroneous conclusions about behavior.

The figures on the following pages each show two curves:

- Blue: 95^{th} percentile SIS RMS URE vs. AOD (in hours)
- Green: the count of points in each bin as a function of AOD

Note that for most SVs, the green curve has a well-defined horizontal plateau that begins near zero AOD, continues for roughly 24 hours, and then drops quickly toward zero. The location of the right-hand drop of the green curve toward zero provides an estimate of the typical upload period for the SV. In cases where the SV is uploaded more frequently, the shape of the green curve will vary reflecting that difference.

A.1 Notes

This section contains some notes on SV-specific behavior observed in the following charts.

- SVN 44/PRN 28: This is the most obvious example of a SV that is being uploaded more frequently than normal. The fact that it is being uploaded more frequently is based on the shape of the dashed green curve which indicates the number of points in each AOD bin. The scale for this curve is on the right-hand vertical axis. The green curve does not exhibit the plateau seen in most plots but instead has a downward slope in the number of points as the AOD increases. If the SV were consistently being uploaded at a given interval, there would still be a plateau, only shorter than the typical plateau. For example, if an SV were being uploaded every 12 hours, one would expect a plateau from somewhere around an hour AOD out to 12 hours AOD. The near linear trend implies that the upload time for this SV is variable over a fairly large range.
- SVN 65/PRN 24: This Block IIF shows indications of occasional contingency uploads. This conclusion is based on the manner in which the SIS URE value line tends to flatten as it approaches the 3 m magnitude and the fact that the number of points starts to decline far earlier than the other Block IIF SVs. This is consistent with the higher 95^{th} percentile URE shown in Table 3.1 and Figure 3.1. It is likely related to the fact that SVN 65/PRN 24 is using a Cesium frequency reference. SVN 72/PRN 8 (which also uses a Cesium frequency reference) shows similar but less pronounced characteristics.

A.2 Block IIA SVs

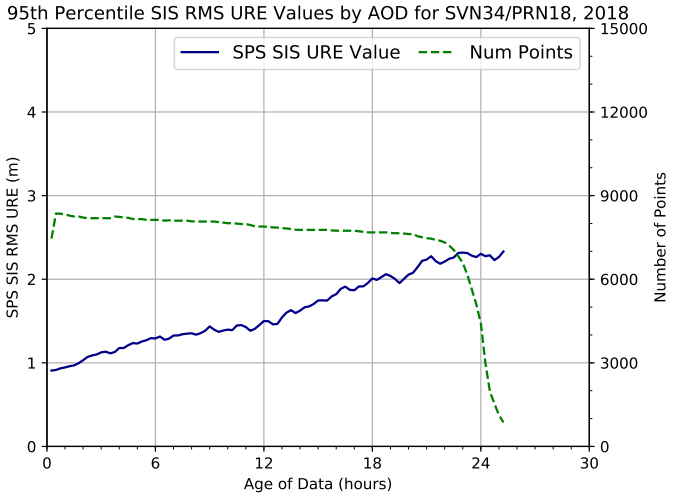

A.3 Block IIR SVs

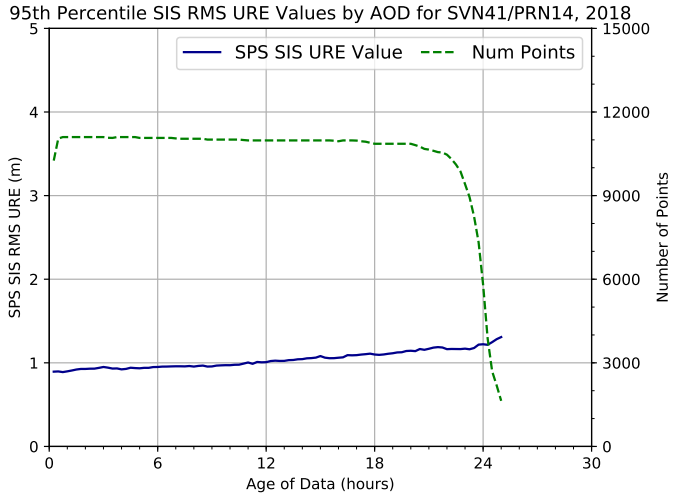

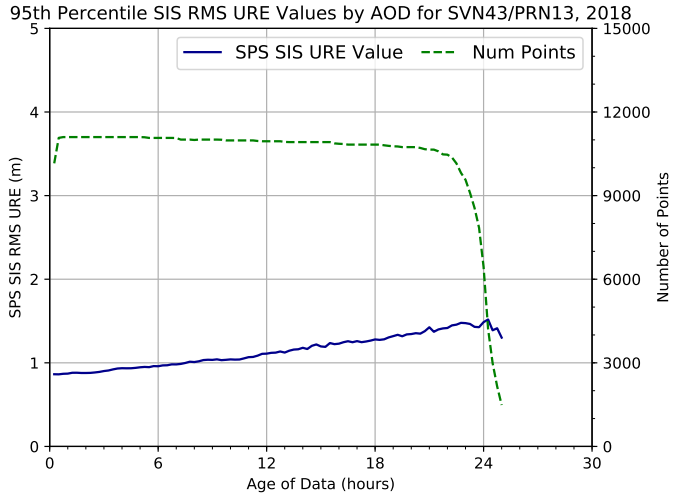

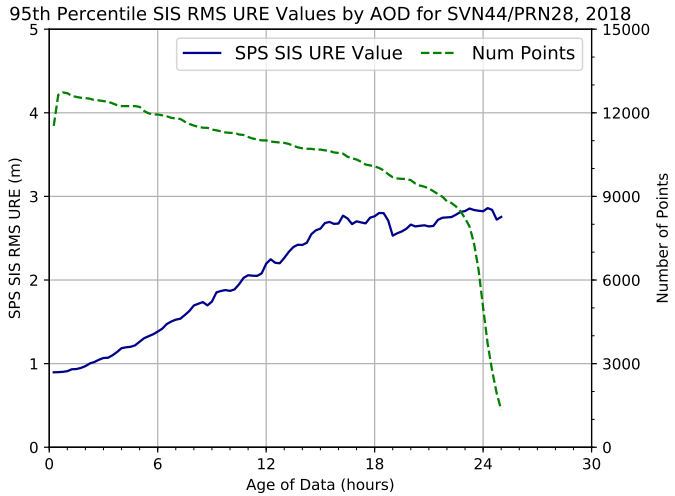

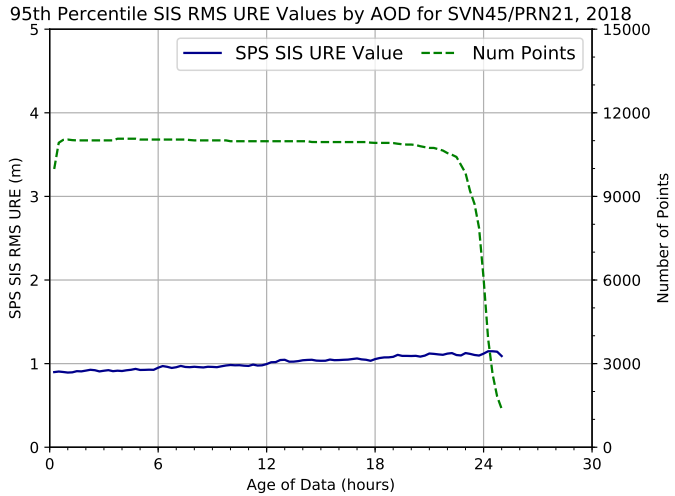

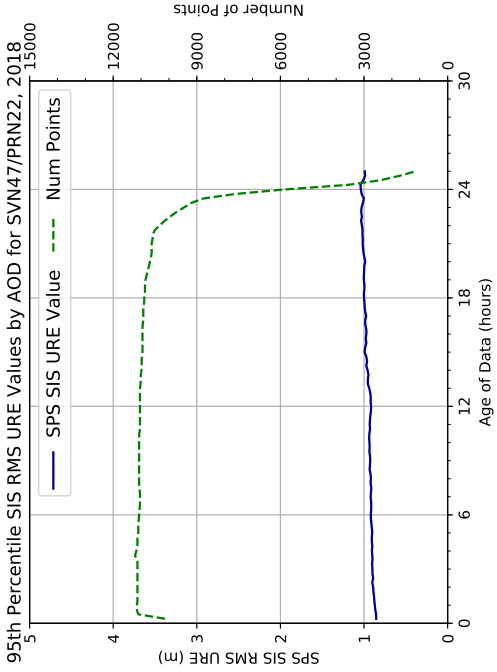
95th Percentile SIS RMS URE Values by AOD for SVN47/PRN22, 2018
SPS SIS URE Value
Num Points
SPS SIS RMS URE (m)
Number of Points
Age of Data (hours)

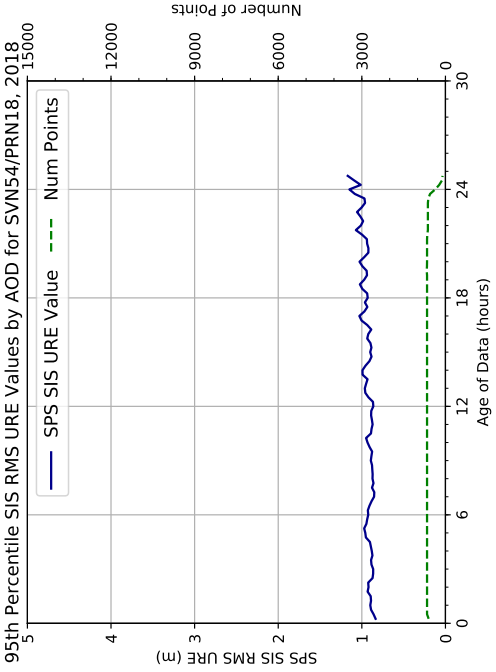
95th Percentile SIS RMS URE Values by AOD for SVN54/PRN18, 2018
SPS SIS URE Value
Num Points
SPS SIS RMS URE (m)
Number of Points
Age of Data (hours)

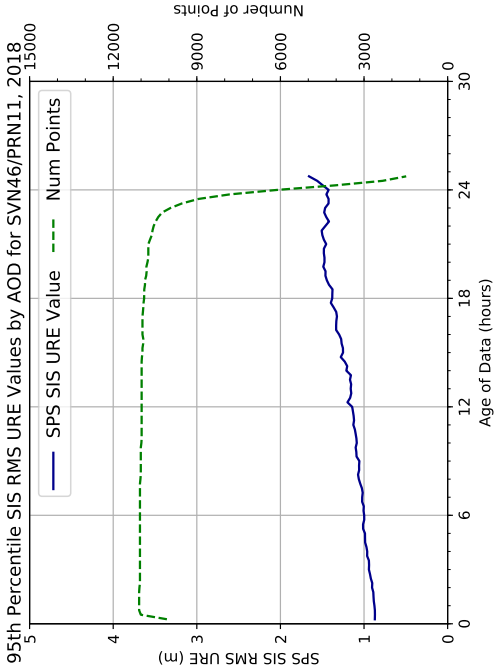
95th Percentile SIS RMS URE Values by AOD for SVN46/PRN11, 2018
SPS SIS URE Value
Num Points
SPS SIS RMS URE (m)
Number of Points
Age of Data (hours)

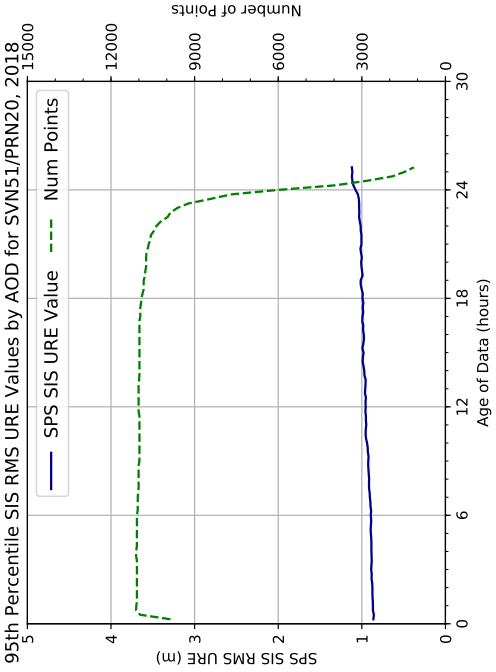
95th Percentile SIS RMS URE Values by AOD for SVN51/PRN20, 2018
SPS SIS URE Value
Num Points
SPS SIS RMS URE (m)
Number of Points
Age of Data (hours)

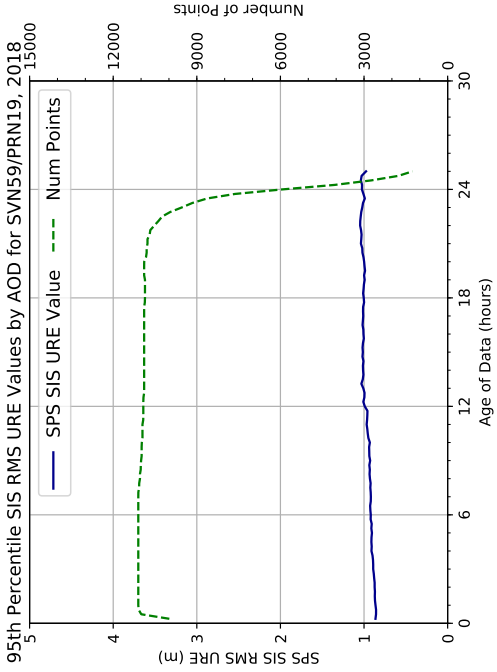
95th Percentile SIS RMS URE Values by AOD for SVN59/PRN19, 2018
SPS SIS URE Value
Num Points
SPS SIS RMS URE (m)
Number of Points
Age of Data (hours)

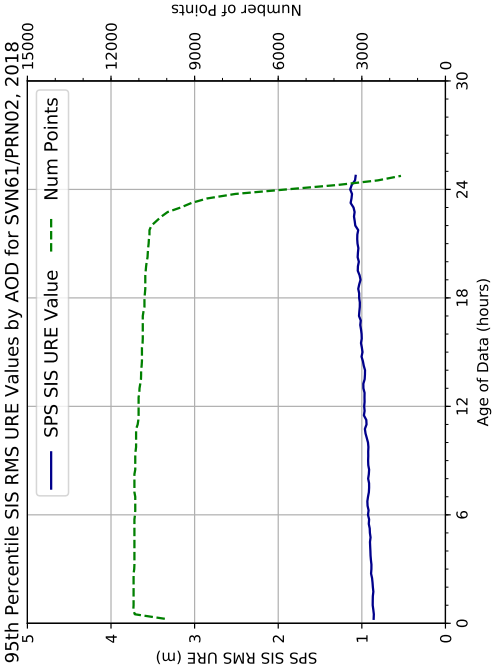
95th Percentile SIS RMS URE Values by AOD for SVN61/PRN02, 2018
SPS SIS URE Value
Num Points
SPS SIS RMS URE (m)
Number of Points
Age of Data (hours)

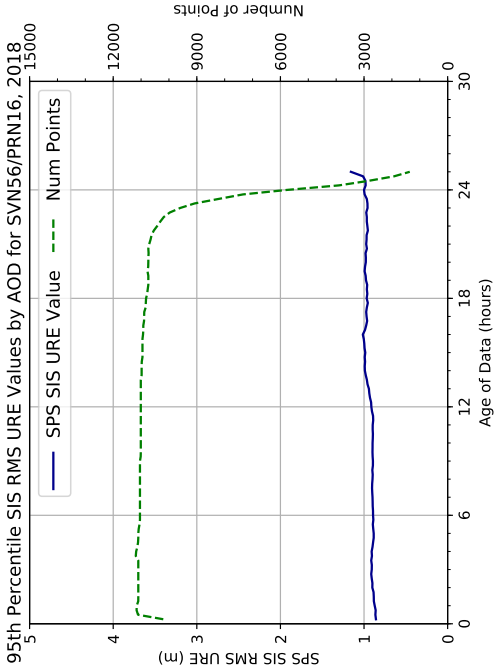
95th Percentile SIS RMS URE Values by AOD for SVN56/PRN16, 2018
SPS SIS URE Value
Num Points
SPS SIS RMS URE (m)
Number of Points
Age of Data (hours)

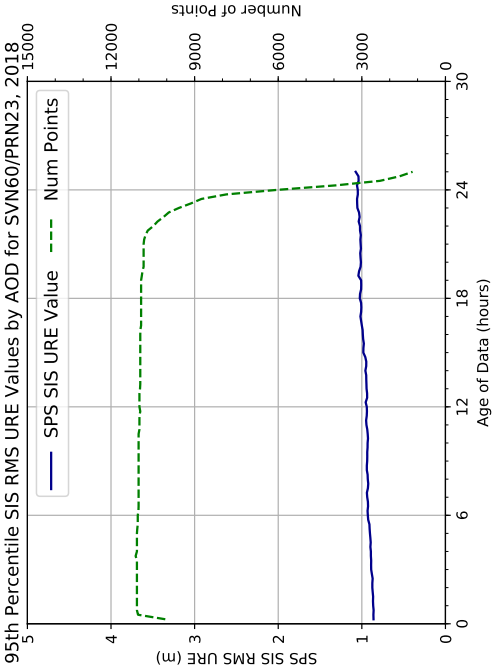
95th Percentile SIS RMS URE Values by AOD for SVN60/PRN23, 2018
SPS SIS URE Value
Num Points
SPS SIS RMS URE (m)
Number of Points
Age of Data (hours)

A.4 Block IIR-M SVs

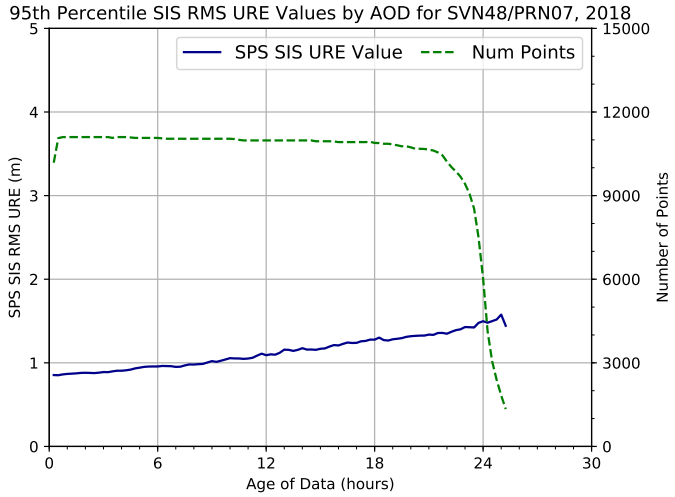

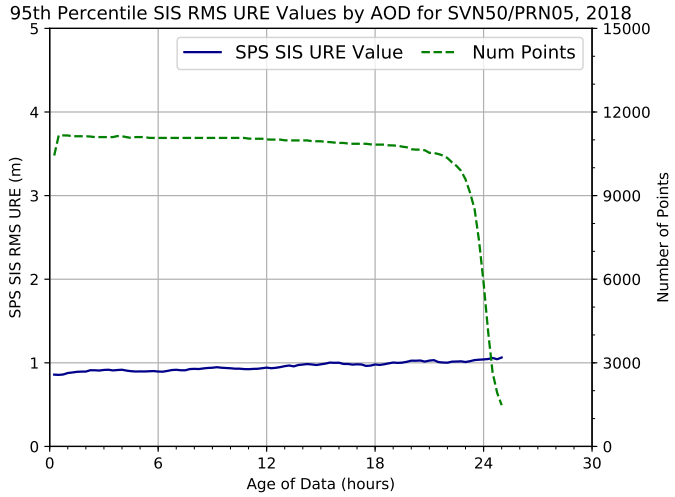

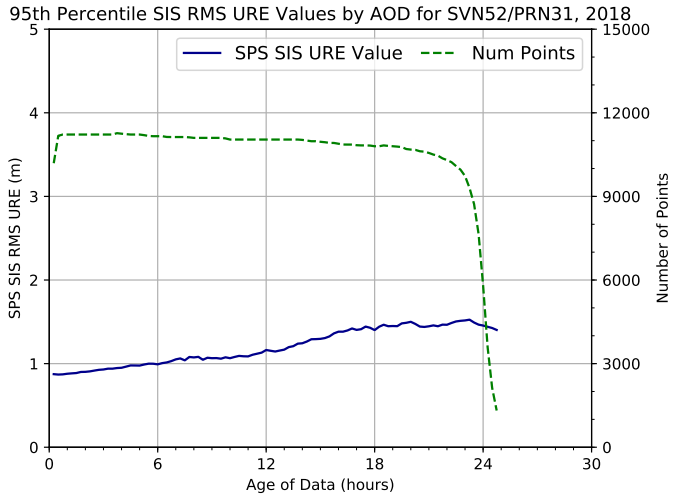

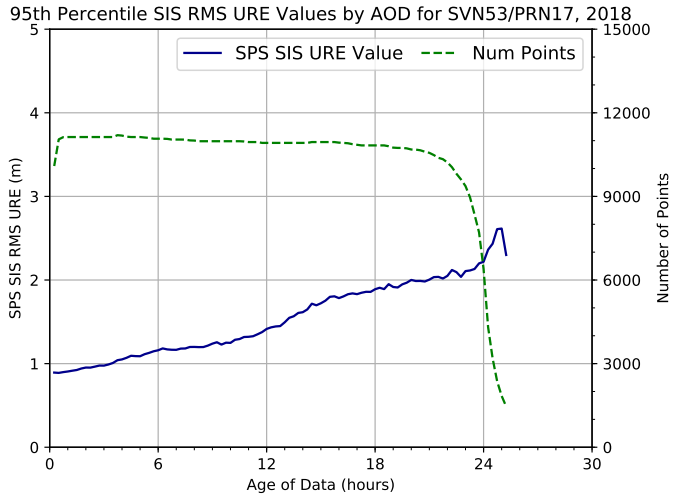

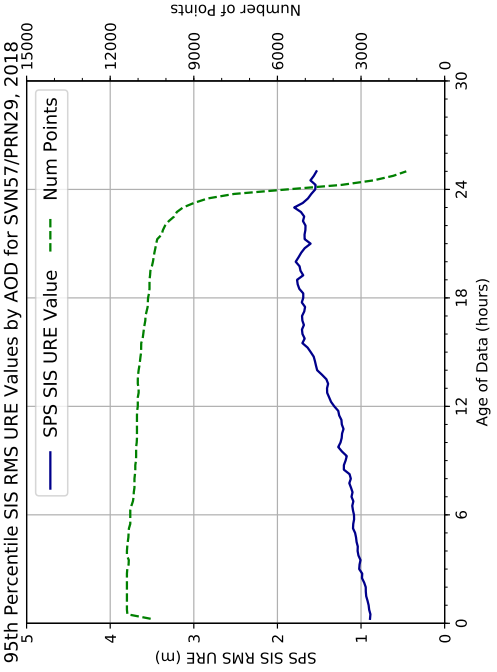
95th Percentile SIS RMS URE Values by AOD for SVN57/PRN29, 2018
SPS SIS URE Value
Num Points
SPS SIS RMS URE (m)
Number of Points
Age of Data (hours)

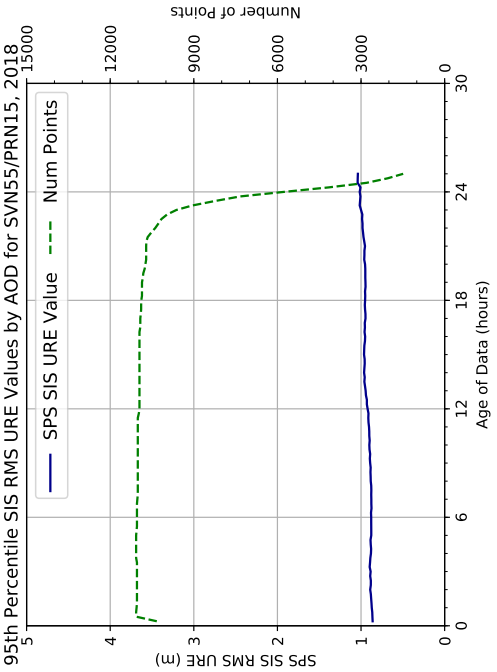
95th Percentile SIS RMS URE Values by AOD for SVN55/PRN15, 2018
SPS SIS URE Value
Num Points
SPS SIS RMS URE (m)
Number of Points
Age of Data (hours)

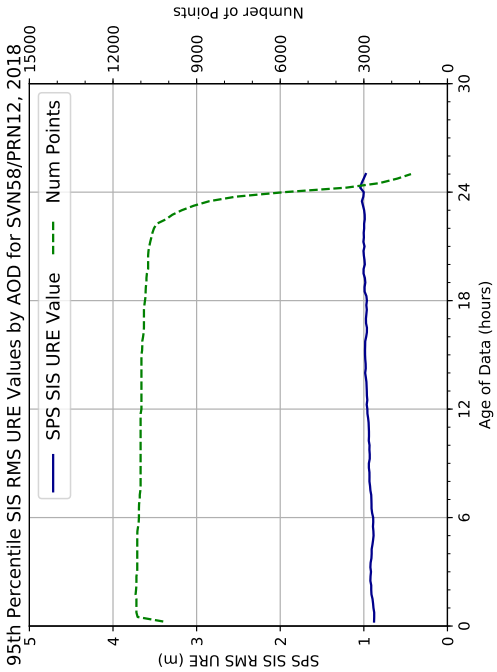
95th Percentile SIS RMS URE Values by AOD for SVN58/PRN12, 2018
SPS SIS URE Value
Num Points
SPS SIS RMS URE (m)
Number of Points
Age of Data (hours)

A.5 Block IIF SVs

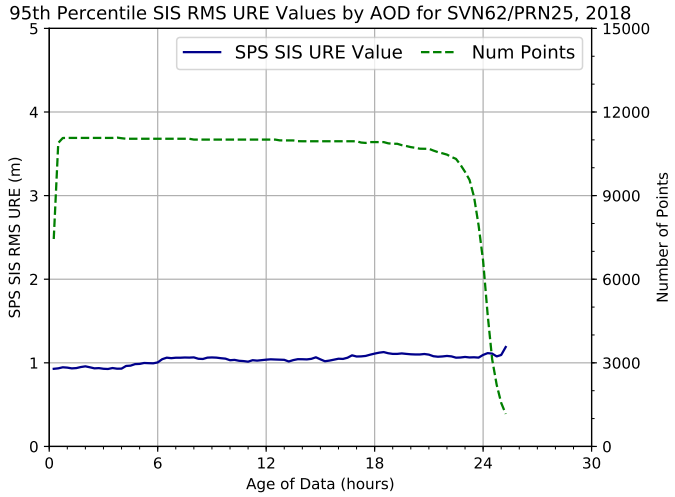

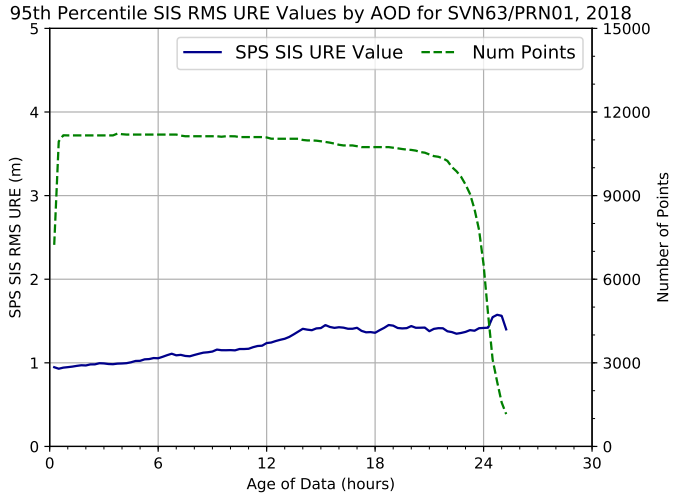

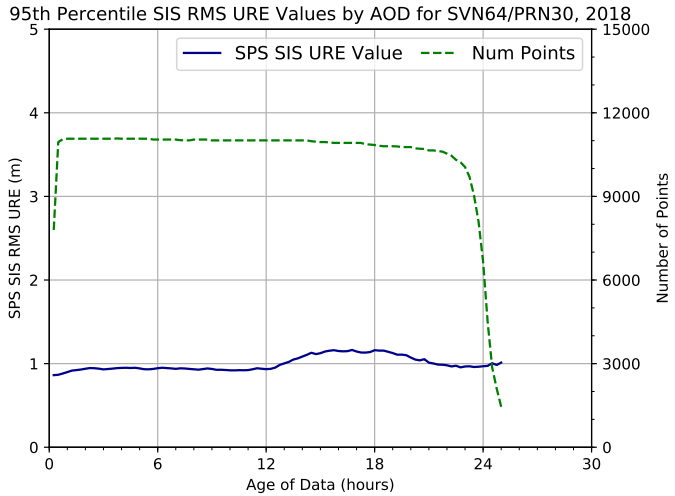

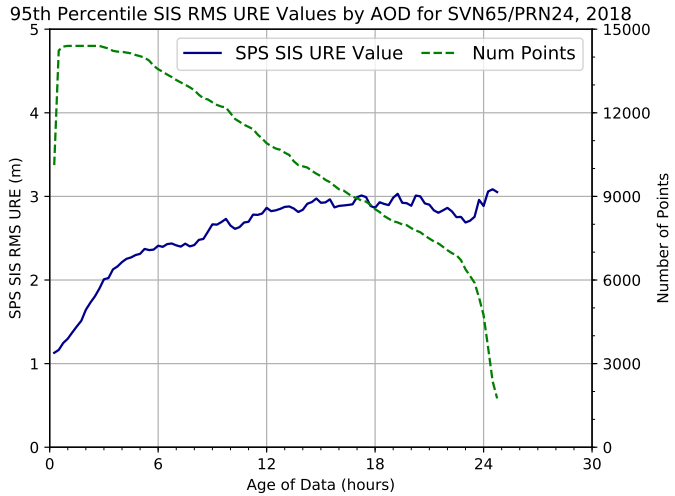

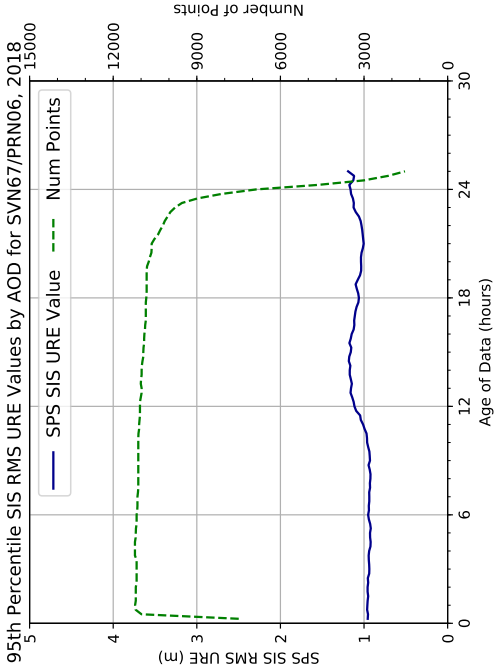
95th Percentile SIS RMS URE Values by AOD for SVN67/PRN06, 2018
SPS SIS URE Value
Num Points
SPS SIS RMS URE (m)
Number of Points
Age of Data (hours)

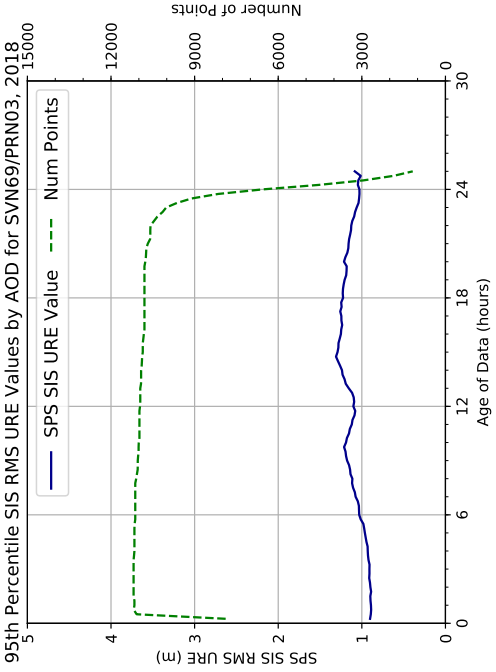
95th Percentile SIS RMS URE Values by AOD for SVN69/PRN03, 2018
SPS SIS URE Value
Num Points
SPS SIS RMS URE (m)
Number of Points
Age of Data (hours)

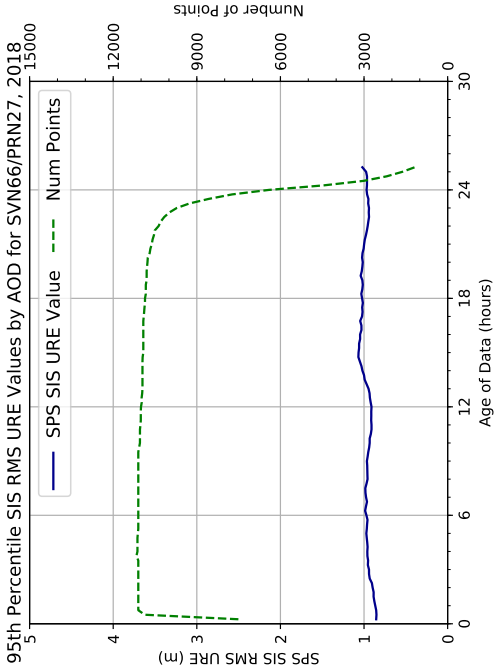
95th Percentile SIS RMS URE Values by AOD for SVN66/PRN27, 2018
SPS SIS URE Value
Num Points
SPS SIS RMS URE (m)
Number of Points
Age of Data (hours)

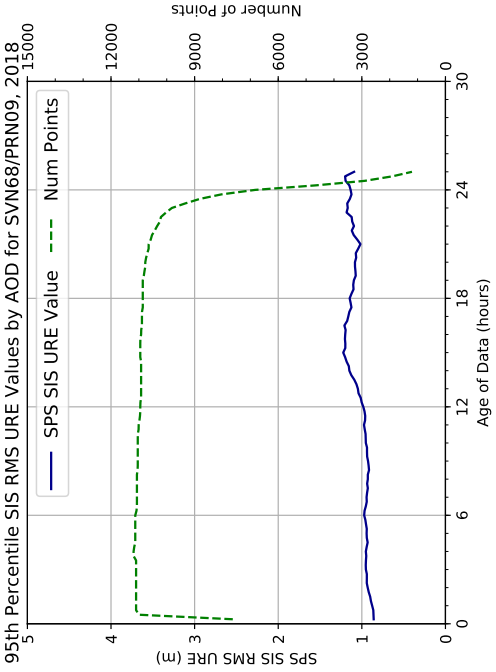
95th Percentile SIS RMS URE Values by AOD for SVN68/PRN09, 2018
SPS SIS URE Value
Num Points
SPS SIS RMS URE (m)
Number of Points
Age of Data (hours)

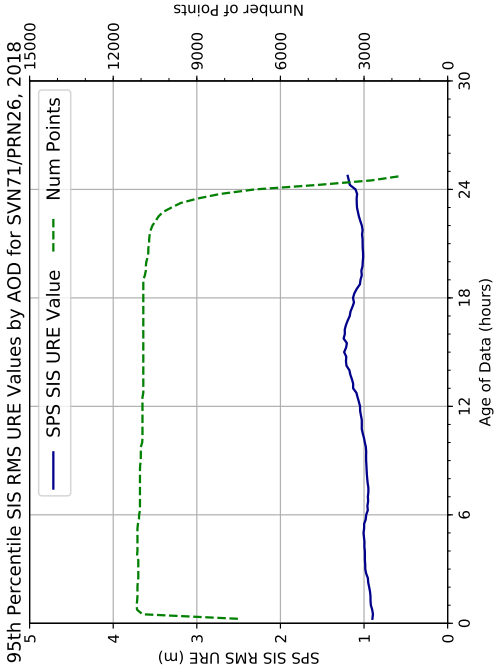
95th Percentile SIS RMS URE Values by AOD for SVN71/PRN26, 2018
SPS SIS URE Value
Num Points
SPS SIS RMS URE (m)
Number of Points
Age of Data (hours)

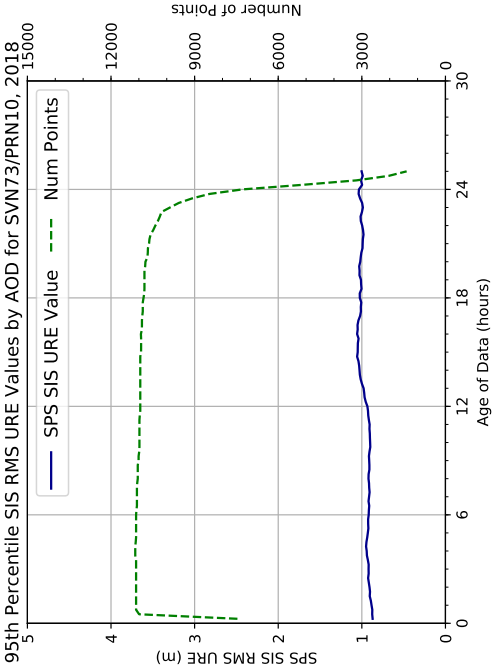
95th Percentile SIS RMS URE Values by AOD for SVN73/PRN10, 2018
SPS SIS URE Value
Num Points
SPS SIS RMS URE (m)
Number of Points
Age of Data (hours)

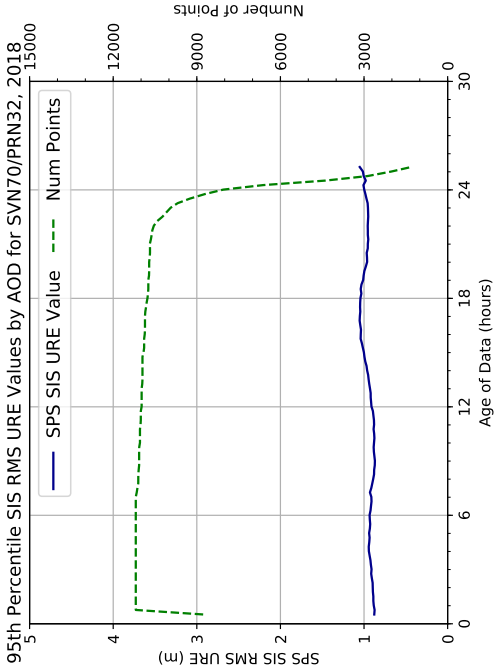
95th Percentile SIS RMS URE Values by AOD for SVN70/PRN32, 2018
SPS SIS URE Value
Num Points
SPS SIS RMS URE (m)
Number of Points
Age of Data (hours)

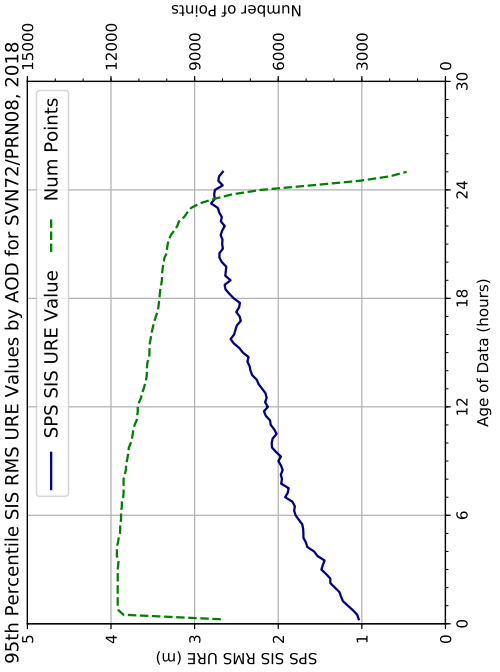
95th Percentile SIS RMS URE Values by AOD for SVN72/PRN08, 2018
SPS SIS URE Value
Num Points
SPS SIS RMS URE (m)
Number of Points
Age of Data (hours)

Appendix B

Analysis Details

B.1 URE Methodology

User range error (URE) represents the accuracy of the broadcast navigation message. There are a number of error sources that affect the URE, including errors in broadcast ephemeris and timing.

Two methods to URE analysis are provided in this report. The first method (Section B.1.2) uses separate statistical processes over space and time to arrive at a URE. The second method (Section B.1.3) derives the URE by a single statistical process but is more computationally demanding.

B.1.1 Clock and Position Values for Broadcast and Truth

The URE values in this report are derived by comparison of the space vehicle (SV) clock and position representations as computed from the broadcast clock and position (BCP) as transmitted in the Legacy Navigation (LNAV) message against the SV truth clock and position data (TCP) provided by a precise orbit calculated after the time of interest.

The broadcast LNAV message data used in the calculations were collected by the National Geospatial-Intelligence Agency (NGA) Monitor Station Network (MSN) (Section B.2). The broadcast LNAV messages provide a set of parameters for an equation which can be evaluated at any time for which the parameters are valid. Our process evaluates the parameters at either a 30 s or 5 min cadence (depending on the setup options).

The TCP values are computed from the archived NGA products. The NGA products used in the calculations are the antenna phase center (APC) precise ephemeris (PE) files available from the NGA public website [13]. The NGA products are published in tabular SP3 format, with positions and clocks provided at a 5 min cadence. When TCP data are needed at a 5 min cadence, a simple table look-up is sufficient. When TCP data are needed at a 30 s cadence, a Lagrange interpolation scheme is used, in which the five points prior to and after the estimation time are used to estimate the SV position. Clock interpolation is handled via a linear interpolation between adjacent points.

B.1.2 95th Percentile Global Average in the SPS PS

The SPSPS08 specifications for URE suggest averaging across the service volume visible to a GPS SV at any specified point in time. The process is illustrated in Figure B.1.

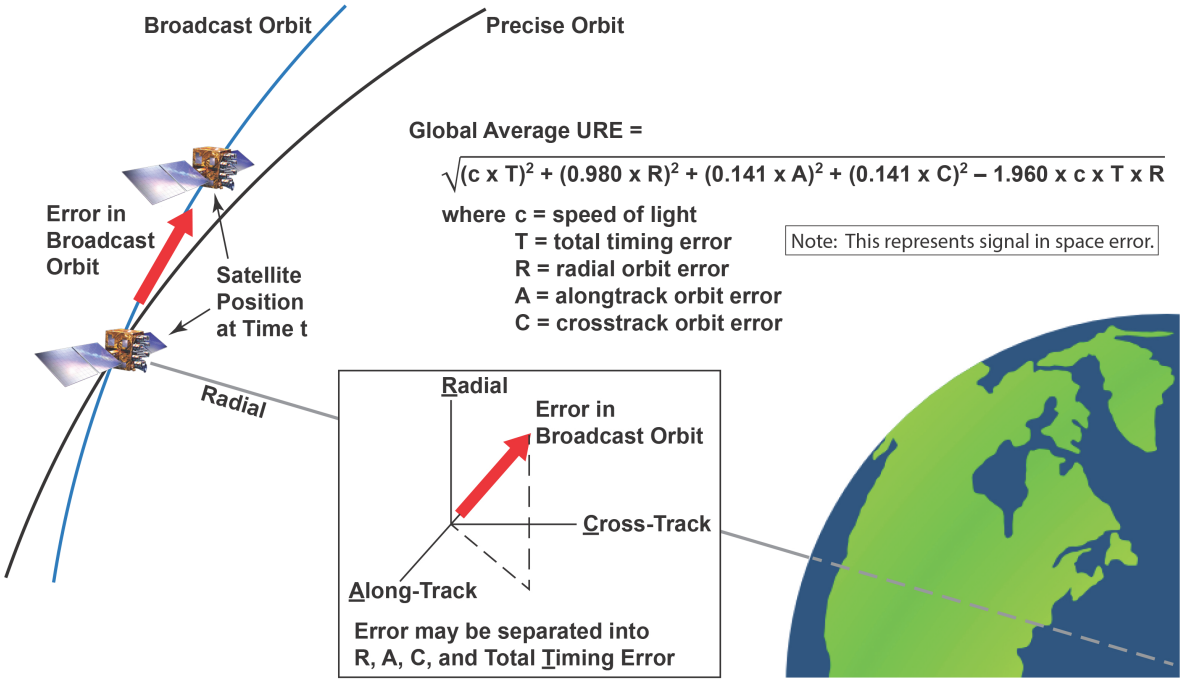

Figure B.1: Global Average URE as defined in SPS PS

The equation shown in Figure B.1 is Equation A-1 of SPSPS08 Section A.4.11. This expression allows the computation of the URE from known errors. Based on the coefficients of this equation, the URE is calculated for a surface corresponding to the WGS 84 radius of the Earth.

For purposes of this report, the Instantaneous RMS SIS URE values were generated at 30 s intervals for all of 2018. The URE was formed by differencing the BCP and TCP to obtain the radial, along-track, cross-track, and time errors at each epoch. These errors were used as inputs to the SPSPS08 Equation A-1.

After the Instantaneous RMS SIS URE values were computed, values for periods when each SV was unhealthy or not broadcasting were discarded. The remaining values were then grouped by monthly period for each SV and sorted; the maximum and the 95^{th} percentile values within a given month were identified for each SV. This is the basis for Table 3.2. The monthly grouping corresponds closely to the 30 day period suggested in Note 2 of SPSPS08 Section 3.4, while being more intuitive to the reader.

B.1.3 An Alternate Method

The previous method computes an SIS Instantaneous RMS URE (an average over space) for a given SV at a 30 s cadence over a month, then selects a 95^{th} percentile value from that set. That is to say, two different statistical processes are combined.

An alternate method is to compute the SIS Instantaneous URE for a large number of locations at each time point and store those results. For each SV, this is done for a series of time points at a selected cadence, and the collection of SIS Instantaneous URE values at each time point are stored. Once the values for all the time points for a month have been computed, the absolute values of SIS Instantaneous URE values for all time points are gathered together in a monthly set. The 95^{th} percentile value is selected from that set.

This method uses an approximation of an equidistant grid over the portion of the Earth visible to the SV with a spacing of roughly 550 km (5° latitude on the surface of the Earth). Considering those points at or above a 5° elevation angle with respect to the SV, this yields a set of 577 SIS Instantaneous URE values for each SV for each evaluation time. Figure B.2 illustrates this set of grid points for a particular SV-time shown as a projection onto the surface of the Earth.

This was done at a cadence of 5 min for each SV for all of 2018 and all 577 values were stored for all time points. Sets of values corresponding to each month were extracted (approximately 5 million values per SV-month). The absolute values and 95^{th} percentile values for each month were selected as the result for the SV-month. This is the basis for Table 3.3.

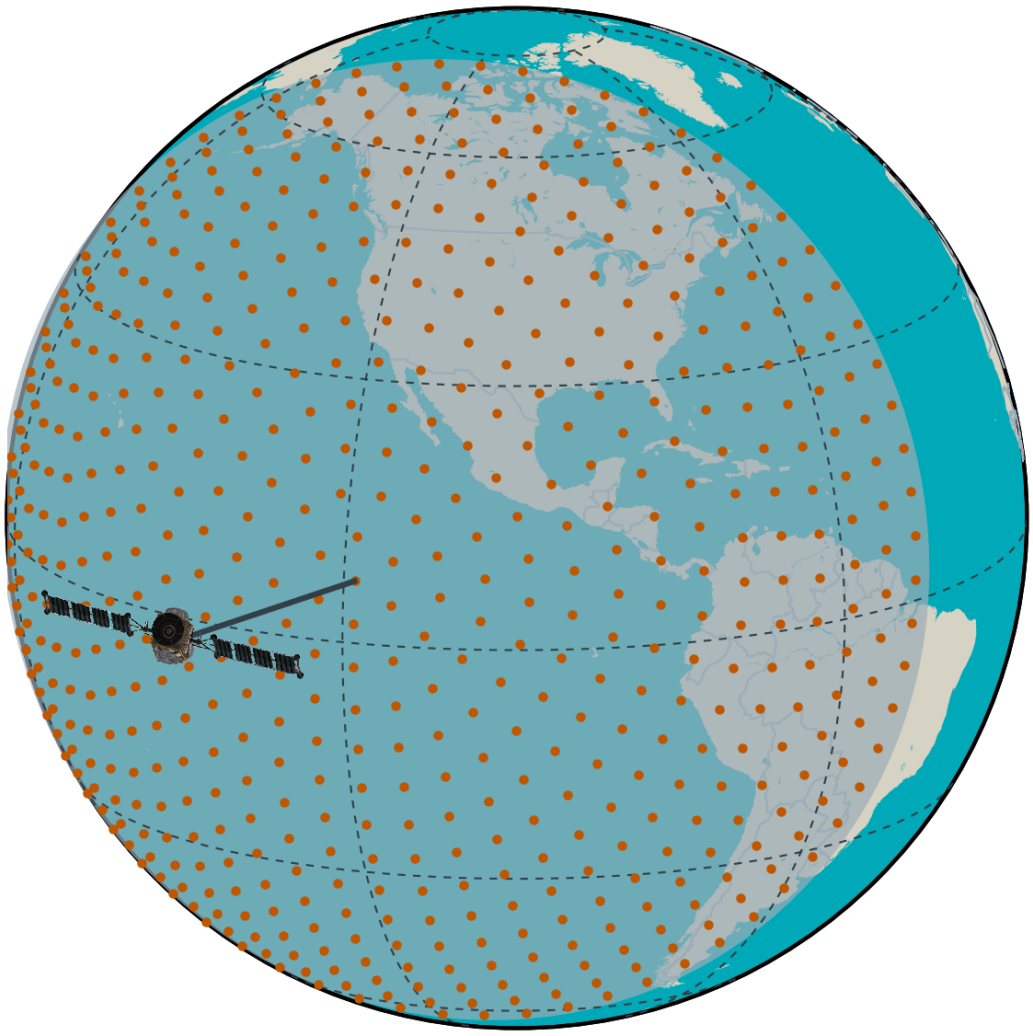

Figure B.2: Illustration of the 577 Point Grid

B.1.4 Limitations of URE Analysis

There are a number of subtleties in this method to computing URE accuracies, and the following paragraphs detail some of these.

The methods described in Sections B.1.1-B.1.3 work well when the estimated URE accuracy is below the required thresholds, as it verifies that the system is operating as expected. However, experience has shown that when an actual problem arises, the use of this procedure, without other cross-check mechanisms, can create some issues and may lead to incorrect results. Consider the following two cases.

- In cases where an SV is removed from service for reasons that invalidate the broadcast ephemeris (such as a clock run-off) we need to compare the time at which the removal from service occurred with the time at which any of the URE accuracy bounds were exceeded to assess whether a violation of the SPS PS metrics occurred. However, because we have relied on the interpolation process to generate 30 s values, we cannot obtain an accurate estimate of the time at which the URE bound was exceeded. As a general rule, the UREs computed in our process should be reviewed when they are contained between two SP3 epochs, one of which contains a clock event.

- When an SV is set unhealthy or cannot be tracked, the PE may provide misleading results. The analyst preparing the PE has several options for handling discontinuities that occur during outages. Therefore, the URE values generated near such events may be incorrect. As a result, it is necessary to avoid accepting UREs into the statistical process under conditions in which the SV could not be tracked or was set unhealthy. This has been done for all the results presented here.

In all cases, when an apparent violation of the URE limits is encountered, we choose to reconcile the analysis described above with the behavior of ORDs formed from the data collected at NGA and IGS sites. Because the observational data used is collected at a 30 s cadence, we obtain a much higher resolution insight into the details of the actual event than we do with the interpolated PE.

B.2 Selection of Broadcast Navigation Message Data

Several of the processes used in deriving the results in this report are dependent on the broadcast navigation message data. In most cases the data needed are the clock, ephemeris, and integrity data (CEI data) contained in subframes 1, 2, and 3 of the GPS legacy navigation message (LNAV). These data are most often required in order to derive the position and/or health status of the transmitting SV.

The goal in selecting the CEI data for a given SV at a given time of interest is to reproduce what the user would have experienced had they been collecting data from that SV at that time. To accomplish this, the process must have access to a complete time-history of navigation message data and it must properly select specific sets of CEI data from that time-history.

The navigation message data supporting this analysis were collected from the NGA MSN. The MSN has complete dual-station visibility to all GPS SVs (and generally much better). The redundant data sets at each navigation message epoch are cross-compared in order to best determine what was actually broadcast from each SV at each navigation message epoch. The MSN data collection process is designed to capture the earliest transmission of each unique set of CEI data. The data are stored in a format that retains all the transmitted bits. As part of the analysis associated with the production of this report, any gaps in the data set are investigated and filled if practical. The results is an archived time-history of the unique CEI data sets transmitted by the constellation.

Wherever the analysis process requires CEI data for a given SV at a given time, it selects the CEI data set from the archive that corresponds to what was being transmitted from the SV at that time. During periods in which new data is being transmitted (data set cutovers), the preceding CEI data set is used until the time the new CEI data set had been completely transmitted and available to the user.

It must be recognized that this may be an inexact reproduction of the experience of any given user. Users may experience delays in the receipt of newly transmitted navigation message data due to obstructions, atmospheric issues, or receiver problems. However, this process is deterministic and reproducible.

B.3 AOD Methodology

The AOD was calculated by finding the upload times based on the t_{oe} offsets as defined in IS-GPS-200 Section 20.3.4.5 and then examining the t_{nmct} under the following assumptions:

- A complete set of the subframe 1, 2, and 3 data broadcast by all SVs of interest is available throughout the time period of interest.
- The term t_{nmct} defined in IS-GPS-200 Section 20.3.3.4.4 represents the time of the Kalman state used to derive the corresponding navigation message.

Given these assumptions, the AOD at any point in time can be determined by the following process:

- Working backward from the time of interest to finding the time when the most recent preceding upload was first broadcast
- Finding the AOD offset (AODO) of the associated subframe 2
- Subtracting the AODO from the t_{oe} (as described in IS-GPS-200 20.3.3.4.4) to determine the time of the Kalman state parameters
- Calculating the difference between the time of interest and the Kalman state parameter time

The search for the preceding upload is necessary because the AODO has a limited range and is not sufficient to maintain an accurate count for a complete upload cycle.

The results of this algorithm are generally consistent with the results provided by MCS analysis. The first assumption is fulfilled by the NGA MSN archive. The remaining assumptions were discussed with systems engineers supporting 2SOPS and are believed to be valid.

The exception to this process is PRN 32. Any SV assigned to PRN 32 presents a minor problem for this analysis. This problem is limited to the type of performance analysis presented in this report. There is no similar concern for a GPS receiver. The AOD values are based on the AODO field in subframe 2. The definition of the AODO field is tied to how AODO is used to determine the age of the data in the NMCT. PRN 32 can never be represented in the NMCT due to the design of the navigation message. Therefore, the AODO field for PRN 32 is never reset to zero at a new upload but remains at the "all ones" state. Therefore, the AOD for PRN 32 cannot be independently derived from the navigation message data. For purposes of this report we examined all upload cutovers through 2018 for all SVs except SVN 70/PRN 32. For each upload cutover we computed the AOD at the time of the upload cutover. We then computed the mean of these samples to determine an average AOD at the time of the upload cutover. There were 11564 samples with an average AOD of 953 sec (about 16 minutes). We assumed this average holds true for SVN 70/PRN 32 and conducted the analysis accordingly.

B.4 Position Methodology

Section 2.4.5 of SPSPS08 provides usage assumptions for the SPS PS and some of the notes in Section 2.4.5 are relevant to the question of position determination. The following is quoted from Section 2.4.5:

"The performance standards in Section 3 of this SPS PS do not take into consideration any error source that is not under direct control of the Space Segment or Control Segment. Specifically excluded errors include those due to the effects of:

- *Signal distortions caused by ionospheric and/or tropospheric scintillation*
- *Residual receiver ionospheric delay compensation errors*
- *Residual receiver tropospheric delay compensation errors*
- *Receiver noise (including received signal power and interference power) and resolution*
- *Multipath and receiver multipath mitigation*
- *User antenna effects*
- *Operator (user) error"*

In addition, at the beginning of Section 3.8, the SPSPS08 explains that in addition to the error exclusions listed in Section 2.4.5, the following assumptions are made regarding the SPS receiver:

"The use of a representative SPS receiver that:

- *is designed in accordance with IS-GPS-200*
- *is tracking the SPS SIS from all satellites in view above a 5° mask angle... It is assumed the receiver is operating in a nominal noise environment...*
- *accomplishes satellite position and geometric range computations in the most current realization of the WGS 84 Earth-Centered, Earth-Fixed (ECEF) coordinate system.*
- *generates a position and time solution from data broadcast by all satellites in view*
- *compensates for dynamic Doppler shift effects on nominal SPS ranging signal carrier phase and C/A code measurements.*
- *processes the health-related information in the SIS and excludes marginal and unhealthy SIS from the position solution.*
- *ensures the use of up-to-date and internally consistent ephemeris and clock data for all satellites it is using in its position solution.*
- *loses track in the event a GPS satellite stops transmitting a trackable SIS.*
- *is operating at a surveyed location (for a time transfer receiver)."*

To address these standards, the following approach was adopted for computing a set of accuracy statistics:

1. 30 s GPS observations were collected from the NGA GPS monitor station network and a similar set of 31 IGS stations. This decision addressed the following concerns:
   (a) All stations selected collect dual-frequency observations. Therefore the first-order ionospheric effects can be eliminated from the results.
   (b) All stations selected collect weather observations. The program that generates the positions uses the weather data to eliminate first order tropospheric effects.
   (c) The receiver thermal noise will not be eliminated, but both the NGA and IGS stations are generally using the best available equipment, so effects will be limited.
   (d) Similarly, multipath cannot be eliminated, but both networks use antennas designed for multipath reduction, and station sites are chosen to avoid the introduction of excessive multipath.
   (e) Antenna phase center locations for such stations are very well known. Therefore, position truth is readily available.
   (f) Despite the similarities, the two networks are processed separately for a variety of reasons.
      i. The NGA GPS network uses receivers capable of tracking the Y-code. As a result, the individual observations have somewhat better SNR than the observations from the IGS stations.
      ii. By contrast, the IGS stations are tracking L1 C/A and L2 codeless, then averaging their observations over 30 s in order to reduce noise on the data.
      iii. The NGA GPS network uses a single receiver which limits the number of receiver-specific traits but leaves the possibility that a systemic problem could affect all receivers. The IGS network uses a variety of receivers, which is some proof against systemic problems from a single receiver, but requires that the processing address a variety of receiver-specific traits.
      iv. The NGA network is operated and maintained by a single organization. Changes are rare and well-controlled. The IGS network is cooperative in nature. While policies are in place to encourage operational standards changes in station behavior are not as well-coordinated.
2. Process the data using a comprehensive set of broadcast ephemerides collected as described in Appendix B.2.

3. Process the collected observations using the PRSOLVE program of the ARL:UT-hosted open source GPS Toolkit (GPSTk)[14]. Note:

   (a) PRSOLVE meets the relevant requirements listed above. For example, SV positions are derived in accordance with IS-GPS-200, the elevation mask is configurable, weather data is used to estimate tropospheric effects, and WGS 84 [12] conventions are used. Data from unhealthy SVs were removed from PRSOLVE using an option to exclude specific satellites.

   (b) PRSOLVE is highly configurable. Several of the items in the preceding list of assumptions are configuration parameters to PRSOLVE.

   (c) Any other organization that wishes to reproduce the results should be able to do so. (Both the algorithm and the data are publically available.)

4. Process the collected 30 s observations in two ways:

   (a) Use all SVs in view without data editing in an autonomous pseudorange solution to generate 30 s position residuals at all sites.

   (b) Use a receiver autonomous integrity monitoring (RAIM) algorithm (another PRSOLVE option) to remove outlier pseudorange measurements from which a "clean" set of 30 s position residuals is generated at all sites. The RAIM algorithm used by PRSOLVE is dependent on several parameters, the two most important of which are the RMS limit on the post-fit residuals (default: 3.0 m) and the number of SVs that can be eliminated in the RAIM process (default: unlimited). This analysis was conducted using the default values.

5. Compute statistics on each set of data independently.

Appendix C

PRN to SVN Mapping for 2018

Throughout the report, SVs have been referred to by both PRN and SVN. The PRN to SVN mapping is time dependent as PRN assignments change. Keeping track of this relationship has become more challenging over the past few years as the number of operational SVs is typically very close to the number of available PRNs. Therefore it is useful to have a summary of the PRN to SVN mapping as a function of time. Figure C.1 presents that mapping for 2018. SVNs on the right vertical axis appear in the order in which they were assigned the PRN values in 2018. Colored bars indicate the range of time each relationship was in effect. Start and end times of relationships are indicated by the dates at the top of the chart.

These data are assembled from the NANUs and the operational advisories, and confirmed by discussion with The Aerospace Corporation staff supporting 2SOPS.

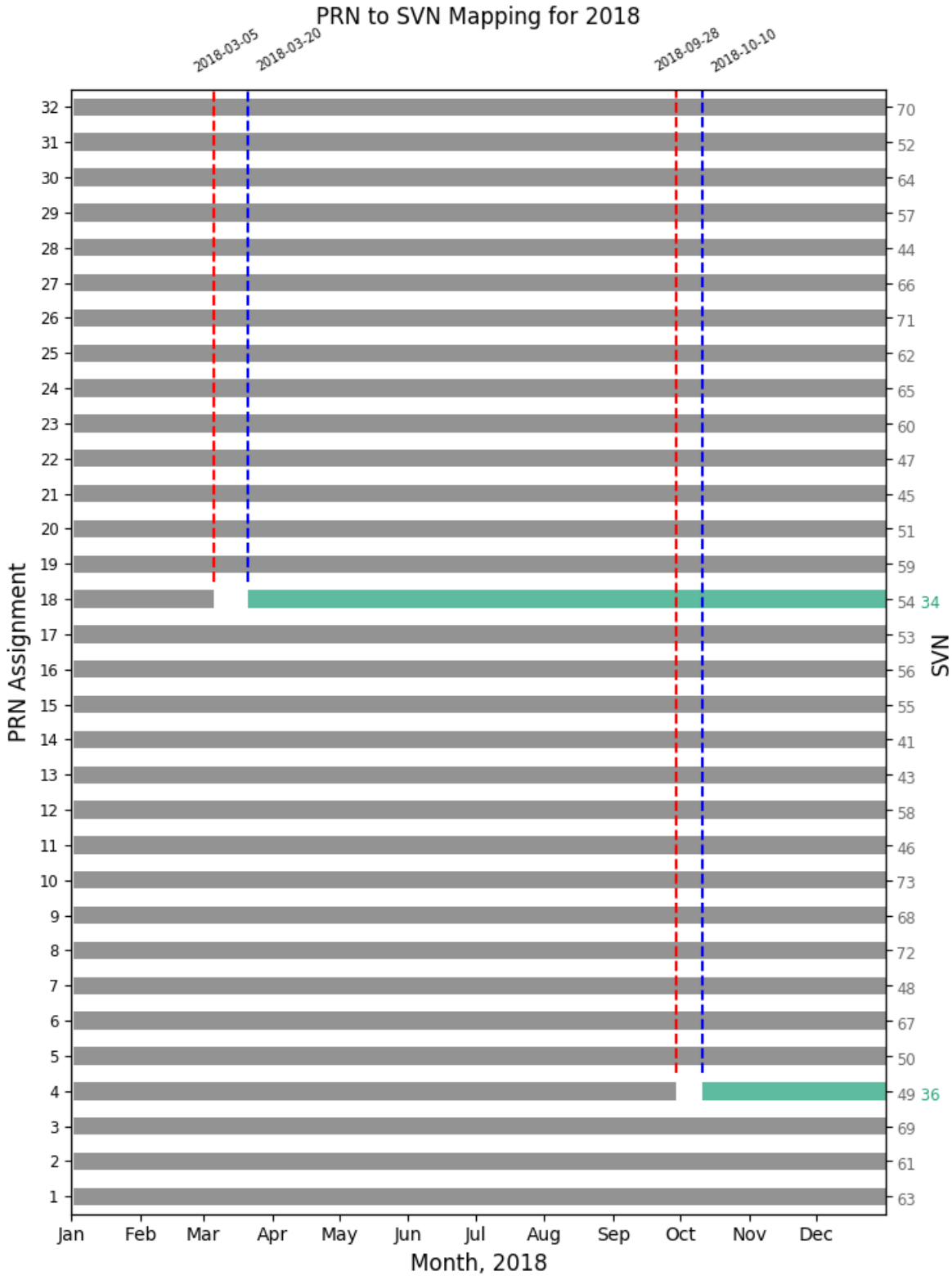

Figure C.1: PRN to SVN Mapping for 2018

Appendix D

NANU Activity in 2018

Several sections in the report make use of NANUs. It is useful to have a time history of the relevant NANUs sorted by SVN. This makes it convenient to determine which NANU(s) should be examined if an anomaly is observed for a particular satellite at a particular time.

Figure D.1 presents a plot of the NANU activity in 2018. Blue bars represent scheduled outages and red bars represent unscheduled outages. Gray bars represent SVs that have been decommissioned. SVN 54 was decommissioned in 2018. Yellow bars indicate scheduled outages with notice of less than 48 hours. There were no such events in 2018. NANU numbers are indicated next to each bar. In the event there is more than one NANU for an outage, the last NANU number is displayed.

Figure D.1: Plot of NANU Activity for 2018

Appendix E

SVN to Plane-Slot Mapping for 2018

Several assertions are related to the performance of the constellation as defined by the plane-slot arrangement specified in the performance standard. Evaluation of these assertions requires information on the plane-slot occupancy during the year.

The constellation definition located in Section 3.2 of the SPSPS08 that provides the plane-slot definitions is an ideal model in the sense that it assumes all SVs have zero eccentricity and nominal inclination. Slots within a plane are defined by the Ground-track Equatorial Crossing (GEC) value (also known as the Geographic Longitude of the Ascending Node (GLAN) value). In the real world, small discrepancies in orbit insertion lead to a situation in which some SVs are less well-positioned than others. The operators manage the SV locations within the constellation in order to achieve the desired coverage (DOP) as documented in Section 3.6 of this report. In some cases, this means assigning plane-slot identifiers to SVs that are fulfilling the responsibility of a particular plane-slot but may not be strictly within the slot as defined by GEC (GLAN). This makes independent verification of plane-slot assignments a challenge.

Information on plane-slot assignment is included in the operational advisory (OA) provided by 2SOPS to the United States Coast Guard (USCG) Navigation Center and defined in ICD-GPS-240. This is a publicly available document and is one of the ways the public is informed of slot assignments. However, the format of the OA does not permit it to clearly convey the status of expanded slots. The format is limited to a letter representing the plane and a number representing the slot. There is no provision of the "fore/aft" designation. The OA designations are also cluttered by use of numbers greater than the number of defined slots. These are "slots of convenience" defined by the operators but have no fixed meaning in terms of position within the constellation. As a result, interpretation of the OA is challenging.

For the past several years, the plane-slot assignments have been provided to ARL:UT by The Aerospace Corporation analysts supporting 2SOPS. The assignments are provided as a set of daily plane-slot relationships. This information source is not publicly available.

Both of these sources are limited in that only a single satellite may be designated as being present in a slot at a given moment. In fact, as satellites are moved within the constellation, there exists occasional periods when more than one SV may be present within the defined boundaries of a slot. From the user's point of view, if a satellite transmitting a healthy signal is present within the slot boundaries, the slot should be counted as occupied.

Figure E.1 provides a graphical illustration of the plane-slot relationships throughout 2018. The contents of Figure E.1 are primarily drawn from the information provided by The Aerospace Corporation and cross-checked against the operational advisories. In the cases where an SV is decommissioned or a new SV is launched, the appropriate NANUs were also checked to confirm dates. The dates when satellites are judged to be present in a slot location are noted only when a change occurs in the plane-slot during the year. This allows the reader to determine when multiple satellites occupied the same slot.

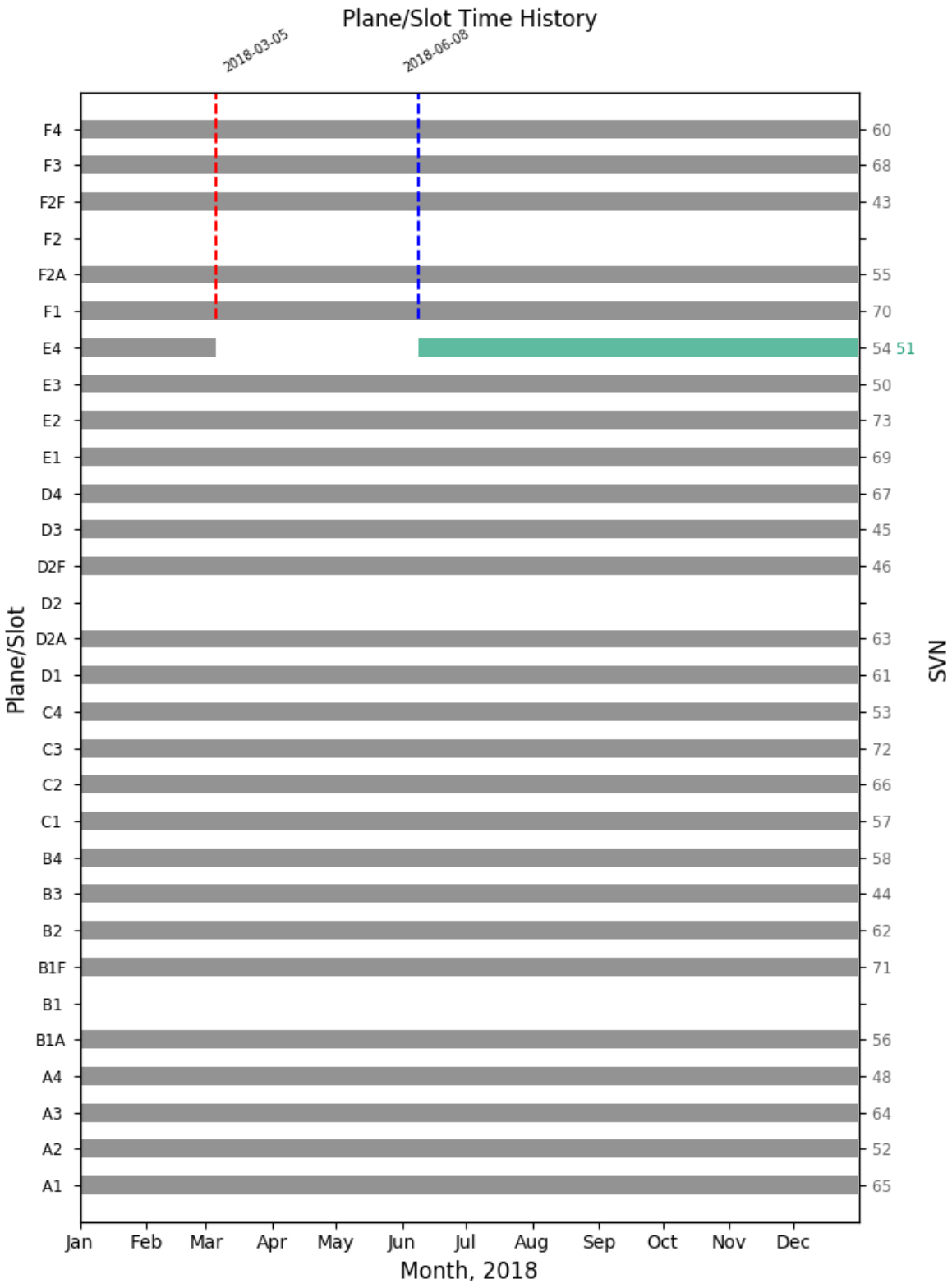

Figure E.1: Time History of Satellite Plane-Slots for 2018

Appendix F

Translation of URE Statistics Among Signals

The URE process described in Appendix B is based on the data broadcast in subframes 1, 2, and 3 of the navigation message and the NGA PE. Both of these estimates of the satellite orbits and clock offsets are referenced to the dual-frequency P(Y)-code signal. Therefore, the URE results are directly related to the Precise Positioning Service (PPS) dual-frequency performance. This appendix explains how these results have been interpreted to apply to the SPS assertions.

The PPS dual-frequency results may be mapped to SPS equivalent results by considering the effects of both the group delay differential and the intersignal bias (ISB) between the P(Y)-code and the C/A-code on L1.

F.1 Group Delay Differential

As described in IS-GPS-200 Section 3.3.1.7, the group delay through the satellite transmission hardware is accounted for in the satellite clock offset. However, there remains a group delay differential effect that comes about due to the fact that the signals passing through the different frequency chains experience slightly different delays. An estimate of the group delay differential is transmitted to the users in the navigation message using the T_{GD} term in subframe 1. Note that T_{GD} is not the group delay differential but the group delay differential scaled to account for the difference between a dual-frequency observation and a single-frequency observation. This is described in IS-GPS-200 Section 20.3.3.3.3.2. This distinction will be relevant below when comparisons to other estimates are discussed.

IS-GPS-200 Section 3.3.1.7.2 states that the random plus non-random variations about the mean of the differential delay shall not exceed 3.0 nsec (95% probability). While this establishes an upper bound on the uncertainty, it does not represent actual performance. The quantization in the T_{GD} term is 0.5 nsec. Therefore, even with perfect estimation, the floor on the uncertainty would be on the order of 0.25 nsec.

If one assumes that T_{GD} is correct and that the user equipment properly applies the correction, then the single-frequency results would be aligned with the dual-frequency results to within that quantization error. However, once the satellite is on orbit it is not possible to directly observe T_{GD}. Instead it must be estimated, and the estimates are subject to a variety of factors including receiver group delay differential effects and ionospheric dispersion. This uncertainty has the effect of inflating the PPS dual-frequency results when these results are interpreted in terms of the PPS single-frequency or SPS services. In fact, because the errors are not directly observable, the best that can be done is to examine the repeatability in the estimate or the agreement between independent estimates and consider these as proxies for the actual uncertainty.

Since 1999, the T_{GD} values have been estimated by Jet Propulsion Laboratory (JPL) and provided to 2SOPS on a quarterly basis. Shortly before this process was instituted there was a study of the proposed estimation process and a comparison of the estimates to those independently developed by two other sources [15]. The day-to-day uncertainty in the JPL estimates appeared to be about 0.3 nsec and the RMS of the differences between the three processes (after removal of a bias) was between 0.2 nsec and 0.7 nsec.

The Center For Orbit Determination (CODE) at the University of Bern estimates the P1-P2 bias [16]. CODE provides a group delay differential estimate for each SV every month. CODE does not provide details on the estimation process, but it must include a constraint that the group differential delay averaged over the constellation is zero as all sets of monthly values exhibit a zero mean.

A comparison of the CODE estimates and the T_{GD} values (scaled by the group differential delay values) shows a $\sim$5 nsec bias between the estimates. This bias can be removed as we are comparing mean-removed vs non-mean removed values. After the bias across the constellation is removed, the level of agreement between the scaled T_{GD} values and the monthly CODE estimates is between 0.1 nsec and 0.8 nsec RMS.

Considering all these factors, for the purpose of this analysis the uncertainty in the T_{GD} is assumed to be 0.5 nsec RMS.

F.2 Intersignal Bias

The ISB represents the difference between two signals on the same frequency. This bias is due to differences in the signal generation chain coupled with dispersive effects in the transmitter due to the differing bandwidths of the signals. It is not possible to observe these effects directly. When examining the signal structure at the nanosecond level the chip edges are not instantaneous transitions with perfectly vertical edges but exhibit rise times that vary by signal. Therefore, measuring the biases requires assumptions about the levels at which one decides a transition is in progress. These assumptions will vary between receivers.

There is no estimate of the ISB provided in the GPS legacy navigation message. However, CODE estimates the bias between the L1 P(Y)-code and the L1 C/A-code [16]. An estimate is provided for each SV every month. When this adjustment process was developed, these estimates were examined for each month in 2013. The monthly mean across all SVs is zero, suggesting the estimation process is artificially enforcing a constraint. The RMS of the monthly values across the constellation is 1.2 nsec for each month. Because there is no estimate of the ISB, this RMS value represents an estimate of the error C/A users experience due to the ISB.

F.3 Adjusting PPS Dual-Frequency Results for SPS

The PPS dual-frequency and SPS cases are based on a different combination and a different code. Therefore, the uncertainties in both T_{GD} and ISB must be considered. The PPS dual-frequency URE results are all stated as 95^{th} percentile (2-sigma) values. This means that the RMS errors estimated in Sections F.1 and F.2 must be multiplied by 1.96 (effectively 2, given that the amount of uncertainty in the values).

If it is assumed that these errors are uncorrelated, the total error may be estimated as:

$$\begin{aligned} \text{Total error} &= \sqrt{((2 * \text{T}_{\text{GD}} \text{ uncertainty})^2 + (2 * \text{ISB uncertainty})^2)} \\ &= \sqrt{((2 * 0.5 \text{ nsec})^2 + (2 * 1.2 \text{ nsec})^2)} \\ &= \sqrt{(1 \text{ nsec}^2 + 5.76 \text{ nsec}^2)} \\ &= 2.6 \text{ nsec} \end{aligned} \tag{F.3.1}$$

Converted to equivalent range at the speed of light and given only a single significant digit is justified, the total error is about 0.8 m. This adjustment may then be combined with the PPS dual-frequency result in a root-sum-square manner.

Appendix G

Acronyms and Abbreviations

Table G.1: List of Acronyms and Abbreviations

2SOPS	2^{nd} Space Operations Squadron
AMCS	Alternate Master Control Station
AOD	Age of Data
AODO	Age of Data Offset
ARL:UT	Applied Research Laboratories, The University of Texas at Austin
BCP	Broadcast Clock and Position
CEI	Clock, Ephemeris, and Integrity
CMPS	Civil Monitoring Performance Specification
CODE	Center For Orbit Determination
DECOM	Decommission
DOP	Dilution of Precision
ECEF	Earth-Centered, Earth-Fixed
FAA	Federal Aviation Administration
FCSTDV	Forecast Delta-V
FCSTEXTD	Forecast Extension
FCSTMX	Forecast Maintenance
FCSTRESCD	Forecast Rescheduled
FCSTUUFN	Forecast Unusable Until Further Notice

GEC	Groundtrack Equatorial Crossing
GLAN	Geographic Longitude of the Ascending Node
GNSS	Global Navigation Satellite System
GPS	Global Positioning System
GPSTk	GPS Toolkit
HDOP	Horizontal Dilution Of Precision
IGS	International GNSS Service
IODC	Issue of Data, Clock
IODE	Issue of Data, Ephemeris
ISB	Intersignal Bias
JPL	Jet Propulsion Laboratory
LNAV	Legacy Navigation Message
LSB	Least Significant Bit
MCS	Master Control Station
MSB	Most Significant Bit
MSI	Misleading Signal Information
MSN	Monitor Station Network
NANU	Notice Advisory to Navstar Users
NAV	Navigation Message
NGA	National Geospatial-Intelligence Agency
NMCT	Navigation Message Correction Table
NTE	Not to Exceed
OA	Operational Advisory
ORD	Observed Range Deviation
PDOP	Position Dilution of Precision
PE	Precise Ephemeris
PPS	Precise Positioning Service

PRN	Pseudo-Random Noise
PVT	Position, Velocity, and Time
RAIM	Receiver Autonomous Integrity Monitoring
RINEX	Receiver Independent Exchange Format
RMS	Root Mean Square
RSS	Root Sum Square
SA	Selective Availability
SINEX	Station Independent Exchange Format
SIS	Signal-in-Space
SMC/GP	Space and Missile Systems Center Global Positioning Systems Directorate
SNR	Signal-to-Noise Ratio
SP3	Standard Product 3
SPS	Standard Positioning Service
SPS PS(SPSPS08)	2008 Standard Positioning Service Performance Standard
SV	Space Vehicle
SVN	Space Vehicle Number
TCP	Truth Clock and Position
T_{GD}	Group Delay
UNUNOREF	Unusable with No Reference
UNUSUFN	Unusable Until Further Notice
URA	User Range Accuracy
URAE	User Range Acceleration Error
URE	User Range Error
URRE	User Range Rate Error
USCG	United States Coast Guard
USNO	U.S. Naval Observatory

UTC	Coordinated Universal Time
UTCOE	UTC Offset Error
UUTCE	User UTC(USNO) Error
WGS 84	World Geodetic System 1984
ZAOD	Zero Age of Data

Bibliography

[1] U.S. Department of Defense. Standard Positioning Service Performance Standard, 4th Edition. http://www.gps.gov/technical/ps/2008-SPS-performance-standard.pdf, 2008.

[2] U.S. Department of Defense. Navstar GPS Space Segment/Navigation User Interfaces, IS-GPS-200, Revision G. https://www.gps.gov/technical/icwg/IS-GPS-200G.pdf, September 2012.

[3] John M. Dow, R.E. Neilan, and C. Rizos. The International GNSS Service in a changing landscape of Global Navigation Satellite Systems. *Journal of Geodesy*, 2009.

[4] B. Renfro, D. Munton, R. Mach, and R. Taylor. Around the World for 26 Years - A Brief History of the NGA Monitor Station Network. In *Proceedings of the Institute of Navigation International Technical Meeting*, Newport Beach, CA, 2012.

[5] U.S. Coast Guard. GPS Constellation Status. https://www.navcen.uscg.gov/?Do=constellationStatus.

[6] U.S. Naval Observatory. Satellite Information. ftp://tycho.usno.navy.mil/pub/gps/gpstd.txt, January 2017.

[7] U.S. Naval Observatory. Daily GPS-UTC Comparison data. ftp://tycho.usno.navy.mil/pub/gps/gps15m/gps_utc_1day.hist.

[8] W. Gurtner and L. Estey. RINEX: The Receiver Independent Exchange Format Version 2.11, 2006.

[9] U.S. Department of Defense. Navstar GPS Control Segment to User Support Community Interfaces, ICD-GPS-240, Revision A, January 2010.

[10] U.S. Department of Transportation. Global Positiong System (GPS) Civil Monitoring Performance Specification, DOT-VNTSC-FAA-09-08, April 2009.

[11] P. Misra and P. Enge. *Global Positioning System: Signals, Measurements, and Performance*. Ganga-Jamuna Press, revised second edition, 2012.

[12] NIMA Technical Report TR8350.2. Department of Defense World Geodetic System 1984, Its Definition and Relationships With Local Geodetic Systems, July 1997.

[13] National Geospatial-Intelligence Agency. NGA Antenna Phase Center Precise Ephemeris products. `ftp://ftp.nga.mil/pub2/gps/pedata`.

[14] B. Tolman et al. The GPS Toolkit - Open Source GPS Software. In *Proceedings of the 17th International Technical Meeting of the Satellite Division of the Institute of Navigation (ION GNSS 2004)*, Long Beach, CA, 2004.

[15] Colleen H. Yinger, William A. Feess, Ray Di Esposti, The Aerospace Corporation, Andy Chasko, Barbara Cosentino, Dave Syse, Holloman Air Force Base, Brian Wilson, Jet Propulsion Laboratory, Maj. Barbara Wheaton, and SMC/CZUT. GPS Satellite Interfrequency Biases, June 1999.

[16] Center for Orbit Determination Europe. GPS satellite bias estimates for 2013. `ftp://ftp.aiub.unibe.ch/CODE/2013`, 2013.